January 2016

Co-orthologs of KATANIN1 Impact Plant Morphology and Show Differential Evolution in Maize

Kin Ho Lau
Purdue University

PURDUE UNIVERSITY
GRADUATE SCHOOL
Thesis/Dissertation Acceptance

This is to certify that the thesis/dissertation prepared

By Kin H. Lau

Entitled

CO-ORTHOLOGS OF KATANIN1 IMPACT PLANT MORPHOLOGY AND SHOW DIFFERENTIAL EVOLUTION IN MAIZE

For the degree of Doctor of Philosophy

Is approved by the final examining committee:

Clifford F. Weil
Chair

Brian P. Dilkes

Mitchell R. Tuinstra

Robert E. Pruitt

To the best of my knowledge and as understood by the student in the Thesis/Dissertation Agreement, Publication Delay, and Certification Disclaimer (Graduate School Form 32), this thesis/dissertation adheres to the provisions of Purdue University's "Policy of Integrity in Research" and the use of copyright material.

Approved by Major Professor(s): Clifford F. Weil

Approved by: Joseph M. Anderson 7/25/2016

Head of the Departmental Graduate Program Date

CO-ORTHOLOGS OF *KATANIN1* IMPACT PLANT MORPHOLOGY AND SHOW DIFFERENTIAL EVOLUTION IN MAIZE

A Dissertation

Submitted to the Faculty

of

Purdue University

by

Kin H. Lau

In Partial Fulfillment of the

Requirements for the Degree

of

Doctor of Philosophy

August 2016

Purdue University

West Lafayette, Indiana

For my family.

ACKNOWLEDGEMENTS

I would like to express my deepest appreciation for my major advisor, Dr. Cliff Weil, for providing funding, lab resources and mentorship that not only made my project possible but allowed me to develop skills as a scientist. I am thankful to my advisory committee for always challenging me to approach my work with a scientific and hypothesis-driven mindset. Much of my growth can be attributed to the committee meetings and exams that were overseen by my committee.

I would like to acknowledge Drs. Amanda Wright and Laurie Smith, for providing the *clt1-2* allele. Thought-provoking discussions with Drs. Wright and Nicholas Miles about my results were also much appreciated. Next, I need to thank Drs. Gerry Neuffer and K. A. Sheridan for creating the *Clt1-1* allele, and Dr. Peter Bommert for the B73 introgression. I would like to thank the Purdue Life Science Microscopy Facility, Genomics Core and Plant Growth Facilities for their help and advice. I want to thank Drs. Karen Hudson, Torbert Rocheford, Steven Scofield, Tesfaye Mengiste, Stan Gelvin, Mary Alice Webb and Bob Pruitt for sharing various equipment and material from their labs.

I would like to thank past and present members of the Weil lab who coincided with my time here. The road to a Ph.D. is not easy but was made much more enjoyable by working with such great people. In particular, I would like to acknowledge the late Mr. Nick Babcock, who was a good friend. Similarly, I want to thank the fellow graduate students, and post-docs I have come to know for their friendship and discussions. Lastly, but most importantly, I want to thank my family for being my support system and believing in me even when I did not. Without them, I would have given up on this pursuit a long time ago.

TABLE OF CONTENTS

Page

Page

Page

LIST OF TABLES

LIST OF FIGURES

Figure Page

ABSTRACT

Lau, Kin H. Ph.D., Purdue University, August 2016. Co-orthologs of KATANIN1 Impact Plant Morphology and Show Differential Evolution in Maize. Major Professor: Clifford Weil.

Understanding how the size and shape of crop plants and their specific organs are genetically controlled may allow for the development of cultivars with improved plant architecture. A microtubule-severing enzyme called katanin p60 is encoded by *KATANIN1* (*KTN1*) in *Arabidopsis* or by an ortholog, *dwarf and gladius leaf1* (*dgl1*), in rice. Katanin p60 has been implicated in the control of anisotropic cell growth, which is cell growth directed in a specific direction instead of equally in all directions. Anisotropic cell growth is crucial for proper plant shape and its disruption in *ktn1/dgl1* mutants leads to morphological changes such as stunted plant height, shorter leaves and reduced inflorescence size.

In this work, characterization of the maize mutant *Clumped tassel1* (*Clt1*) led to the discovery of a putative dominant-negative allele of a *KTN1* ortholog. Results indicate that the causative lesion is a missense mutation in the adenosine triphosphatase (ATPase) domain that, we hypothesize, disrupts the ability of the protein to hydrolyze ATP. In general, the phenotype of *Clt1-1* was analogous to the phenotypes reported for *ktn1/dgl1* mutants in *Arabidopsis* and rice, with reduced plant stature and more compact organs. *Clt1-1* represents the first report of a dominant-negative allele of *KTN1* or its orthologs among plant species, though similar mutants have been described in animal systems. By expressing it in specific tissues, the discovery of *Clt1-1* can potentially be used to decouple the pleiotropic effects of *KTN1* so that each effect can be studied without being confounded by other aspects of the phenotype, or to reduce the size of particular organs for agronomic purposes.

In order to learn more about the mechanism of *clt1*, an enhancer/suppressor screen was conducted, using natural variation. Through this approach, multiple deleterious alleles of *ktn1b*, the other maize ortholog of *KTN1*, were identified. These alleles, whose effects are masked in the inbred parents presumably by redundant function from *clt1*, helped uncover functional differences between *clt1* and *ktn1b*. First, *clt1* appears to provide less function than *ktn1b* for the elongation of upper internodes. Conversely, *clt1* seems to be more important than *ktn1b* for overall plant development because, in *Clt1-1* heterozygotes, losing functionality in the other *clt1* allele has a much more severe developmental impact than in one of the *ktn1b* alleles.

Consistent with a more important biological role for *clt1*, sequencing data suggests that purifying selection is relaxed for *ktn1b*. Introns in *ktn1b* appear to have expanded dramatically compared to sorghum homologs, whereas *clt1* retains homology with the sorghum homologs along most of the gene. Furthermore, examination of publicly available whole-genome sequencing data for approximately one thousand maize lines indicates a substantially greater ratio of nonsynonymous to synonymous nucleotide diversity (π_a/π_s) and more frequent occurrence of deleterious mutations in the coding sequence of *ktn1b* than in *clt1*. In summary, the results from this work indicate overlapping but not fully redundant functions between *clt1* and *ktn1b* in maize, and suggest an evolutionary bias for the retention of *clt1* over *ktn1b*.

CHAPTER 1. INTRODUCTION

1.1 A brief introduction to the cytoskeleton

Cytoskeleton is present in cells from all organisms although its specific functions vary. It is often described as the scaffolding of the cell, helping organize the contents of the cell so that specific components are in the right place at the right time to allow cellular functions to be carried out. The tasks of the cytoskeleton are diverse, delegated among at least three different long chained protein structures: actin, microtubules and, in animal cells, intermediate filaments.

Microtubules are hollow cylindrical structures that consist of a circular arrangement of thirteen parallel chains, called protofilaments (Ledbetter and Porter, 1964). Each protofilament consists of α- and β-tubulin heterodimers lined up end to end with α-tubulin subunits pointing towards the “plus end” and β-tubulin pointing to the “minus end” (Borisy, 1967; Meza et al., 1972). Key functions of microtubules include, firstly, the formation of spindle fibers during mitosis and meiosis, that pull sister chromatids or homologous chromosomes to opposite poles of the dividing cell (Flemming, 1880). Secondly, microtubules are a major component of both the preprophase band, which encircles the dividing cell before and during prophase indicating the location of the plane of cell division, and the phragmoplast that actually guides the formation of the new cell wall that separates two daughter cells at cytokinesis (Pickett-Heaps and Northcote, 1966b, 1966a). The third major role of microtubules involves their localization directly below the cell membrane, in a region called the cell cortex. These cortical microtubules (CMTs) form internal rings around the cell that have been likened to “hoops around a barrel” (Ledbetter and Porter, 1963) and help direct cell growth and shape.

1.2 Cell growth direction is controlled by an intricate relationship between CMTs and cellulose microfibrils in the cell wall

The cytoplasm exerts turgor pressure pushing outwards against the cell wall, which resists deformation (also known as strain). This ability of the cell wall to maintain cell shape is mainly due to the presence of cellulose, which consists of a long chain of beta-(1,4)-linked D-glucose units. When turgor pressure is stronger than the stiffness of the cell wall, the cell wall stretches and the cell can grow (Ray et al., 1972). If cell wall stiffness is uniform in all directions, then the cell will grow equally in all directions to form a sphere (isotropic growth). However, plant architecture necessitates the formation of non-spherical cells and it is thought that the pattern in which new cellulose microfibrils (CMFs) form facilitates this by reducing the stiffness of the cell wall in certain directions. CMFs have long been believed to promote growth in a particular direction (growth anisotropy) by organizing into arrays transverse to the main growth axis where they restrict lateral growth and in effect make the cell more susceptible to longitudinal deformation by turgor pressure (Green, 1962). This idea is supported based on the pattern of new CMFs formed in elongating tissues and on the observation that disruption of this pattern leads to spherical instead of cylindrical cells. Interestingly, studies suggest that CMTs help CMFs achieve orientations needed for properly regulating cell growth, an idea called the alignment hypothesis (reviewed in Baskin, 2001). Paul Green ((Green, 1962) first proposed the alignment hypothesis based on the observation that colchicine, a chemical known to inhibit tubulin polymerization, causes the transverse alignment of CMFs in internode cells of *Nitella* (a multicellular algae) to become disorganized. Remarkably, CMTs would not be directly observed until a year later when the introduction of the fixative glutaraldehyde allowed CMTs to be visualized for the first time. Consistent with Green's hypothesis, it was found that CMT and CMF orientations mirror each other (Ledbetter and Porter, 1963).

1.2.1 Live-cell confocal microscopy sheds light on possible mechanisms behind the alignment hypothesis

More recently, the use of fluorescent protein fusions in *Arabidopsis thaliana* has revealed how CMTs can direct the deposition of CMFs. Tagged cellulose synthase (CESA) complexes, consisting of CESA1, CESA3, and CESA6 for primary cell wall synthesis (Hill et al., 2014), showed directly that the path of CESA complexes during CMF deposition at the cell membrane aligns with the CMT patterns underneath (Paredez et al., 2006). Additionally, several lines of evidence suggest that CMTs are even involved in the transport of CESA complexes *to* the plasma membrane. CESA complexes are transported to the cell cortex via either small sub-cellular compartments called small CESA compartments/microtubule-associated cellulose synthase compartments (SmaCCs/MASCs) or the Golgi apparatus (Gutierrez et al., 2009; Crowell et al., 2009). Once at the cell cortex, sites where CESA complexes are deposited into the plasma membrane often coincide with CMTs. Interestingly, treatment with oryzalin (a microtubule depolymerizing chemical) does not affect the rate of delivery of CESA to the plasma membrane but does inhibit stable accumulation of SmaCCs/MASCs at the cell cortex suggesting that CMTs are involved in guiding CESA deposition but is not required for it (Gutierrez et al., 2009). Indeed, CESA motility at the cell cortex prior to exocytosis tracks with the depolymerizing ends of CMTs and the velocity of CESA particles in the cell cortex is significantly reduced by the MT-stabilizing chemical, taxol (Gutierrez et al., 2009). Taken together, these findings suggest that, on arrival at the cell cortex, SmaCCs/MASCs bind to the depolymerizing end of CMTs that then pull them towards the plasma membrane where the CESA complex gets integrated. Thus, CMTs not only guide the direction of synthesis of CESA complexes, but also have a role in positioning the deposition of CESA complexes.

The association between CESA trajectory at the plasma membrane and CMT pattern is dependent on a microtubule-binding protein called CELLULOSE SYNTHASE INTERACTING1 (CSI1) that co-localizes with CESA at the cell membrane (Bringmann et al., 2012; Li et al., 2012) and binds with the CESA6 sub-unit of CESA complexes in yeast two-hybrid experiments (Gu et al., 2010). CSI1 mutants decouple CESA

trajectories in the plasma membrane from CMT patterns (Bringmann et al., 2012; Li et al., 2012). However, insertion sites of CESA remain associated with microtubules (Bringmann et al., 2012), suggesting that interaction between CESA complexes and CMT is dependent on CSI1 only after CESA establishment in the plasma membrane.

1.2.2 Nuances of the alignment hypothesis

Although evidence of the importance of CMT in guiding CMF orientation is strong, there have been inconsistencies with the model that CMT influence cell elongation simply by aligning CMF. While disruption of microtubules by relatively brief treatment with oryzalin causes CESA trajectories to be disorganized as expected, CESA trajectories become parallel again if the treatment time is extended, suggesting that CESA follows intact microtubules if they are present but is capable of maintaining uniform trajectories even in their absence via an unknown mechanism (Paredez et al., 2006). Similarly, another study using *Arabidopsis* showed that inducing CMT disorganization using a temperature-sensitive mutant, *mor1-1*, do not lead to distinguishable changes in the orientation and uniformity of CMF despite severe effects on that of CMT and cell shape (Sugimoto, 2003). That disrupting CMTs consistently leads to more isotropic cells but not consistently to CMF disorganization, suggests that other factors in addition to CMF orientation may be required for anisotropic growth.

One of these additional factors appears to be the crystallinity of cellulose, which is inversely proportional to its extensibility. As mentioned above, cellulose is a long chain of beta-(1,4)-linked D-glucose units; 18 to 24 of these glucan chains associate to form a CMF. These CMFs are cross-linked by pectin and hemicelluloses that heavily influence the degree of crystallinity of the resulting cellulose complex. In wildtype *Arabidopsis*, cell elongation can be induced by growing plants at elevated temperatures (Fujita et al., 2011). This increase in cell elongation is accompanied by reductions in cell wall crystallinity. In contrast, elevated temperature had no effect on either cell elongation or cellulose crystallinity in the CMT-defective mutant *mor1-1*, suggesting that anisotropic cell growth requires both transverse orientation of CMFs and a reduction in cellulose crystallinity. This model proposes that although most CMF remain transversely

aligned in MT-defective cells, the CMFs that remain longitudinal provide substantial resistance against turgor pressure along the main growth axis because of unreduced cellulose crystallinity and leading to isotropic cell growth.

In summary, CMTs play a central role in not only controlling the pattern of CMF deposition, but also in the delivery of CESA to the plasma membrane and in influencing the chemical properties of CMF. Thus, CMTs are a key control point for anisotropic growth, cell shape and, thus, overall plant shape.

1.3 Katanin, a microtubule-severing enzyme, and its diverse roles in plants

1.3.1 Discovery of katanin and its mechanism of action

Katanin was first identified from sea urchin egg extract by assaying chromatography fractions for microtubule severing activity. SDS-PAGE of the active fractions revealed and a 60kd and an 81kd polypeptide that are referred to as katanin p60 and p80 respectively (McNally and Vale, 1993). Co-immunoprecipitation of baculovirus-expressed katanin p60 and p80 confirmed that these proteins can form complexes, and that each subunit has distinct functions (Hartman et al., 1998). The p60 subunit has a conserved adenosine triphosphatase (ATPase) domain on the carboxyl end (Hartman et al., 1998) that makes it a member of a superfamily called ATPases Associated to a variety of cellular Activities (AAA) (Confalonieri and Duguet, 1995), and can sever microtubules *in vitro* in the presence of adenosine triphosphate (ATP) (McNally and Vale, 1993). In contrast, the p80 subunit has no microtubule severing activity but, because it localizes to centrosomes when transfected by itself into mammalian cells (Hartman et al., 1998), is thought to guide the katanin p60-p80 complex to the centrosomes where katanin aggregates as observed in sea urchin (McNally et al., 1996).

Findings from a key *in vitro* study (Hartman and Vale, 1999) suggest that ATPase activity, and thus microtubule severing, by katanin p60 is likely to depend on the formation of katanin p60 homo-hexamer rings—which have been observed through electron microscopy and corroborated by estimated molecular mass of oligomerized katanin p60 (Hartman et al., 1998; Hartman and Vale, 1999). In this study, Hartman and

Vale (1999) used fluorescence resonance energy transfer (FRET) between katanin p60 subunits tagged with cyan fluorescence protein (CFP) and yellow fluorescence protein (YFP) to quantify oligomerization. They found that oligomerization of katanin p60 requires ATP and that, provided ATP is present, microtubules induce the oligomerization of katanin p60 even further. However, very high concentrations of microtubules actually inhibited oligomerization possibly by reducing interactions between katanin p60 monomers. At different concentrations of microtubules, changes in oligomerization and ATPase activity were strongly correlated, suggesting that the ATPase activity of katanin p60 requires oligomerization. In addition, they used a co-sedimentation assay to show that the binding affinity of katanin p60 to microtubules increases substantially in the presence of ATP. Taking these results together, Hartman and Vale (1999) formulated a model where katanin p60 monomers form hexamers in the presence of ATP and microtubules, binds to microtubules and uses the energy of ATP hydrolysis to induce microtubule severing. Subsequently, the katanin complex breaks back down to monomers due to the lack of ATP to promote oligomerization.

1.3.2 Mutants of katanin p60 in *Arabidopsis* indicate roles in CMT organization, anisotropic growth and cell division

Mutants of *KATANIN1* (*KTN1*), encoding katanin p60 in *Arabidopsis*, show pleiotropic effects and consequently have been identified repeatedly in mutant screens for different traits. These traits include reduced hypocotyl elongation due to shorter and wider cells (*botero1*, *bot1*) (Bichet et al., 2001), inflorescence stems that break with less force (*fragile fiber2*, *fra2*) (Burk et al., 2001), disrupted identity of hair cells in roots (*ectopic root hair3*, *erh3*) (Webb et al., 2002) and constitutive expression of transgenic luciferase controlled by the promoter of the gibberellin (GA) biosynthetic enzyme, *GA5* (encoding GA 20-oxidase), which is normally repressed by exogenous GA_3 (*LUCIFERASE super expressor1*, *lue1*) (Meier et al., 2001; Bouquin et al., 2003). In general, loss-of-function mutants have wider and shorter cells, leading to reduced size of many features including leaves, internodes between flowers on an inflorescence, floral organs and roots. These aberrant cell shapes are consistent with a loss of anisotropic

growth due to disorganization of CMTs resulting in randomly aligned CMT arrays in tissue that normally have uniformly transverse CMT arrays to promote cell elongation (Bichet et al., 2001; Burk and Ye, 2002; Bouquin et al., 2003). Thus, *Arabidopsis ktn1* mutants underscore the importance of uniform CMT arrays for anisotropic growth and also suggest that katanin p60 has an essential role in either propagating or maintaining such uniformity, a topic that will be discussed in more detail in later sections.

Beyond simple loss of growth anisotropy, the inability to properly organize CMTs in *ktn1* mutants also seems to impair the formation of complex cell shapes. For example, it is thought that lobed cells, such as those found in the epidermis, are produced by outgrowths of a cell due to constrictive forces initiated by rings of CMTs at the base of each cell lobe that presumably direct the deposition of rings of CMFs (Jung and Wernicke, 1990). Consistent with an inability to properly form uniform CMT arrays, *ktn1* mutants have visibly less interdigitation in leaf epidermal cells (Burk et al., 2001). Similarly, branching of unicellular trichomes on *Arabidopsis* leaves is reduced in *ktn1* mutants (Burk et al., 2001), probably because the initiation of trichome branches also involves rings of CMTs at the initiation site (Sambade et al., 2014).

Katanin also plays roles in cell division, as evidenced by crooked cell files and frequent non-transverse division planes in *ktn1* mutants (Bichet et al., 2001; Burk et al., 2001). Several cytological defects involving microtubules have been observed that may explain this aberrant cell patterning (Panteris et al., 2011). Just before the start of mitosis, the preprophase band, which normally predicts the eventual cell division plane, aligns perpendicular to the tissue growth axis as expected in *ktn1* mutants, but is more diffuse and disorganized compared with the condensed and parallel microtubules in wildtype preprophase bands. Prophase spindles are the first stage where alignment defects become readily apparent; while normal prophase spindles converge at the two poles where the daughter nuclei eventually form, spindles converge at multiple poles in *ktn1* mutants. While functional, bi-polar spindles do eventually form in metaphase, the axis between the two poles are often obliquely aligned as opposed to being parallel to the tissue growth axis. These oblique spindles are proceeded by, and probably cause, a substantial amount of obliquely aligned phragmoplasts that lead to abnormal cell division planes that often

do not reflect the orientation of the preprophase band. Furthermore, delays in transitions between stages of mitosis were observed, where preprophase bands linger into metaphase, phragmoplast microtubules remain attached to the daughter nuclei in late cytokinesis (Panteris et al., 2011) and even CMTs in newly divided cells show attachment points to the nucleus (Burk et al., 2001). Finally, consistent with roles in controlling the mitotic processes described above, fluorescently-tagged katanin co-localizes with preprophase bands, spindle poles and at the ends of phragmoplast microtubules proximal to the daughter nuclei (Panteris et al., 2011).

1.4 Katanin-mediated microtubule-severing at microtubule crossover sites and branching nucleation sites is essential for CMT organization and reorientation

1.4.1 A brief overview of microtubule dynamics

Understanding the role katanin can play in the cell requires an understanding of microtubule dynamics inside cells. Microtubules are initiated in a process called nucleation, where α- and β-tubulin heterodimers further polymerize to form the protofilaments of a microtubule. While microtubules can form spontaneously *in vitro* (Weisenberg, 1972), *in vivo* nucleation is usually facilitated by a protein complex, consisting of γ-tubulin (Oakley and Oakley, 1989) and its associated proteins (GCPs), called the γ-tubulin ring complex (γ-TuRC) that may act as a template to assemble nascent protofilaments into a microtubule (Oakley et al., 1990; Horio et al., 1991; Zheng et al., 1995). Microtubules are dynamic molecules that can switch between polymerization and depolymerization at the ‘plus-end’ (Mitchison and Kirschner, 1984) and periodic pausing and depolymerization at the ‘minus-end’ (Desai and Mitchison, 1997). The α- and β-tubulin dimers that are incorporated at the plus-end are stabilized by a guanosine triphosphate (GTP) molecule that is bound to the β-tubulin subunit (Downing and Nogales, 1998; Nogales et al., 1998). However, these GTP molecules are gradually hydrolyzed to GDP after the tubulin dimer is incorporated into the microtubule. When incorporation of new tubulin dimers occurs faster than hydrolysis of the GTP attached to recently added dimers, a ‘GTP cap’ is created at the plus-end that is thought

to inhibit depolymerization of the microtubule (Carlier and Pantaloni, 1981; Carlier et al., 1984). In contrast, when the rate of GTP hydrolysis becomes greater than the rate of incorporation of new, GTP-bound dimers, this apparent cap is lost, which may lead to 'catastrophe' where the microtubule plus-end undergoes very rapid depolymerization (Mitchison and Kirschner, 1984). In this model, catastrophe can be stopped by the addition of GTP-bound tubulin dimers that reconstitute the GTP cap and 'rescue' the microtubule. Interestingly, when the rate of polymerization at the plus-end matches that of depolymerization at the minus-end, the length of the microtubule remains constant but the microtubule, in effect, gets transported in the direction of the plus-end, a process called 'treadmilling' (Margolis and Wilson, 1978).

1.4.2 Direct evidence that katanin-mediated microtubule-severing helps promote parallel CMT organization in elongating cells

Confocal microscopy of fluorescence-tagged GCPs and microtubules showed that γ-tubulin complexes often bind to extant microtubules (Murata et al., 2005) and that nucleation from pre-existing microtubules happens approximately 10 times more frequently compared with *de novo* nucleation by γ-tubulin complexes not bound to existing microtubules (Nakamura et al., 2010). Importantly, nucleation proceeds parallel to the bound microtubule 38% of the time, thereby increasing the number of microtubules oriented in the original direction, but the rest of the time nucleation branches out at a 40-45° angle with the plus end of the new microtubule almost always growing on the same side as the plus-end of the mother microtubule (Murata et al., 2005; Chan et al., 2009). Such branching, nascent microtubules can be severed from the mother microtubule, but mutant analysis showed this severing is dependent on functional KTN1 (Nakamura et al., 2010). After being severed from the mother microtubule, the new microtubule treadmills to other regions of the cell cortex and eventually collides with other microtubules. The outcome of such collisions may be dependent on the angle of incidence (Dixit and Cyr, 2004). In tobacco BY-2 culture cells, shallow incident angles (<40°) lead to stable attachment of the growing 'plus' end to the obstructing microtubule, forming a bundle ~90% of the time. In contrast, steep incident angles (>40°) lead to 'crossover' ~40% of

the time, where the growing microtubule continues on its original trajectory past the obstructing microtubule, presumably by going over it, and catastrophe of the incident microtubule ~60% of the time (Dixit and Cyr, 2004). However, this high frequency of catastrophe has not been replicated in whole plants.

In contrast, in *Arabidopsis* petiole tissue where CMTs are organized into uniform transverse arrays, 91% of steep-angle collisions result in crossovers (Wightman and Turner, 2007). However, the growing microtubule frequently gets severed at the crossover site and the resulting lagging strand often undergoes catastrophe, offering an alternate mechanism for suppressing microtubules that are misaligned relative to the predominant direction of CMTs in a particular cell, referred to as discordant microtubules (Wightman and Turner, 2007). Furthermore, some microtubules grew in curved trajectories such that depolymerization of the discordant lagging strand leaves a leading strand that has better co-alignment with the obstructing microtubule. A subsequent study in *Arabidopsis* hypocotyl tissue reported 85% of severing events led to complete depolymerization of the lagging strand (Zhang et al., 2013). Interestingly, this study also found that severing at crossovers in *Arabidopsis* hypocotyl tissue was abolished in *ktn1* mutants and that KTN1 protein localized to crossovers prior to severing, suggesting that severing at crossover sites is carried out by KTN1. Furthermore, the *ktn1* mutant was unable to generate parallel CMT arrays when CMTs are depolymerized by cold treatment and then allowed to recover suggesting that KTN1 is required to even generate parallel CMTs and not just to maintain them. In support of the importance of microtubule severing for promoting uniformly oriented CMTs, the rate of microtubule severing is much lower in the non-parallel, net-like arrangement of pavement cells (despite having more crossovers) than in the parallel, transverse arrays of petiole cells, though the exact severing frequencies were different using two different microtubule visualization methods (Wightman and Turner, 2007). Together, these data suggest that KTN1-dependent severing at crossover sites promote the depolymerization of discordant CMTs, which helps cells achieve uniform, parallel CMT arrays.

1.4.3 Direct evidence that katanin-mediated microtubule-severing helps promote parallel CMT organization in localized bands that allow cell lobing

As mentioned earlier, functional KTN1 is required in *Arabidopsis* to form the uniform CMT 'bands' that wrap around the indented regions of epidermal pavement cells, restricting growth in those regions to help give rise to a lobed cell shape (Lin et al., 2013). Studies of these cells and their shape has revealed interactions between KTN1 and other proteins that impact cell shape. KTN1 interacts physically with *ROP-interactive CRIB motif-containing1 (RIC1*) (Lin et al., 2013), which is activated by binding with ROP6, a Rho guanosine triphosphatase (GTPase) (Fu et al., 2009). An imbalance in this interaction disrupts lobe formation in pavement cells. For example, overexpression of either *RIC1* or *ROP6* causes exceptionally uniform, parallel CMT arrays over the entire cell, leading to rectangular pavement cells with minimal lobing (Fu et al., 2005, 2009). Conversely, loss-of-function *ric1, rop6 or ktn1* alleles cause disorganization of the lobe-associated CMT 'bands', leading to wider lobes that are most severe in the *ktn1* mutant, which is epistatic to both *ric1* and *rop6* (Lin et al., 2013). Additionally, RIC1 localizes to CMTs like KTN1, and enhances *in vitro* microtubule severing by KTN1 (Lin et al., 2013). Together, these results suggest that RIC1 and ROP6 activate KTN1-mediated CMT severing to promote lobe-associated CMT 'bands' that help form the lobed shapes of pavement cells, presumably by activating severing at indented regions of the cell preferentially.

Findings from Xu et al. (2010) suggest that auxin signaling could underlie such localized control of KTN1-severing. First, a quadruple mutant of auxin biosynthesis genes, *yucca (yuc) 1*/*2*/*4*/*5* shows a reduced number of lobes in pavement cells that can be rescued by exogenous synthetic auxin, naphthalene-1-acetic acid (NAA). Second, the association of RIC1 with CMTs is severely weakened in *yuc1*/*2*/*4*/*6*, while addition of NAA in backgrounds with functional auxin signaling leads to more abundant accumulation of RIC1 on CMTs. Third, active ROP6, assayed by the amount of ROP6 pulled down by epitope-tagged RIC1, is increased by NAA treatment in protoplasts, suggesting that auxin can promote RIC1-ROP6 interactions. Finally, the auxin efflux protein PINFORMED1 (PIN1) (Okada et al., 1991; Gälweiler et al., 1998; Petrásek et al.,

2006) localizes to the tips of pavement cell lobes, where it presumably facilitates the efflux of auxin that may induce the RIC1-ROP6 pathway in the indentation regions of the adjacent, interdigitating cell. In summary, these results suggest localized activation of KTN1 at indentation regions in lobed pavement cells by RIC1 and ROP6 in response to local, sub-cellular auxin maxima. Further evidence for interactions between KTN1 function and auxin signaling in shoot apical meristems (SAM) is discussed in more detail below.

1.4.4 Katanin-mediated severing underlies a novel, γ-tubulin-independent type of nucleation that helps reorient CMTs in hypocotyls exposed to blue light

Changes in CMTs mediated by katanin are important in other aspects of plant growth and development. The findings discussed above suggest that, in the presence of uniform parallel CMT arrays, there is a biased destabilization of CMTs that are oriented in discordant directions relative to the majority of other microtubules. Therefore, in order to change the predominant orientation of CMTs, there may need to be a rapid increase in the number of microtubules adopting the new orientation before they can depolymerize. One such mechanism is dependent on katanin and was uncovered by observing the reorientation of CMTs from transverse to longitudinal orientations in hypocotyl tissue of *Arabidopsis* after exposure to blue light—a process involved in bending the hypocotyl towards the light source by inhibiting cell elongation on one side (Lindeboom et al., 2013).

The authors observed that 62% of new microtubules initiated after light exposure nucleated from crossover sites and that these crossover-dependent nucleations tended to produce daughter microtubules that were almost parallel to the mother microtubule as opposed to the ~40° angle that predominates for nucleations that branch from a non-crossover microtubule. These nucleations from crossovers were 1.7 times more likely to nucleate from the growing microtubule than the microtubule being collided into, providing a mechanism to amplify growing, discordant microtubules. Surprisingly, 97% of γ-tubulin-mediated nucleation events, identified using tagged GCP proteins, occur at

non-crossover sites, suggesting a novel, γ-tubulin-independent microtubule nucleation mechanism causes these nucleations at crossover sites.

As mentioned previously, microtubule severing is abolished in *Arabidopsis ktn1* mutants and *ktn1* mutants are also severely inhibited in their rate of reorientation of microtubules in response to blue light, suggesting that KTN1 is required for severing at CMT crossovers in this response as well. Consistent with this idea, fluorescence-tagged KTN1 localizes to crossovers in blue-light treated *Arabidopsis* hypocotyls as predicted. These results suggest that blue light exposure causes KTN1 to sever discordant, growing microtubules at crossover sites to create a new discordant microtubule each time, because the lagging strand continues polymerizing at the plus-end instead of undergoing catastrophe. In fact, the authors were able to track single microtubules that led to the formation of ~7 new microtubules in less than 8 minutes due to a recursive pattern where crossovers lead to new discordant microtubules that then form more crossovers. Thus, this KTN1-mediated mechanism can rapidly amplify discordant microtubules in response to blue light.

1.5 Coordinating primordia initiation at the SAM involves katanin-dependent auxin-regulated reorganization of CMTs

1.5.1 The shoot apical meristem

The SAM controls the development of all above-ground structures in plants. It is a dome-shaped organ with undifferentiated pluripotent cells at the top in a region called the central zone (CZ) that continuously supplies cells to the peripheral zone (PZ) below it. While cells in the CZ divide and grow slowly, cells in the PZ divide and grow more rapidly, and begin differentiating into specialized cells that initiate and form new organs, such as leaves. The pattern that new primordia are initiated at the SAM is called phyllotaxis and helps determine overall plant shape and architecture. At older growth stages, the SAM can transition into an inflorescence meristem (IM) where the pattern of primordia initiation heavily influences inflorescence traits such as spikelet density; thus, factors that regulate the spatio-temporal pattern of primordia initiation is of tremendous

agronomic value. Auxin is a key growth regulator in plants and one of its roles in the plant is to control organ initiation and morphology. Part of that function is mediated through katanin and the severing of microtubules.

1.5.2 Auxin maxima precede primordium initiation at the SAM

Understanding the interaction of auxin and katanin in organ formation in the plant shoot requires some understanding of how auxin functions in the shoot apical meristem. Auxin transport is crucial for organ initiation. When auxin transport is inhibited – either by growing plants in auxin transport inhibitors such as *N*-1-naphthylphthalamic acid (NPA) or in mutants of genes such as *PIN1* (Okada et al., 1991), which encodes a transmembrane auxin efflux protein (Gälweiler et al., 1998; Petrásek et al., 2006) – *Arabidopsis* inflorescence stems become 'pin-shaped' due to an impairment in forming flowers. Exogenous application of auxin to the SAM rescues the ability to form lateral organs (Reinhardt et al., 2000). In fact, localized applications of auxin to the PZ leads to formation of primordia at the site of application suggesting that primordia formation is induced by auxin accumulation at incipient primordium sites; the size of the organ correlates with the concentration of exogenous auxin applied. Application of auxin to the center of the meristem leads to the formation of a ring of primordia surrounding the center of the meristem which itself remains devoid of primordia, suggesting that all parts of the PZ are capable of forming primordia when auxin is in excess, but functional differences between the PZ and the CZ prevents primordia initiation in the meristem center regardless of auxin level.

Monitoring of auxin accumulation patterns in the SAM using the auxin-responsive *DR5* promoter element controlling β-glucuronidase (GUS) or green fluorescent protein (GFP) expression confirmed directly that auxin gets transported to and accumulates at sites of incipient leaf and floral primordium initiation through a process called polar auxin transport (PAT) (Benková et al., 2003). Because of the phenotype of *pin1* mutants, the PIN1 efflux protein was suspected to be important for creating these auxin flux patterns that regulate phyllotaxis. Indeed, fluorescence-tagged PIN1 showed that PIN1 in the L1 layer (topmost layer) of the SAM localizes to the side

of each cell facing towards the incipient primordium, consistent with a role in directing auxin flow towards the incipient primordium (Reinhardt et al., 2003; Benková et al., 2003). At the site of incipient primordium, PIN1 cell localization is distributed on all sides of the cell to pool auxin at that location. After primordium outgrowth, PIN1 in the inner layers becomes polarized towards the base of the primordium where they may direct auxin back to the meristem and to new incipient primordia, while avoiding the L1 layer in the vicinity of the nascent primordium to prevent induction of ectopic primordia (Reinhardt et al., 2003).

The importance of PIN efflux proteins and their facilitation of PAT is likely to be conserved in maize (*Zea mays*). Dissected maize seedling SAM are unable to initiate any new leaf primordia when cultured in NPA-containing media but resume leaf initiation once transferred to media without NPA, suggesting that PAT in maize, as in *Arabidopsis*, is crucial for primordia initiation (Scanlon, 2003). Similarly, watering young plants in the process of developing tassels with NPA or hydroxyfluorene-9-carboxylic acid (HFCA), another PAT inhibitor, showed that PAT is required for initiation of branches and spikelets in the maize tassel (Wu and McSteen, 2007). Like *Arabidopsis*, auxin maxima precede the initiation of primordia in both the vegetative and reproductive phases of maize, as shown by *DR5*-modulated expression of red fluorescent protein (RFP) (Gallavotti et al., 2008). As in *Arabidopsis*, *PIN1* function is likely to be involved in creating the auxin flux pattern in maize meristems; fluorescence-tagged ZmPIN1a, a homolog of AtPIN1, is upregulated at incipient primordia and shows polar sub-cellular localization consistent with a role in directing and accumulating auxin at sites of primordia initiation.

1.5.3 Auxin-based inhibition of katanin activity at the SAM may help effectuate primordium outgrowth

Whereas the importance of PAT for signaling primordia initiation has been well-documented, relatively little progress has been made in identifying the mechanisms downstream of auxin maxima that actually effectuate primordia initiation. However, recent findings implicate the maintenance of CMT uniformity and orientation, involving

KTN1, in regulating primordia initiation (Hamant et al., 2008; Sassi et al., 2014). In the SAMs of wildtype untreated plants, CMT orientation is variable from cell to cell at the very top of the SAM but arranged in supra-cellular concentric circles around the SAM in the PZ (Hamant et al., 2008), and breakdown of this concentric CMT pattern at incipient primordium sites precedes primordia outgrowth and coincides with auxin maxima visualized using a *DR5* reporter (Sassi et al., 2014).

Looking at SAMs from the top down and measuring the angle between mean CMT orientation of individual cells and a radial line drawn from the meristem center to each cell, Sassi et al. (2014) quantified CMT orientations in the SAMs of NPA-induced 'pin-shaped' stems. As expected if auxin leads to disorganized CMTs in the SAM, the distribution of CMT orientations of individual cells in the SAM of wildtype NPA-grown plants were centered at 80° to 90°, but addition of auxin leads to random patterns with CMT orientations distributed roughly equally from 10° to 90°. In the SAMs of NPA-grown *ktn1* and *rop6* mutants (ROP6 interacts with KTN1, as discussed above), CMTs in the PZ of the SAM are not arranged concentrically and CMT organization does not respond to addition of auxin. Both before and after auxin application, distribution of CMT orientations in *ktn1* is spread roughly equivalently from 0° to 90°, while the distribution for *rop6* was skewed left but not distinctly centered at 80° to 90° like the wildtype and visually indistinguishable before and after auxin application. Thus, KTN1 and ROP6 functions are critical for maintaining the concentric arrangement of CMTs that are disrupted by exogenous auxin in the SAM of NPA-grown plants.

Consistent with the hypothesis that KTN1-mediated maintenance of the concentric CMT arrangement around the SAM inhibits primordia formation, NPA is much less effective at inhibiting primordia formation in the absence of functional KTN1 (Sassi et al., 2014). In wildtype NPA-grown plants, ~55% of plants initiated no flowers and ~2% initiated three or more flowers compared to ~10% and ~30% respectively for a *ktn1* mutant. Similarly, NPA was substantially less effective at inhibiting flower initiation in mutants of *RIC1* and *ROP6*, which interact with KTN1 as discussed above, or when MTs were disrupted chemically using oryzalin. Together, the findings by Sassi et al. (2014) suggest that concentric arrangements of CMTs around the meristem center of the

SAM inhibits primordia initiation and auxin maxima at incipient primordia may repress KTN1 activity leading to disorganized CMTs that allows outgrowth at that site. Interestingly, this model conflicts with the idea that auxin maxima induce the ROP6-RIC1-KTN1 pathway at indentation regions in the lobed pavement cells and may indicate different upstream auxin sensing and signaling elements that allow auxin to induce KTN1 activity in pavement cells but repress it at incipient primordia sites in the SAM.

1.6 Cortical microtubule patterns are directed by mechanical stress via a katanin-dependent mechanism and influence SAM morphology

CMTs in the SAM of *Arabidopsis* are arranged in specific patterns depending on the region of the meristem being observed (Hamant et al., 2008). As mentioned above, CMTs are not arranged in any predominant direction from cell to cell at the top of the SAM – but in the PZ, CMTs are aligned circumferentially around the circumference of the stem cylinder. Additionally, CMTs are aligned uniformly along the crease created at the boundary domain separating a growing primordium and the meristematic dome. Disruption of these CMT patterns by transferring plants to media containing oryzalin resulted in isotropic cells in the SAM as expected and also a failure to form the crease at the boundary domain (Hamant et al., 2008). The degree of curvature at the boundary domain is developmentally important – likely contributing to induction at the boundary domain of *SHOOT MERISTEMLESS* (*STM*), a homeobox transcription factor that is required at the boundary domain to allow organ separation and prevent organs that end up being fused to the stem (Landrein et al., 2015).

The CMT patterns at the SAM are likely to be heavily influenced by directions of maximal stress based on two chief observations (Hamant et al., 2008). First, although stress is difficult to measure specifically for the sub-regions of the SAM, modeling based on the geometry of the SAM predicts that stress, like CMTs, occurs equivalently in all directions at the top of the meristem. In contrast, at the boundary domain and around the lower parts of the meristem, predicted stress is anisotropic and mirror that of CMT patterns. Second, modifying stress patterns by ablating cells at the top of the meristematic dome or by compressing the SAM between two blades both produce new CMT patterns

that align in parallel with the new predicted stress directions. Together these two findings suggest that CMTs in the SAM tend to align in the same direction as maximal mechanical stress at the different regions of the SAM.

The mechanism of how mechanical stress is perceived and how it may cause changes in CMT orientation is not clear, but it involves the function of KTN1 (Uyttewaal et al., 2012). Compared to wildtype, CMTs in the SAMs of a loss-of-function *ktn1* mutant are much less effectively reoriented along new stress patterns created artificially such as by cell ablation and tissue compression. The combination of defective response to stress and the other functions of KTN1 discussed previously appears to cause major structural anomalies in the SAM of the *ktn1* mutant (Uyttewaal et al., 2012). The dome shape of the SAM is flattened and folding at the boundary domain is much less sharp in *ktn1* compared with wildtype. The distinctive concentric arrangement of CMTs in the PZ as described above is not present in *ktn1*, resembling the lack of cell to cell alignment in the CZ. For individual cells, CMT arrays are more isotropic, which predictably leads to reduced cell growth anisotropy and may partially explain the inability to maintain a dome-shaped meristem that presumably requires tight control of growth anisotropy.

Surprisingly for a genotype where control of cell growth is impaired, local growth variability calculated for each cell by comparing its growth rate with its immediate neighbors was substantially lower in the *ktn1* mutant (Uyttewaal et al., 2012). This suggests that local growth variability is developmentally important and may also contribute to the abnormal SAM shape in the *ktn1* mutant. In particular, local growth variability in the wildtype SAM is conspicuously higher at the boundary domain compared to adjacent cells on either the meristem or the primordium side; however, this variability is much weakened in the *ktn1* mutant and has been proposed to contribute to the defective folding at the boundary domain. Because the boundary domain is predicted to have highly anisotropic stress along the crease (Hamant et al., 2008), Uyttewaal et al. (2012) proposed that stress may instigate growth heterogeneity. Growing cells during initial outgrowth of a primordium creates stress by pulling on the cell walls of neighboring cells that are growing at slower rates, which may respond by depositing CMF along the direction of the stress to resist deformation. Following this idea,

Uyttewaal et al. (2012) further propose that reinforcing the slower growing cells against deformation creates additional stress which accelerates the growth of the fast growing cells even more due to the presumed role of stress in inducing growth heterogeneity. Thus, in this model, growth heterogeneity and mechanical stress create a positive feedback loop that could allow rapid growth rate changes that may be required to form sharp creases at boundary domains and allow for proper organ outgrowth.

1.7 Katanin function in other plants besides *Arabidopsis*

Mutant analyses of katanin p60 in plants have been reported only for *Arabidopsis* and, to a much lesser extent, rice (*Oryza sativa*), where the *AtKTN1* ortholog is named *dwarf and gladius leaf1* (*dgl1*). In general, the rice mutant *dgl1* has phenotypes that are analogous to many of those described above for *Arabidopsis*, with reduced plant height, compact organs and disorganized CMTs (Komorisono et al., 2005). The SAM appears to be shorter and narrower compared to wildtype rice, but these differences were not quantified. Although the size of floral organs is reduced, the effect of *dgl1* on panicle traits such as the density of flowers was not reported. Overall, there is a need to more carefully characterize mutants of *KTN1* homologs in other species, especially commercially important crops, because it is clear that katanin is crucial for controlling plant architecture and could thus have a large impact on crop yields.

The findings described in this work was centered around the maize (*Zea mays*) mutant *Clumped tassel1* (*Clt1*), which proved to be a dominant-negative allele in a maize ortholog of *AtKTN1*, of which there are two in the maize genome. Evidence will be described in Chapter 2 that are consistent with this *Clt1* allele encoding protein that inhibit the ATPase function of katanin complexes that it gets incorporated into. A dominant-negative allele such as this, which has never been identified in plants, could potentially be useful for inhibition of katanin function in specific tissues using a transgenic construct of *Clt1* controlled by tissue-specific promoters. As shown above, the functions of katanin are diverse and many are overlapping; it is possible that a more intricate understanding of katanin function can be obtained by inactivating katanin function in specific places or times. An example of such an experiment is proposed in

Chapter 2 of this work to decouple the predicted effects of maize katanin on meristem size and inhibition of primordia initiation.

Most effects of *Clt1* on plant and organ shape were reminiscent of those in *ktn1* and *dgl1* in *Arabidopsis* and rice respectively. However, the tassel meristem in *Clt1* heterozygotes were surprisingly wider than wildtype, whereas the SAM and ear meristem were shorter and narrower like the SAM in rice *dgl1*. Another surprising finding was uncovered in an enhancer-suppressor screen using the natural diversity among the founder lines of the Nested Association Mapping (NAM) population (McMullen et al., 2009); a novel *Clt1* phenotype was identified where the upper internodes were especially compressed compared with the lower internodes. Findings will be discussed in Chapter 3 that strongly suggest this modifier gene is caused by defects in the other *KTN1* ortholog in maize, which was named *ktn1b*. Comparison of nucleotide diversity based on whole-genome sequencing data from the maize HapMap3 project (Bukowski et al., 2015) indicated that purifying selection is stronger on *clt1* than *ktn1b* in maize. Consistent with this idea, a comparison with sorghum homologs suggests that promoter and intron regions in *ktn1b* have diverged more than *clt1* subsequent to the whole-genome duplication that created these two homoeologs. Overall, the findings in this work highlight key differences between *clt1* and *ktn1b* function in maize compared with *Arabidopsis KTN1*.

1.8 References

Baskin, T.I. (2001). On the alignment of cellulose microfibrils by cortical microtubules: A review and a model. Protoplasma **215**: 150–171.

Benková, E., Michniewicz, M., Sauer, M., Teichmann, T., Seifertová, D., Jürgens, G., and Friml, J. (2003). Local, Efflux-Dependent Auxin Gradients as a Common Module for Plant Organ Formation. Cell **115**: 591–602.

Bichet, A., Desnos, T., Turner, S., Grandjean, O., Hofte, H., and Höfte, H. (2001). BOTERO1 is required for normal orientation of cortical microtubules and anisotropic cell expansion in Arabidopsis. Plant J **25**: 137–148.

Borisy, G.G. (1967). The mechanism of action of colchicine: Binding of Colchincine-3H to Cellular Protein. J. Cell Biol. **34**: 525–533.

Bouquin, T., Mattsson, O., Naested, H., Foster, R., and Mundy, J. (2003). The Arabidopsis lue1 mutant defines a katanin p60 ortholog involved in hormonal control of microtubule orientation during cell growth. J Cell Sci **116**: 791–801.

Bringmann, M., Li, E., Sampathkumar, A., Kocabek, T., Hauser, M.-T., and Persson, S. (2012). POM-POM2/cellulose synthase interacting1 is essential for the functional association of cellulose synthase and microtubules in Arabidopsis. Plant Cell **24**: 163–77.

Bukowski, R. et al. (2015). Construction of the third generation Zea mays haplotype map (Cold Spring Harbor Labs Journals).

Burk, D.H., Liu, B., Zhong, R., Morrison, W.H., and Ye, Z.-H.H. (2001). A katanin-like protein regulates normal cell wall biosynthesis and cell elongation. Plant Cell **13**: 807–827.

Burk, D.H. and Ye, Z.H. (2002). Alteration of Oriented Deposition of Cellulose Microfibrils by Mutation of a Katanin-Like Microtubule-Severing Protein. Plant Cell **14**: 2145–2160.

Carlier, M.F., Hill, T.L., and Chen, Y. (1984). Interference of GTP hydrolysis in the mechanism of microtubule assembly: an experimental study. Proc. Natl. Acad. Sci. U. S. A. **81**: 771–5.

Carlier, M.F. and Pantaloni, D. (1981). Kinetic analysis of guanosine 5’-triphosphate hydrolysis associated with tubulin polymerization. Biochemistry **20**: 1918–1924.

Chan, J., Sambade, A., Calder, G., and Lloyd, C. (2009). Arabidopsis cortical microtubules are initiated along, as well as branching from, existing microtubules. Plant Cell **21**: 2298–306.

Confalonieri, F. and Duguet, M. (1995). A 200-amino acid ATPase module in search of a basic function. BioEssays **17**: 639–50.

Crowell, E.F., Bischoff, V., Desprez, T., Rolland, A., Stierhof, Y.-D., Schumacher, K., Gonneau, M., Höfte, H., and Vernhettes, S. (2009). Pausing of Golgi bodies on microtubules regulates secretion of cellulose synthase complexes in Arabidopsis. Plant Cell **21**: 1141–54.

Desai, A. and Mitchison, T.J. (1997). Microtubule polymerization dynamics. Annu. Rev. Cell Dev. Biol. **13**: 83–117.

Dixit, R. and Cyr, R. (2004). Encounters between dynamic cortical microtubules promote ordering of the cortical array through angle-dependent modifications of microtubule behavior. Plant Cell **16**: 3274–84.

Downing, K.H. and Nogales, E. (1998). Tubulin structure: insights into microtubule properties and functions. Curr. Opin. Struct. Biol. **8**: 785–91.

Flemming, W. (1880). Beiträge zur Kenntniss der Zelle und Ihrer Lebenserscheinungen. Arch. für Mikroskopische Anat. **18**: 151–259.

Fu, Y., Gu, Y., Zheng, Z., Wasteneys, G., and Yang, Z. (2005). Arabidopsis interdigitating cell growth requires two antagonistic pathways with opposing action on cell morphogenesis. Cell **120**: 687–700.

Fu, Y., Xu, T., Zhu, L., Wen, M., and Yang, Z. (2009). A ROP GTPase signaling pathway controls cortical microtubule ordering and cell expansion in Arabidopsis. Curr. Biol. **19**: 1827–32.

Fujita, M., Himmelspach, R., Hocart, C.H., Williamson, R.E., Mansfield, S.D., and Wasteneys, G.O. (2011). Cortical microtubules optimize cell-wall crystallinity to drive unidirectional growth in Arabidopsis. Plant J. **66**: 915–28.

Gallavotti, A., Yang, Y., Schmidt, R.J., and Jackson, D. (2008). The Relationship between auxin transport and maize branching. Plant Physiol. **147**: 1913–23.

Gälweiler, L., Guan, C., Müller, A., Wisman, E., Mendgen, K., Yephremov, A., and Palme, K. (1998). Regulation of Polar Auxin Transport by AtPIN1 in *Arabidopsis* Vascular Tissue. Science (80-.). **282**: 2226–2230.

Green, P.B. (1962). Mechanism for Plant Cellular Morphogenesis. Science **138**: 1404–5.

Gu, Y., Kaplinsky, N., Bringmann, M., Cobb, A., Carroll, A., Sampathkumar, A., Baskin, T.I., Persson, S., and Somerville, C.R. (2010). Identification of a cellulose synthase-associated protein required for cellulose biosynthesis. Proc. Natl. Acad. Sci. U. S. A. **107**: 12866–71.

Gutierrez, R., Lindeboom, J.J., Paredez, A.R., Emons, A.M.C., and Ehrhardt, D.W. (2009). Arabidopsis cortical microtubules position cellulose synthase delivery to the plasma membrane and interact with cellulose synthase trafficking compartments. Nat. Cell Biol. **11**: 797–806.

Hamant, O., Heisler, M.G., Jönsson, H., Krupinski, P., Uyttewaal, M., Bokov, P., Corson, F., Sahlin, P., Boudaoud, A., Meyerowitz, E.M., Couder, Y., and Traas, J. (2008). Developmental patterning by mechanical signals in Arabidopsis. Science **322**: 1650–5.

Hartman, J.J., Mahr, J., McNally, K., Okawa, K., Iwamatsu, A., Thomas, S., Cheesman, S., Heuser, J., Vale, R.D., and McNally, F.J. (1998). Katanin, a Microtubule-Severing Protein, Is a Novel AAA ATPase that Targets to the Centrosome Using a WD40-Containing Subunit. Cell **93**: 277–287.

Hartman, J.J. and Vale, R.D. (1999). Microtubule disassembly by ATP-dependent oligomerization of the AAA enzyme katanin. Science (80-.). **286**: 782–785.

Hill, J.L., Hammudi, M.B., and Tien, M. (2014). The Arabidopsis cellulose synthase complex: a proposed hexamer of CESA trimers in an equimolar stoichiometry. Plant Cell **26**: 4834–42.

Horio, T., Uzawa, S., Jung, M.K., Oakley, B.R., Tanaka, K., and Yanagida, M. (1991). The fission yeast gamma-tubulin is essential for mitosis and is localized at microtubule organizing centers. J. Cell Sci. **99**: 693–700.

Jung, G. and Wernicke, W. (1990). Cell shaping and microtubules in developing mesophyll of wheat (Triticum aestivum L.). Protoplasma **153**: 141–148.

Komorisono, M., Ueguchi-Tanaka, M., Aichi, I., Hasegawa, Y., Ashikari, M., Kitano, H., Matsuoka, M., and Sazuka, T. (2005). Analysis of the rice mutant dwarf and gladius leaf 1. Aberrant katanin-mediated microtubule organization causes up-regulation of gibberellin biosynthetic genes independently of gibberellin signaling. Plant Physiol. **138**: 1982–93.

Landrein, B. et al. (2015). Mechanical stress contributes to the expression of the STM homeobox gene in Arabidopsis shoot meristems. Elife **4**: e07811.

Ledbetter, M.C. and Porter, K.R. (1963). A “microtubule” in plant cell fine structure. J. Cell Biol. **19**: 239–250.

Ledbetter, M.C. and Porter, K.R. (1964). Morphology of Microtubules of Plant Cell. Science **144**: 872–4.

Li, S., Lei, L., Somerville, C.R., and Gu, Y. (2012). Cellulose synthase interactive protein 1 (CSI1) links microtubules and cellulose synthase complexes. Proc. Natl. Acad. Sci. U. S. A. **109**: 185–90.

Lin, D., Cao, L., Zhou, Z., Zhu, L., Ehrhardt, D., Yang, Z., and Fu, Y. (2013). Rho GTPase signaling activates microtubule severing to promote microtubule ordering in Arabidopsis. Curr. Biol. **23**: 290–7.

Lindeboom, J.J., Nakamura, M., Hibbel, A., Shundyak, K., Gutierrez, R., Ketelaar, T., Emons, A.M.C., Mulder, B.M., Kirik, V., and Ehrhardt, D.W. (2013). A mechanism for reorientation of cortical microtubule arrays driven by microtubule severing. Science (80-.). **342**: 1245533.

Margolis, R.L. and Wilson, L. (1978). Opposite end assembly and disassembly of microtubules at steady state in vitro. Cell **13**: 1–8.

McMullen, M.D. et al. (2009). Genetic properties of the maize nested association mapping population. Science **325**: 737–40.

McNally, F., Okawa, K., Iwamatsu, A., and Vale, R. (1996). Katanin, the microtubule-severing ATPase, is concentrated at centrosomes. J. Cell Sci. **109**: 561–567.

McNally, F.J. and Vale, R.D. (1993). Identification of katanin, an ATPase that severs and disassembles stable microtubules. Cell **75**: 419–429.

Meier, C., Bouquin, T., Nielsen, M.E., Raventos, D., Mattsson, O., Rocher, A., Schomburg, F., Amasino, R.M., and Mundy, J. (2001). Gibberellin response mutants identified by luciferase imaging. Plant J. **25**: 509–519.

Meza, I., Huang, B., and Bryan, J. (1972). Chemical heterogeneity of protofilaments forming the outer doublets from sea urchin flagella. Exp. Cell Res. **74**: 535–540.

Mitchison, T. and Kirschner, M. (1984). Dynamic instability of microtubule growth. Nature **312**: 237–242.

Murata, T., Sonobe, S., Baskin, T.I., Hyodo, S., Hasezawa, S., Nagata, T., Horio, T., and Hasebe, M. (2005). Microtubule-dependent microtubule nucleation based on recruitment of gamma-tubulin in higher plants. Nat. Cell Biol. **7**: 961–8.

Nakamura, M., Ehrhardt, D.W., and Hashimoto, T. (2010). Microtubule and katanin-dependent dynamics of microtubule nucleation complexes in the acentrosomal Arabidopsis cortical array. Nat. Cell Biol. **12**: 1064–70.

Nogales, E., Wolf, S.G., and Downing, K.H. (1998). Structure of the alpha beta tubulin dimer by electron crystallography. Nature **391**: 199–203.

Oakley, B.R., Oakley, C.E., Yoon, Y., and Jung, M.K. (1990). γ-tubulin is a component of the spindle pole body that is essential for microtubule function in Aspergillus nidulans. Cell **61**: 1289–1301.

Oakley, C.E. and Oakley, B.R. (1989). Identification of gamma-tubulin, a new member of the tubulin superfamily encoded by mipA gene of Aspergillus nidulans. Nature **338**: 662–4.

Okada, K., Ueda, J., Komaki, M.K., Bell, C.J., and Shimura, Y. (1991). Requirement of the Auxin Polar Transport System in Early Stages of Arabidopsis Floral Bud Formation. Plant Cell **3**: 677–684.

Panteris, E., Adamakis, I.-D.S., Voulgari, G., and Papadopoulou, G. (2011). A role for katanin in plant cell division: microtubule organization in dividing root cells of fra2 and lue1Arabidopsis thaliana mutants. Cytoskeleton (Hoboken). **68**: 401–13.

Paredez, A.R., Somerville, C.R., and Ehrhardt, D.W. (2006). Visualization of cellulose synthase demonstrates functional association with microtubules. Science **312**: 1491–5.

Petrásek, J. et al. (2006). PIN proteins perform a rate-limiting function in cellular auxin efflux. Science (80-.). **312**: 914–8.

Pickett-Heaps, J.D. and Northcote, D.H. (1966a). Cell Division in the Formation of the Stomatal Complex of the Young Leaves of Wheat. J. Cell Sci. **1**: 121–128.

Pickett-Heaps, J.D. and Northcote, D.H. (1966b). Organization of microtubules and endoplasmic reticulum during mitosis and cytokinesis in wheat meristems. J. Cell Sci. **1**: 109–20.

Ray, P.M., Green, P.B., and Cleland, R. (1972). Role of Turgor in Plant Cell Growth. Nature **239**: 163–164.

Reinhardt, D., Mandel, T., and Kuhlemeier, C. (2000). Auxin Regulates the Initiation and Radial Position of Plant Lateral Organs. Plant Cell **12**: 1–12.

Reinhardt, D., Pesce, E.-R., Stieger, P., Mandel, T., Baltensperger, K., Bennett, M., Traas, J., Friml, J., and Kuhlemeier, C. (2003). Regulation of phyllotaxis by polar auxin transport. Nature **426**: 255–60.

Sambade, A., Findlay, K., Schäffner, A.R., Lloyd, C.W., and Buschmann, H. (2014). Actin-Dependent and -Independent Functions of Cortical Microtubules in the Differentiation of Arabidopsis Leaf Trichomes. Plant Cell **26**: 1629–1644.

Sassi, M. et al. (2014). An auxin-mediated shift toward growth isotropy promotes organ formation at the shoot meristem in Arabidopsis. Curr. Biol. **24**: 2335–42.

Scanlon, M.J. (2003). The polar auxin transport inhibitor N-1-naphthylphthalamic acid disrupts leaf initiation, KNOX protein regulation, and formation of leaf margins in maize. Plant Physiol. **133**: 597–605.

Sugimoto, K. (2003). Mutation or Drug-Dependent Microtubule Disruption Causes Radial Swelling without Altering Parallel Cellulose Microfibril Deposition in Arabidopsis Root Cells. PLANT CELL ONLINE **15**: 1414–1429.

Uyttewaal, M., Burian, A., Alim, K., Landrein, B., Borowska-Wykręt, D., Dedieu, A., Peaucelle, A., Ludynia, M., Traas, J., Boudaoud, A., Kwiatkowska, D., and Hamant, O. (2012). Mechanical stress acts via katanin to amplify differences in growth rate between adjacent cells in Arabidopsis. Cell **149**: 439–51.

Webb, M., Jouannic, S., Foreman, J., Linstead, P., and Dolan, L. (2002). Cell specification in the Arabidopsis root epidermis requires the activity of ECTOPIC ROOT HAIR 3--a katanin-p60 protein. Development **129**: 123–31.

Weisenberg, R.C. (1972). Microtubule Formation in vitro in Solutions Containing Low Calcium Concentrations. Science (80-.). **177**: 1104–1105.

Wightman, R. and Turner, S.R. (2007). Severing at sites of microtubule crossover contributes to microtubule alignment in cortical arrays. Plant J. **52**: 742–51.

Wu, X. and McSteen, P. (2007). The role of auxin transport during inflorescence development in maize (Zea mays, Poaceae). Am. J. Bot. **94**: 1745–55.

Xu, T., Wen, M., Nagawa, S., Fu, Y., Chen, J.-G., Wu, M.-J., Perrot-Rechenmann, C., Friml, J., Jones, A.M., and Yang, Z. (2010). Cell surface- and rho GTPase-based auxin signaling controls cellular interdigitation in Arabidopsis. Cell **143**: 99–110.

Zhang, Q., Fishel, E., Bertroche, T., and Dixit, R. (2013). Microtubule severing at crossover sites by katanin generates ordered cortical microtubule arrays in Arabidopsis. Curr. Biol. **23**: 2191–5.

Zheng, Y., Wong, M.L., Alberts, B., and Mitchison, T. (1995). Nucleation of microtubule assembly by a gamma-tubulin-containing ring complex. Nature **378**: 578–83.

CHAPTER 2. CHARACTERIZATION AND MAPPING OF THE SEMI-DOMINANT MAIZE MUTANT *CLUMPED TASSEL1*

2.1 Introduction

The gene *KATANIN1* (*KTN1*) encoding the microtubule-severing p60 component of katanin has been studied using mutants in *Arabidopsis thaliana* and rice (*Oryza sativa*; the rice ortholog is named *dwarf and gladius leaf1*, *dgl1*), but not in any other plant species. In both species, loss of *KTN1* (or *dgl1*) function leads to shorter plant stature and more compact organs (Bichet et al., 2001; Burk et al., 2001; Komorisono et al., 2005). Examination of cellular structure in elongating tissue showed that cells in *ktn1* and *dgl1* mutants tend to be shorter and wider, and vary more in both shape and size compared to wildtype where cells are mostly uniformly rectangular (Bichet et al., 2001; Burk et al., 2001; Komorisono et al., 2005). These defects suggest a failure in anisotropic growth, which is cell growth that predominates in a particular direction leading to cells that are rectangular instead of spherical. The loss of anisotropic growth is likely a major reason for the decrease in plant height and reduction in organ size, though *KTN1* has also been implicated in allowing proper microtubule arrangements during the different mitotic stages (Panteris et al., 2011) and hormonal responses (Bouquin et al., 2003; Komorisono et al., 2005), which likely also affect the architecture of *ktn1* plants.

The role of *KTN1* in regulating anisotropic growth can be linked to its role in organizing cortical microtubules (CMTs). Internal turgor pressure drives cell growth by deforming the cell but this is counteracted by restrictive cellulose microfibrils (CMF) in the cell wall (Ray et al., 1972). The ability of CMFs to resist deformation is related to its deposition pattern (Green, 1962). Randomly organized CMFs make the cell wall equally susceptible to deformation in all directions, leading to isotropic growth and non-rectangular cells. Rectangular cells require CMFs that are uniformly arranged perpendicular to the main growth axis making the cell wall more susceptible to

longitudinal deformation but resistant to lateral expansion. These CMF patterns are correlated with the pattern of cortical microtubules which form a layer directly underneath the plasma membrane and are thought to guide the trajectories of cellulose synthase complexes (CesA) depositing CMFs in the cell wall (Paredez et al., 2006). Thus, organized CMTs promote the organized CMFs that are required for anisotropic growth.

The mechanism of the organization of the CMTs themselves is not fully understood, but studies in *Arabidopsis* indicate that *KTN1* is required. KTN1 preferentially severs microtubules where two non-parallel microtubules have intersected, called a crossover (Zhang et al., 2013). Severing at these crossover sites help increase parallel CMTs by promoting depolymerization or realignment of CMTs that are oriented differently from the predominant orientation (Wightman and Turner, 2007). As expected, *ktn1* mutants in *Arabidopsis* have disorganized CMTs and CMFs, which likely cause the non-rectangular cells described above (Burk et al., 2001).

While *KTN1/dgl1* in *Arabidopsis* and rice have no closely related paralogs, there are two *KTN1* co-orthologs in maize (*Zea mays*) (Figure 2.1A). In this chapter, results will be discussed that indicate the maize mutant *Clumped tassel1-1* (*Clt1-1*) is caused by a lesion in the Chr 8 paralog (GRMZM2G017305), which we have named *ktn1a*/*clt1*, and acts as a dominant negative allele. Consistent with functional redundancy between *clt1* and the Chr 3 *KTN1* paralog, which we have named *ktn1b* (GRMZM2G054715), a putative loss-of-function allele, *clt1-2*, has no effect unless combined with the dominant negative allele, *Clt1-1*. Based on these results, a model will be presented that proposes a molecular mechanism for the *Clt1-1* and *clt1-2* alleles. The effects of *Clt1-1* on plant morphology, organ shape and meristem size will also be presented and discussed.

2.2 Materials and Methods

2.2.1 Phylogenetic analysis of plant *AtKTN1* orthologs

Closely related homologs of AtKTN1 were identified by a BLAST search on Phytozome (Goodstein et al., 2012) using AtKTN1 protein sequence against the predicted proteomes of *Arabidopsis thaliana* TAIR10 (to confirm lack of closely related paralogs)

and grass species consisting of *Zea mays* AGPv3, *Sorghum bicolor* v3.1, *Setaria italica* v2.2 and *Brachypodium distachyon* v3.1. Sequences included in this analysis had alignment scores ranging from 670 to 806, while the next highest hit had an alignment score of only 282 and homology only around the ATPases Associated to a variety of cellular Activities (AAA) family ATPase domain, which is conserved in proteins besides katanin p60 (Confalonieri and Duguet, 1995).

Predicted coding sequences were loaded into MEGA7 (Kumar et al., 2016), where they were aligned using the MUSCLE algorithm (Edgar, 2004) and used to calculate a maximum likelihood tree.

2.2.2 Genetic stock

The *Clt1-1* mutant was generated via ethyl methanesulfonate (EMS) pollen mutagenesis in an unknown genetic background by Drs. M. G. Neuffer and K. A. Sheridan. Seed stock was obtained for this work through the Maize Genetics Cooperation Stock Center and from Dr. Peter Bommert who kindly gifted a stock of *Clt1-1* that had been backcrossed 8 times into B73.

A mutant named *discordia3* (*dcd3*) was identified by Dr. Laurie Smith in an EMS mutagenesis screen for defective asymmetric cell divisions in leaf stomata and was propagated by Dr. Amanda Wright. Wright mapped *dcd3* to regions on Chr 8 and Chr3, containing *ktn1a* and *ktn1b* respectively, that must both be *dcd3* to observe the mutant phenotype (personal communication). Wright also conducted sequencing that uncovered a 1 bp deletion in *ktn1a* in the *dcd3* mutant, which will be referred to as *clt1-2* for the rest of this work. Several missense polymorphisms were found in *ktn1b-dcd3* but no obvious causative lesion was identified. The *dcd3* stock provided by Wright had been backcrossed 4 times with B73.

Wildtype Columbia-0 (Col-0) seed was obtained from the lab of Dr. Tesfaye Mengiste. Seed stock of the *LUCIFERASE super expressor1* (*lue1*) allele of *KTN1*, caused by a nonsense mutation, was obtained from the *Arabidopsis* Biological Resource Center (ABRC; Columbus, Ohio). *Agrobacterium tumefaciens* strain GV3101::pMP90

was obtained from Dr. Stan Gelvin. The binary vector pCB302 (Xiang et al., 1999) was obtained from Dr. Bob Pruitt.

2.2.3 Plant growth

For maize, mature plant measurements for *Clt1-1* single mutants were done on plants grown in the field in West Lafayette, Indiana during the summer. All meristem data and the data from the cross between *Clt1-1* and *clt1-2* were obtained from plants grown in the greenhouse under 16 hour days, daytime temperatures 28-32°C and nighttime temperatures 18-22°C.

For *Arabidopsis*, all plants were grown in a growth chamber under 16 hours of light and 24°C temperature. The soil substrate was Redi-Earth supplemented with a few pellets of Osmocote fertilizer around each plant.

2.2.4 Phenotypic measurements

For maize, plant height was measured from the ground to the ligule of the flag leaf blade. Internode lengths were estimated by measuring the vertical distance between the ligules of leaves originating from nodes flanking that internode. Internodes 1, 2, 3, 7, 8 and 9, counted from the tassel, were measured in this fashion. Leaf length was measured from the ligule to the tip for the 5th leaf from the tassel. Leaf width was also measured for the 5th leaf from the tassel from one leaf margin to the other at the widest point of the leaf and perpendicular to the mid-vein. Tassel length was measured from the lowest tassel branch to the tip of the tassel rachis. Rachis length was measured from the highest branch to the tip of the rachis. Spikelet density per cm was estimated by cutting off the top 2cm of the tassel rachis, counting the number of spikelets in the 5cm region below that and dividing by 5.

For *Arabidopsis* transformed with maize *clt1* constructs, siliques were measured from the most distal 10-12 fully elongated siliques from the ends of 4 inflorescences, totaling at least 38 siliques per plant at the onset of senescence. Using a camera at a fixed distance from the specimen, an image was captured for the siliques of each plant and ImageJ was used to measure the lengths of each silique.

2.2.5 Leaf epidermal impressions

A thick layer of clear nail polish was applied to the adaxial surface of a particular leaf, as specified in the figures, for each plant. The location on the leaf was at roughly mid-length between the ligule and leaf tip, and mid-way between the leaf margin and the left or right side of the mid-vein. The nail polish was allowed to dry for at least 2 hours, removed using clear packing tape and adhered to a microscope slide. Images were captured using a standard light microscope connected to a camera.

2.2.6 Scanning electron microscopy of tassel and ear primordia

Tassels were dissected 5 weeks after planting when most tassels were 1-3 mm long for both wildtype and *Clt1-1*/+ plants. Plants outside of this range were not measured. Ears were dissected 6 weeks after planting for wildtype plants and 4 days later for *Clt1-1*/+ plants so that the lengths of ears observed for both genotypes were between 1-3 mm.

For both tissue types, primordia were dissected and immediately immersed in ice-cold FAA consisting of 3.7% formalin, 50% ethanol and 10% acetic acid. A vacuum was applied briefly to expedite infiltration. Fixation was carried out overnight at 4°C. Tissue were dehydrated by ethanol series, CO_2 critical point dried and sputter-coated with platinum. SEM visualization was done using an FEI NanoSEM 200 at 5 kV accelerating voltage.

2.2.7 Dissection of shoot apical meristems (SAM)

Approximately 1 mm thick tissue blocks, containing the SAM, were dissected from seedlings 14 days after planting (Jackson and Hake, 1999). Tissue were fixed in FAA overnight, dehydrated by an ethanol series, transferred to 1:1 ethanol: methyl salicylate and then finally to 100% methyl salicylate. After at least 6 hours of clearing, the tissue blocks were placed on microscope slides and imaged using a light microscope.

2.2.8 Positional cloning of *Clt1-1*

Previous work using translocation lines mapped *Clt1-1* to a 21.8 Mb interval on the long arm of chromosome 8 (MaizeGDB; Andorf et al., 2016). In this work, the *Clt1-1* interval was first refined by genotyping the B73-introgressed stock of *Clt1-1* with SNP markers spanning this 21.8 Mb interval to delineate the non-B73 linkage block containing *Clt1-1*. Twenty one SNP markers where 22/26 or more Nested Association Mapping (NAM) founder lines had a different genotype from B73 were chosen from the maize HapMap1 dataset (Gore et al., 2009) to maximize the probability of getting a marker polymorphic between B73 and the unknown progenitor background of *Clt1-1*. Flanking sequences were sent to LGC genomics (formerly KBioscience) for KASP assays to be designed and made.

KASP assays are based on having two allele-specific primers attached to quenched fluorophores with different excitation and emission wavelengths that compete to amplify with a common gene-specific reverse primer. Amplification eliminates quenching of the fluorophore of a particular primer and the final fluorescence signals of individual samples after PCR indicate their genotypes. KASP assays were run according to the manufacturer's instructions, on a Roche LightCycler 480. Of the 21 markers (Table 2.1), only 15 markers could successfully assay the SNP, with the others producing ambiguous results between B73 and positive controls, MS71 and CML333, which were reported in the HapMap1 dataset to be polymorphic with B73 at those SNPs (Table 2.2).

Genotyping 3 *Clt1-1*/+ and 3 wildtype plants from a cross between B73 x *Clt1-1*/+ (BC9 to B73) identified a 6.6 Mb non-B73 linkage block within the original 21.8 Mb interval (Table 2.2). Subsequently, 2 more polymorphic KASP assays were made for SNPs (ss230245925 and ss230245955) within this reduced region, and a mapping population of 259 plants from B73 x *Clt1-1*/+ (BC9 or BC10 to B73) crosses was used to fine-map *Clt1-1* to an even smaller interval. Mutants that genotyped as homozygous B73 or wildtype siblings that genotyped as heterozygous were counted as recombinants for that marker. The final two recombinants with the closest right-flanking breakpoints were confirmed to be *Clt1-1*/+ at *ktn1a* using the *Clt1-1* DraI dCAP marker described below,

consistent with their mutant phenotype. This test was needed in the absence of a left-flanking marker and verified that *ktn1a* was still within the mapped interval.

2.2.9 Next-generation sequencing (NGS) of *Clt1-1*

Genomic DNA was isolated from 2 *Clt1-1* homozygous plants (BC9 to B73) and sent to the Yale Center for Genome Analysis (West Haven, CT) where a barcoded library was created for each sample and sequenced together on a single lane using a HiSeq 2500. FASTQ files were returned and then analyzed as described below. Sequence reads were first trimmed to remove barcode sequences using Trimmomatic (Bolger et al., 2014), then aligned to the reference genome B73 AGPv3.21 using the 'mem' algorithm in Burrows-Wheeler Aligner (BWA-MEM; Li, 2013). The resulting Sequence Alignment/Map (SAM) files were converted to BAM (binary version of SAM) files using Picard tools (http://picard.sourceforge.net) which also marked reads that were PCR duplicates. BAM files were processed with Genome Analysis Toolkit (GATK; McKenna et al., 2010) using the recommended steps (DePristo et al., 2011; Van der Auwera et al., 2013), and known variant sites from HapMap2 (Chia et al., 2012) for calibration, to result in a variant calls format (VCF) file containing the variant sites called between the samples and the reference. The number of variant sites called in 300 kb non-overlapping windows along Chr 8 was counted using VCFtools (https://sourceforge.net/projects/vcftools/) to support results from positional cloning.

This VCF file was processed with SNPEff (Cingolani et al., 2012), which was used to annotate variant sites with predicted effects on splice sites and protein sequence after filtering for variant sites that are not listed in a dataset of known variant sites (HapMap2), variants occurring within exons or introns (to include splice site mutations), only G to A or C to T SNPs which are characteristic of EMS-induced mutations, 5x or greater depth in at least one of the samples, quality score (QUAL) 30 or greater, root mean square of mapping quality (MQ) 40 or greater and homozygosity for the variant allele in both samples. Strand bias was not globally filtered against but was checked for the candidate gene identified as reported in the results section. Impact of a missense SNP on protein function was predicted using the bioinformatics tool Sorting Intolerant From

Tolerant (SIFT; Ng and Henikoff, 2001, 2003) which uses sequence homology as an indicator of the importance of each amino acid. Finally, Sanger sequencing using BigDye (Applied Biosystems) was carried out for the entire genomic sequence of GRMZM2G017305 (see Table 2.3 for primer sequences)

2.2.10 Genotyping of maize *Clt1-1* and *Arabidopsis ktn1-lue1*

Using the online tool dCAPS finder 2.0 (Neff et al., 2002), a derived Cleaved Amplified Polymorphic Sequences (dCAPS) assay was designed that directly genotypes the C to T substitution causing the serine to phenylalanine change in *Clt1-1*. The forward primer is 5'-TAATTTTCCTAGATGTTGCTCGTGT-3' and the reverse primer is 5'-ACCATCAATTTGCACTAGAAGTTTA-3' where the underlined base is modified from the actual sequence in order to form a DraI restriction site in the presence of the *Clt1-1* SNP. For the *Arabidopsis* transformation experiment, an exon-binding forward primer was designed, 5'-TAATGTTTCCTCTGCAACACTGG-3', which is compatible with the above reverse primer and also produces amplicons that are cut by DraI for the *Clt1-1* allele only. The *ktn1-lue1* lesion was genotyped using forward primer 5'-ATTGGCAGCTACCAACTTCCCGCG-3' and reverse primer 5'-TGCGTTGGACCAGTAGAGAG-3' where the underlined base in the forward primer is modified from the actual sequence in order to form a SacII restriction site in the Col-0 allele but not in *ktn1-lue1*.

2.2.11 Expression cassettes of maize *clt1* alleles and transformation into *Arabidopsis*

To test the effect of maize *Clt1-1* and *clt1-B73* in *Arabidopsis*, the coding sequence (CDS) of each allele was cloned and positioned between the *Arabidopsis KTN1* promoter and 5'UTR on the 5' end, and the *Arabidopsis KTN1* 3'UTR and 3' downstream region on the 3' end to account for potential species-specific regulation. The left end of the 5' regulatory region and the right end of the 3' regulatory region were chosen based on a successful complementation experiment using the entire genomic region of *KTN1* in Bouquin et al. (2003). Overexpression of the constructs was not attempted because overexpression of *KTN1* in *Arabidopsis* causes defects similar to loss

of *KTN1* function (Bouquin et al., 2003). The specific steps undertaken to produce this construct is described below.

Using RNA from ~1 cm long developing tassels of *Clt1-1*/+ (B73) plants, cDNA was produced using an oligo-dT primer and SuperScriptIII reverse transcriptase (Invitrogen). *Clt1-1* and *clt1-B73* cDNA were first amplified using external nested primers 5'-ACACTGCACGTGTACGAACCTA-3' and 5'-TGAGATACGTTTGACAGCAGAAA-3' to avoid amplifying *ktn1b*. To splice together the *Arabidopsis KTN1* 5' regulatory sequence with maize *clt1* CDS with no intervening base pairs, overlap-extension of PCR products was employed (Heckman and Pease, 2007). The *Arabidopsis* 5' regulatory sequence was amplified from Col-0 genomic DNA using a forward primer with an EcoRI restriction site on the 5' end to facilitate cloning, 5'-GCATGAATTCATTGTTGGTCCTGGCCAGTCA-3', and a reverse primer 5'-CCATTTCCTCTTTTACTAAAAAAATAGCCTATTCCAA-3'. The maize CDS was amplified from the external nested PCR product using a forward primer 5'-TTGGAATAGGCTATTTTTTTAGTAAAAGAGGAAATGGCGAATCCCCTAGCG-3' where the first 33 bp are identical to the last 33 bp of the *Arabidopsis* 5' regulatory sequence and a reverse primer with a SacII restriction site on the 5' end to facilitate cloning 5'-GCATCCGCGGTCAGGCAGACCCAAACTCAG. Next, the PCR products from the two reactions were purified and equimolar amounts of each were combined for the overlap PCR using the forward primer that amplified the 5' regulatory region of *KTN1* and the reverse primer that amplified the *clt1* CDS. The resulting fusion PCR product was gel-purified and cloned into an *E. coli* plasmid pPICZαA (Invitrogen) using the EcoRI and SacII sites.

The 3' regulatory region of *KTN1* was amplified using a forward primer with a SacII site 5'-GCATCCGCGGTTAAACCCACTTTTTTTAATTTAGTGTCAAAAGATGTGT-3' and a reverse primer with an XbaI site 5'-GCATTCTAGAACATCCGGAGTCCTCCTTAGC-3'. The product of this PCR was subcloned downstream of the *clt1* CDS in the fusion construct. All amplifications were done using proof-reading Phusion polymerase (New England BioLabs) and constructs

were sequenced by BigDye reactions (see Table 2.3 for primer sequences) to ensure there were no PCR errors. The three-component construct was then cut out and cloned into the binary vector pCB302 using EcoRI and XbaI to digest both insert and vector. The pCB302 vector containing the construct was then transformed into *Agrobacterium* strain GV3101::pMP90 using the 'freeze-thaw' method (Höfgen and Willmitzer, 1988) as modified by Weigel and Glazebrook (2002). This was used to transform Col-0 and *ktn1-lue1 Arabidopsis* plants using the floral dip method (Clough and Bent, 1998). Seedling transformants were screened by spraying with 0.006% glufosinate and then transplanted to individual pots. Subsequently, successful transformation was further verified by PCR using primers specific for maize *clt1*.

2.2.12 Testing for interaction between *Clt1-1* and *clt1-2*

To test for interaction between *Clt1-1* and *clt1-2*, *clt1-2*/+ was crossed to *Clt1-1*/+. To avoid potential confounding effects from the Chr 3 *dcd3* mutation, *clt1-2*/+; +/+ plants were identified by genotyping the F2 progeny of a double heterozygous *dcd3* plant for crossing to *Clt1-1*/+. To genotype *clt1-2*, the forward primer 5'-AAGCAAGAATGTATCATTCTGC-3' and the reverse primer 5'-TGAACCTATGCATATTCCAGG-3' were used to amplify a region within *clt1*. The resulting amplicon is cut by MspI in the B73 allele but not in the *dcd3* allele. To genotype the Chr 3 *KTN1* paralog, the forward primer 5'-CGTTGGAATCTCTGCCGCTA-3' and the reverse primer 5'- ATGAAAACCGTTGCCGTGAG-3' were used to amplify a portion of the *ktn1b* promoter region. The resulting amplicon is cut by SspI in the *dcd3* allele but not in the B73 allele.

2.3 Results

2.3.1 Putative orthologs of *AtKTN1* among maize and its close relatives

Phylogenetic analysis of *AtKTN1*-like genes among different grass species indicated that there are two orthologs within sorghum and maize (Figure 2.1A). In contrast, there is only one katanin p60 ortholog in *Setaria italica* (Seita.5G273100),

which is basal to maize and sorghum both in this analysis of the katanin gene only and in a whole-genome phylogeny of several grass species (Zhang et al., 2012), suggesting that the duplicate genes in maize and sorghum were created after the split from *Setaria italica*. However, separate duplications within sorghum and maize likely created these two pairs of paralogs because the two sorghum paralogs (Sobic.003G259400 and Sobic.010G114200) form a highly supported clade between themselves (Figure 2.1A).

The two maize katanin p60 paralogs occur on Chr 3 and Chr 8, which share large regions of synteny with sorghum Chr 3, containing Sobic.003G259400, but not Chr 10 containing Sobic.010G114200 (Figure 2.1B). Previous work by other researchers found that these two maize syntenic blocks have low synonymous mutation rates compared with sorghum Chr 3, suggesting they were created by a recent maize-specific whole-genome duplication and not by earlier whole-genome duplication events that predate the divergence of maize and sorghum (Schnable et al., 2011). In summary, these results are most consistent with a scenario where maize *clt1* and *ktn1b* are orthologous to Sobic.003G259400 and created by the maize-specific whole-genome duplication, while Sobic.010G114200 was created by a sorghum-specific gene duplication.

2.3.2 The *Clt1-1* phenotype

Clt1-1 is a semi-dominant mutant, with phenotypic defects in general being more severe in the homozygote. Multiple traits are affected in *Clt1-1* and the overall phenotype is reminiscent of the *ktn1* mutants in *Arabidopsis* and rice with reduced plant stature and more compact shapes to most organs (Bichet et al., 2001; Burk et al., 2001; Komorisono et al., 2005). Plant height of the *Clt1-1* homozygote was approximately one quarter that of the wildtype plant (Figure 2.2A) and shortened internodes contributed greatly to this with the internodes of homozygotes estimated by leaf distance being between 16-40% compared to wildtype depending on the internode being observed (Figure 2.2B). Leaves in the mutant were both shorter and narrower, and had leaf tips with wider angles (Table 2.4; Figure 2.2C). Leaf epidermal cells showed dramatic patterning defects in the *Clt1-1* homozygote (Figure 2.2D). Cell files were meandering instead of straight as observed in the wildtype and heterozygous mutant (Figure 2.2D). Whereas wildtype cells were of a

uniform size and rectangular, cells in the homozygous mutant were shorter in general but varied widely in both size and shape. The subsidiary cells that flank the guard cells of stomata were often deformed, indicating defective asymmetric cell divisions that normally create the subsidiary cell and an adjacent pavement cell that is larger. The shorter cells in the *Clt1-1* homozygote suggests that *Clt1-1* causes defects in cell elongation, while the abnormal cell shapes and non-linear cell files suggest that proper placement of cell division planes is also impaired.

The *Clt1-1* tassel was shorter due to reduced length of the main rachis and branches, and also due to shorter spacing between tassel branches (Figure 2.3A). Pedicels, glumes and anthers were all shorter in *Clt1-1*/+ spikelets than wildtype (Figure 2.3B). Spikelet density in the *Clt1-1* heterozygote was ~58% higher than wildtype (Figure 2.3C). In a B73 inbred background, the *Clt1-1* homozygote typically do not make functional tassels and fail to make any spikelets (Figure 2.3A). When *Clt1-1* is outcrossed to other backgrounds, *Clt1-1* homozygotes can make very small tassels possibly because of reduced inbreeding depression (Figure 2.3D). These tassels had even higher spikelet density than the heterozygote but pollen shed was weak and anthers were smaller (Figure 2.3E). *Clt1-1* heterozygotes often do not make ears especially in an inbred B73 background and *Clt1-1* homozygotes never made ears in either inbred B73 or mixed backgrounds. The ears of *Clt1-1* heterozygotes were shorter than wildtype, had disorganized kernel rows and poor seed set (Figure 2.3F). In contrast to the cylindrical shape of wildtype ears, *Clt1-1*/+ ears were sometimes flattened, especially at the tip (Figure 2.3G). Like the tassels, ears were more vigorous in outcrossed plants but remained shorter than wildtype with disorganized kernel rows and flattened tips (Figure 2.3H,I).

Larger meristems in several plant species have been shown to increase organ initiation, and in maize, enlarged inflorescence meristems often lead to increased kernel row number in the ear and higher spikelet density in the tassel (reviewed in Pautler et al., 2013). Thus, we examined the meristems of tassel primordia in *Clt1-1*/+ plants using scanning electron microscopy (SEM) (Figure 2.4A) to explore whether meristem size is involved in the increased spikelet density of *Clt1-1* tassels. Indeed, the tassel meristems

of *Clt1-1*/+ plants were ~32% wider than wildtype (Figure 2.4B). On the other hand, ear and SAM width were comparable between *Clt1-1*/+ mutants and wildtype (Figure 2.4C,D). In contrast to meristem width, meristem height was reduced in all three tissues examined (Figure 2.4A-D).

2.3.3 Mapping *Clt1-1* to a lesion in an ortholog of *KTN1* on Chr 8

Previous work mapped *Clt1-1* to a 21.8 Mb interval on the long arm of chromosome 8, data which is publicly available (MaizeGDB; Andorf et al., 2016). To refine the interval for *Clt1-1*, the non-B73 linkage block containing *Clt1-1* in a B73 introgression was delineated. A ~6.6 Mb region was identified that was interspersed with markers that genotyped as heterozygous and was flanked by regions genotyping as B73 homozygous in *Clt1-1* heterozygotes (Table 2.2). Subsequently, more individuals from a B73 x *Clt1-1*/+ (B73) cross were genotyped and identification of recombinants reduced the *Clt1-1* interval further with a new right flanking marker, ss230245925, at 150,879,259 bp (Figure 2.5A). No polymorphic markers could be identified to demarcate the left boundary of the non-B73 linkage block, even with the testing of two additional markers (ss230245196 and ss230245225) at the putative left boundary. A potential explanation is that *Clt1-1* is very close to the left boundary of the linkage block. Considering that lack of polymorphism between the *Clt1-1* progenitor background and B73 at a particular marker could not be differentiated from bona fide homozygosity for B73, marker ss230245130 was taken as the putative left boundary instead of the closest "B73-fixed" marker. This produced an interval containing 16 genes that could underlie *Clt1-1*, including *ktn1a*.

To identify the causative lesion among these 16 genes, genomic DNA from two *Clt1-1* homozygotes in a B73 background were sequenced. After aligning the reads to B73 AGPv3.21, average per base coverages of 6.4x and 6.7x were achieved for the two *Clt1-1* samples for reads aligned to chromosomal DNA. After applying filters as described in the methods, the only mutation within the interval delineated by positional cloning that affected the CDS of any gene was a single missense mutation in GRMZM2G017305 (*ktn1a*; Chr 8:150,792,636-150,799,106). This variant site had a

Phred-scaled P-value from Fisher's exact test for strand bias (FS) of 0 indicating no strand bias during sequencing. This mutation, a C to T transition, causes a serine to phenylalanine change in the ATPase domain of *ktn1a* (Figure 2.5B) and was predicted to be deleterious by SIFT with a score of 0. This SNP was confirmed by both a dCAPS marker (Figure 2.5C) and Sanger sequencing, which also showed that there is 100% identity with B73 at all other positions, including the 5' UTR, exons, introns and the part of the 3' UTR that was sequenced (Appendix A). Tracking the non-B73 linkage block containing *Clt1-1* by plotting the number of variant calls in genomic windows along Chr 8 (Figure 2.5D) was consistent with the interval obtained through positional cloning. In support of *Clt1-1* being very close to the left boundary of the *Clt1-1* linkage block, the location of *ktn1a*—the putative causative gene—coincided with a region of sharply reduced number of variant sites.

2.3.4 Transformation of *Clt1-1* and *clt1-B73* into *Arabidopsis*

Transforming *Clt1-1* and *clt1-B73* into Col-0 *Arabidopsis* showed that *Clt1-1* has a dominant effect causing siliques to be shorter and wider in T1 plants, similar to siliques obtained from *Arabidopsis ktn1-lue1* plants which have defective *KTN1* (Figure 2.6A). Of the 9 transformants recovered for the B73 allele, none produced such shortened siliques. Six out of the 13 transformants for *Clt1-1* produced siliques that were significantly shorter than the shortest *clt1-B73* plant (Figure 2.6B). The *Clt1-1* transformants that did not produce substantially shortened siliques might have landed in genomic regions that caused weak transcription but this was not tested. Interestingly, features such as inflorescence height and leaf shape were not obviously different between the transformants with the *Clt1-1* allele and the *clt1-B73* allele (not shown) suggesting that *Clt1-1* has a stronger effect in *Arabidopsis* siliques than other tissue types for unknown reasons. Genotype of the transformed construct, either *clt1-B73* or *Clt1-1*, was verified by PCR to be the correct genotype in all events except for event #8 for *Clt1-1* which amplified poorly (Figure 2.6C,D). Note that the primers designed for the maize construct does not amplify genomic DNA from untransformed Col-0 indicating specificity for the transgenic construct.

Transformations of the same constructs into *ktn1-lue1 Arabidopsis*, which produce truncated KTN1 due to a premature stop codon (Bouquin et al., 2003), showed that function is conserved between *ktn1a* in maize and *KTN1* in *Arabidopsis*. The *clt1-B73* allele was sufficient for restoring plant height and silique length in 3 out of 4 PCR-validated T1 *ktn1-lue1* plants (Figure 2.7B,C). Pollen or seed contamination was ruled out by PCR confirmation that all plants were still homozygous for *ktn1-lue1* at the native *KTN1* gene (Figure 2.7D). Conversely, *Clt1-1* was unable to complement *ktn1-lue1* in all 8 PCR-validated transformants suggesting that normal function is lost in this allele (Figure 2.7A,C-D).

2.3.5 Cross between *Clt1-1* and *clt1-2* shows synergistic interaction

Further support for *ktn1a* being the causative gene of *Clt1-1* came from a second *ktn1a* allele. This allele, *clt1-2*, was discovered in a mutant called *dcd3* that produces a mild phenotype, resembling *Clt1-1*/+ plants (Figure 2.8A-D), when homozygous for *clt1-2* and a Chr 3 locus that contains *ktn1b*. The *dcd3* allele of *ktn1b* has several missense polymorphisms compared with B73 but no obvious causative lesion. The *clt1-2* allele has a 1bp deletion that causes a frameshift near the 3' end (Figure 2.8E). The *Arabidopsis fragile fiber2* (*fra2*) allele of *KTN1* is caused by a 1 bp deletion that occurs downstream of the position corresponding to this *clt1-2* lesion (Burk et al., 2001). Since *fra2* causes a strong mutant phenotype, *clt1-2* is likely to be deleterious also. Furthermore, the frameshift changes the sequence of a domain required for oligomerization of a related enzyme called VACUOLAR PROTEIN SORTING4 (VPS4; see discussion).

Unlike *Clt1-1*, *clt1-2* mutants with wildtype *ktn1b* were indistinguishable from wildtype plants even when homozygous (not shown) potentially due to redundant function from its homoeolog, *ktn1b*. However, combining *clt1-2* with *Clt1-1* results in a synergistic effect. The overall plant shape and stature of *Clt1-1*/*clt1-2* heterozygotes resembled *Clt1-1* homozygotes (Figure 2.9A,B). *Clt1-1* homozygotes produced healthier tassels in the greenhouse than in the field (Figure 2.3A), and these were also similar to the tassels produced by *Clt1-1*/*clt1-2* plants with both being very short and having high spikelet density (Figure 2.9C). Like *Clt1-1* homozygotes, *Clt1-1*/*clt1-2* heterozygotes

produced more non-rectangular pavement cells and deformed stomatal subsidiary cells in the leaf epidermis than *Clt1-1*/+ or homozygous wildtype (Figure 2.9D-F). Plant height, leaf length and central rachis length all were consistent with a synergistic interaction between *Clt1-1* and *clt-2*, with the *clt1-2* allele having a significant effect only when combined with *Clt1-1* (Figure 2.9G-I).

2.4 Discussion

2.4.1 A model for the mechanisms of the *Clt1-1* and *clt1-2* mutations

Functional katanin is composed of hexamers of KTN1 sub-units (Hartman et al., 1998; Hartman and Vale, 1999). Such protein homo-multimers are vulnerable to the formation of dominant-negative mutations due to 'poisoning' effects of non-functional subunits on the overall function of the complex. This work is the first report of a dominant-negative allele of *KTN1* in plants, though there have been reports of similar alleles generated by site-directed mutagenesis of sea urchin and human *KTN1* cDNA (Hartman and Vale, 1999; McNally et al., 2000). Interestingly, these alleles were also missense mutations in the ATPase domain, at two different positions though both were at different residues than the *Clt1-1* lesion. In vitro experiments showed that these mutant forms of KTN1 are unable to sever microtubules (McNally et al., 2000), unable to hydrolyze adenosine triphosphate (ATP) and form relatively stable KTN1 oligomers in the presence of ATP compared with wildtype KTN1 oligomers which are transient (Hartman and Vale, 1999). Hartman and Vale (1999) proposed that in the presence of ATP, KTN1 subunits will form hexamers that bind to microtubules and the hydrolysis of ATP causes both microtubule severing and de-oligomerization of the KTN1 hexamer. Thus, wildtype KTN1 subunits once bound to KTN1 subunits with defective ATPase domains may become stably oligomerized and unable to sever microtubules due to defects in hydrolyzing ATP, providing a potential mechanism for the dominant-negative effect of *Clt1-1* in maize (Figure 2.10).

The *clt1-2* allele works by a different mechanism than *Clt1-1* because there are no visible defects even in *clt1-2* homozygotes. The affected residues in the *clt1-2* allele

correspond to a domain that is essential for homo-oligomerization of VPS4 (Vajjhala et al., 2006), an enzyme involved in endosomal trafficking and is a member of the ATPases Associated to a variety of cellular Activities (AAA) superfamily (Confalonieri and Duguet, 1995) that includes KTN1. In *Saccharomyces cerevisiae* VPS4, disruption of the C-terminal oligomerization domain and utilizing this disrupted isoform as both bait and prey in a yeast two-hybrid experiment produces no interaction suggesting that this C-terminal domain facilitates self-interactions (Vajjhala et al., 2006). Thus, protein encoded by *clt1-2* may be incapable of or at least less efficient at forming oligomers (Figure 2.10). Consistent with our model for the mechanism of *Clt1-1*, the effects of a dominant-negative allele of Sc*VPS4*, also created by a missense mutation in the ATPase domain (Babst et al., 1997), can be mitigated by also disrupting the C-terminal oligomerization domain suggesting that the dominant-negative effect requires incorporation into VPS4 oligomers (Vajjhala et al., 2006).

Interestingly, the *dcd3* mutant has a relatively mild phenotype (Figure 2.8A-D) relative to *Clt1-1* homozygotes (Figure 2.2A), despite being a putative double mutant of both *ktn1a* and *ktn1b*. Because *ktn1b-dcd3* harbors several missense polymorphisms compared to the B73 allele, but no other obviously deleterious changes, we hypothesize that *ktn1b-dcd3* is a weak *ktn1b* allele. Consistent with this, a putative null mutant in rice where the entire KTN1 ATPase domain is deleted has a severe phenotype resembling *Clt1-1* homozygotes more than the *dcd3* mutant (Komorisono et al., 2005). For example, plant height in the rice mutant is approximately 1/3 of wildtype, while the maize *dcd3* mutant is about half the height of wildtype. However, it is possible that removal of KTN1 function in maize simply has a milder effect than in rice. Moreover, a "gain-of-function" scenario can be proposed for *Clt1-1* where KTN1 complexes 'poisoned' by *Clt1-1* subunits fail to dissociate from and accumulate on microtubules. Although it is unclear how such hypothetical non-dissociations might affect normal cell function, examination of double mutants with high-confidence null or strong loss-of-function alleles for both *KTN1* paralogs in maize will be needed to eliminate the possibility of a gain-of-function effect in *Clt1-1* due to such non-dissociations. We have discovered such alleles for *ktn1b* occurring naturally among diverse inbred lines, and these will be discussed in Chapter 3.

The pleiotropic effects of losing the function of *KTN1* or its orthologs makes interpretation of certain aspects of the phenotype difficult. Provided that future experiments show that there are no major 'gain-of-function' aspects to *Clt1-1*, this putative dominant-negative allele could be useful for transgenic approaches to deactivate CLT1 and KTN1B in specific tissues or at particular time points in order to decouple the various aspects of the pleiotropic phenotype. In this regard, one possible experiment is proposed below. Regardless of the molecular mechanism of *Clt1-1*, the discovery of the causative gene of *Clt1* provides a potential tool for genetically modulating plant and organ size. For example, mild expression of *Clt1-1*, restricted to elongating internodes, could hypothetically result in a cultivar that is more resistant to lodging without substantial impact on other agronomic traits, though an internodes-specific gene has not been reported as yet to my knowledge. Such a protein-level approach should minimize off-targets that are a common issue in RNA interference approaches (Mohr et al., 2014).

2.4.2 The role of katanin in meristem morphology

In *Arabidopsis*, *ktn1* mutants produce SAMs that are flatter and less dome-shaped (Uyttewaal et al., 2012), and this is consistent with the shorter meristems for all meristem types observed in this work (Figure 2.4A-D). Loss of *KTN1* in *Arabidopsis* leads to reduced capacity to realign CMTs in response to mechanical stress, which may be involved in creating the less-domed SAMs in *ktn1* mutants (Uyttewaal et al., 2012). Differential growth rates between neighboring cells are assumed to generate intricate stress patterns in the meristem that may act as developmental cues. *KTN1* is required for CMTs to realign along changing stress patterns (Uyttewaal et al., 2012) which presumably template for corresponding patterns of CMFs that heavily influence subsequent cell growth patterns. Thus, in a model proposed by Uyttewaal et al. (2012), a feedback loop exists in wildtype meristems involving cell growth, stress patterns and CMT arrangements but is broken in *ktn1* mutants. Furthermore, cell growth in the inflorescence meristem of *Arabidopsis ktn1* mutants are ~37% less anisotropic than wildtype (Uyttewaal et al., 2012), which probably also influences meristem shape.

The widening of tassel meristems in *Clt1-1*/+ plants represents the first report of larger meristems due to loss of *KTN1* function, and could result from wider cells due to loss of growth anisotropy though this was not tested in this work. In contrast, both the SAM and ear meristems in *Clt1-1*/+ plants are shorter and narrower (Figure 2.4C,D), similar to the SAM in loss-of-function *ktn1* mutants in rice (Komorisono et al., 2005). These opposing responses of the tassel and ear meristems in *Clt1-1*/+ mirror that of the maize mutants, *fasciated ear2* (*fea2*) and *thick tassel dwarf1* (*td1*), in which the ears are disproportionately widened relative to the tassels (Taguchi-Shiobara et al., 2001; Bommert et al., 2005). FEA2 and TD1 are thought to be negative regulators of cell division in the meristem, and their mutants have enlarged meristems that are thought to be caused by over-proliferation of meristem cells. In contrast, *Clt1-1* mutants could potentially have lower cell division rates because transitions through the different microtubule arrangements during mitosis are delayed in *Arabidopsis ktn1* mutants (Panteris et al., 2011). To explain the severe phenotype in the ears compared to the tassels in *fea2* and *td1* mutants, Taguchi-Shiobara et al. (2001) and Bommert et al. (2005) postulated that the maize ear is more sensitive to genetic perturbation due to strong selection for large ears during domestication. Extending this postulation, potential cell division defects caused by *Clt1-1* may have a stronger negative effect on meristem size in the maize ear compared with the tassel and negate other effects of *Clt1-1* that may promote wider meristems, such as less rectangular cells.

2.4.3 The effect of *Clt1-1* on primordia initiation

The increased spikelet density in *Clt1-1*/+ tassels may be caused by the wider meristems, which are thought to promote primordia initiation by allowing more space for new primordia to initiate; other mutants with larger tassel meristems also have higher spikelet density (for example, Taguchi-Shiobara et al., 2001; Bommert et al., 2005, 2013). Alternatively, *KTN1* is also necessary for maintaining concentric patterns of CMTs around the SAM that are thought to inhibit primordia initiation (Sassi et al., 2014). Thus, the increased spikelet density in *Clt1-1*/+ could also result from loss of these restrictive concentric CMT arrangements in the tassel meristem, allowing more primordia

to initiate. However, the estimated total spikelets is not statistically different from wildtype (Table 2.4). One explanation is that spikelet initiation rate is actually not increased substantially in *Clt1-1*/+ plants and the elevated spikelet density results simply from reduced spacing between spikelets, for example due to shorter intervening cells. Another explanation is that the shortened meristem and putatively faster spikelet initiation in the *Clt1-1*/+ tassel causes premature depletion of the meristem, and thus unchanged total spikelets despite a higher rate of spikelet initiation. To test this, a double mutant with mutants such as *td1* or *fea2*, described above, could be made. If the number of spikelets initiated in *Clt1-1*/+ tassels is limited by depletion of the meristem, increasing the meristem size may help counteract this. Thus, we would predict a synergistic effect on total tassel spikelets in double mutants between *Clt1-1* and one of these other mutants, which also have positive effects on spikelet density by themselves.

As stated above, future work will be needed to rule out potential 'gain-of-function' effects of *Clt1-1*. If that can be proven, *Clt1-1* could be used to differentiate the potential effects of reduced inhibition of primordia initiation versus widened meristems on tassel spikelet initiation. Expression of *Clt1-1* could be attempted in the central zone (CZ) and, in separate plants, at the peripheral zone (PZ) of the meristem using transgenic constructs under transcriptional control by, for example, the promoters of *knotted1* (*kn1*) (Jackson et al., 1994) or *aberrant phyllotaxy2* (*abphyl2*) (Yang et al., 2015) respectively; in situ RNA hybridizations have shown that *kn1* is expressed in the CZ but not at the PZ, while *abphyl2* is expressed in the PZ but not the CZ. Thus, we predict that the *kn1* promoter construct would cause wider and shorter tassel meristems but not affect the concentric CMTs that limit primordia initiation, while the *abphyl2* promoter construct would have minimal effects on meristem shape but remove the restrictive concentric CMTs. The tassel spikelet density and total counts from these two transgenic lines could then be compared to test the relative contributions of loss of CLT1 (and presumably KTN1B) activity in the CZ versus the PZ towards increased tassel spikelet initiation.

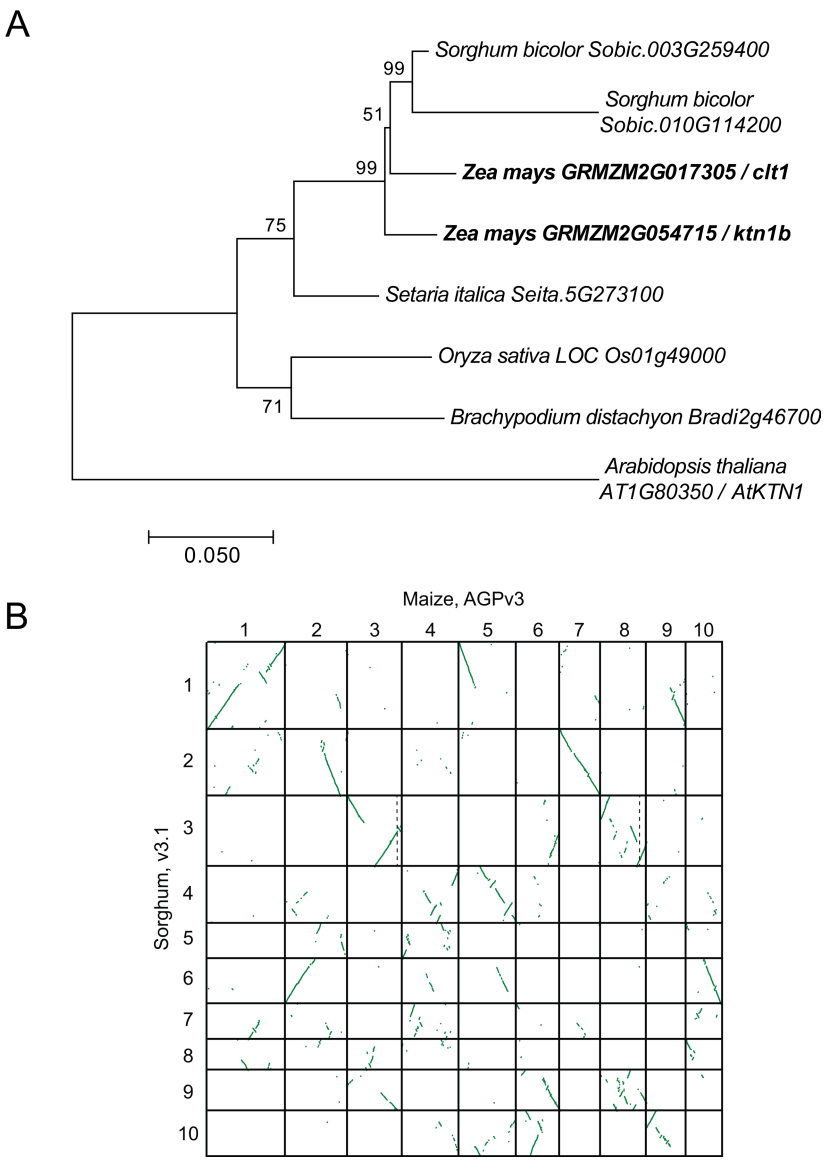

Figure 2.1 Phylogeny of *AtKTN1* orthologs among several plant species and syntenic gene blocks between maize and sorghum.

(A) The evolutionary history of the coding sequences of predicted proteins from the indicated plant species with the highest sequence similarity (protein BLAST query) with AtKTN1. The Maximum Likelihood method based on the Tamura-Nei model (Tamura and Nei, 1993) was used within the MEGA7 software (Kumar et al., 2016). The percentage of trees in which the associated taxa clustered together is shown next to the branches, based on 1,000 permutations. The tree is drawn to scale, with branch lengths measured in the number of substitutions per site. Maize *ktn1a*/*clt1* and *ktn1b* are indicated by bold font. (B) Regions of synteny between the maize and sorghum genomes. Generated by SynMap (Lyons et al., 2008). Dotted lines indicate the approximate locations of maize *clt1* and *ktn1b* in maize.

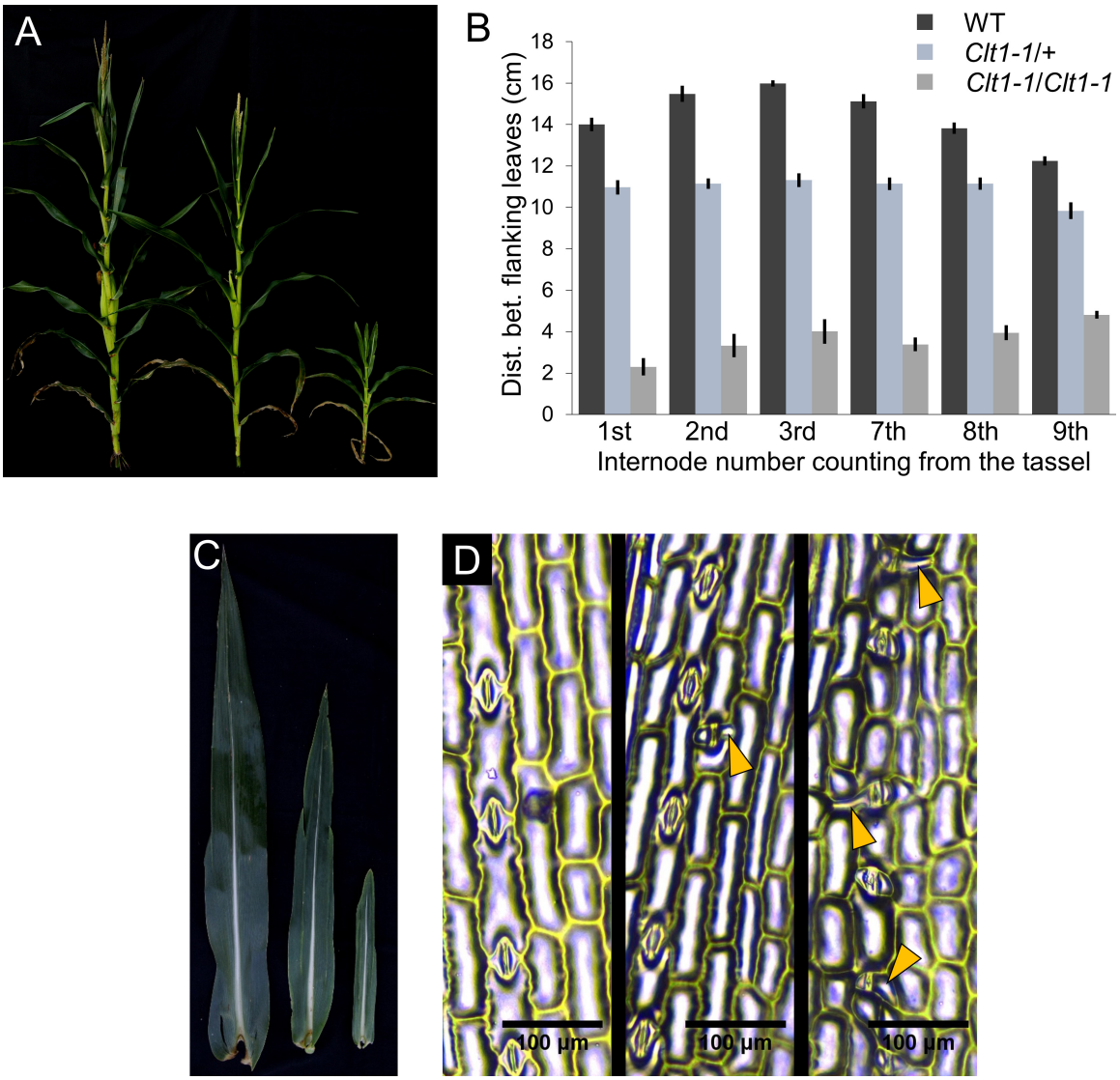

Figure 2.2 Phenotype of *Clt1-1*.

(A,C,D) Comparisons of wildtype (left), *Clt1-1* heterozygote (middle) and *Clt1-1* homozygote (right) for (A) plant height, (C) leaf size and shape (5th leaf from the tassel), and (D) shape of epidermal cells from the adaxial surface of the third leaf. Arrowheads indicate irregularly shaped stomatal subsidiary cells. (B) Mean distances between the ligules of leaves initiated from the top and bottom nodes of each internode for the indicated genotypes. Internodes were numbered starting from the tassel (n = ≥8; ± standard error).

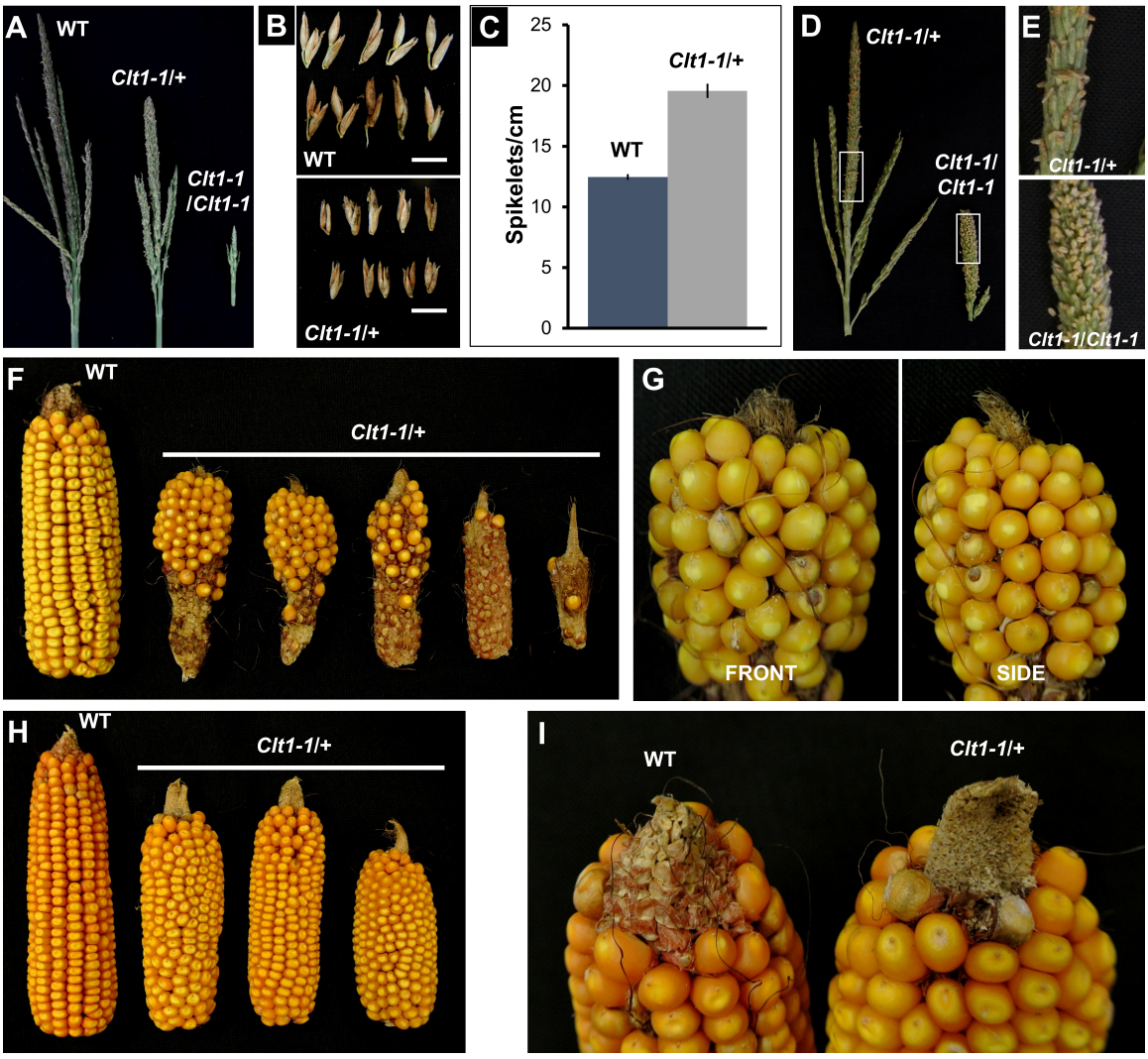

Figure 2.3 Tassel and ear phenotypes of *Clt1-1*

Inflorescence phenotypes of *Clt1-1* in (A-C, F, G) a B73 background or (D, E, H, I) in the F3 generation of a cross between PHJ40 and *Clt1-1* (B73). (A, D) Comparison of tassels from the indicated genotypes. (B) Close-up of spikelets removed from the tassel. Scale bars represent 1 cm. (C) Mean spikelet density for indicated genotypes (n=20; ± standard error; Welch's t-test, p = 3.28E-11). (E) Close-up of the tassels in panel (D) as indicated by the white boxes to show the spikelet phenotype. (F, H) Comparison of ears from the indicated genotypes. Multiple *Clt1-1*/+ ears shown to illustrate the range of phenotypes. (G) Front and side views of a *Clt1-1*/+ ear from (F) showing a flattened ear tip. (I) Close-up of two ears from (H) showing a normal ear tip and a flattened *Clt1-1*/+ ear tip.

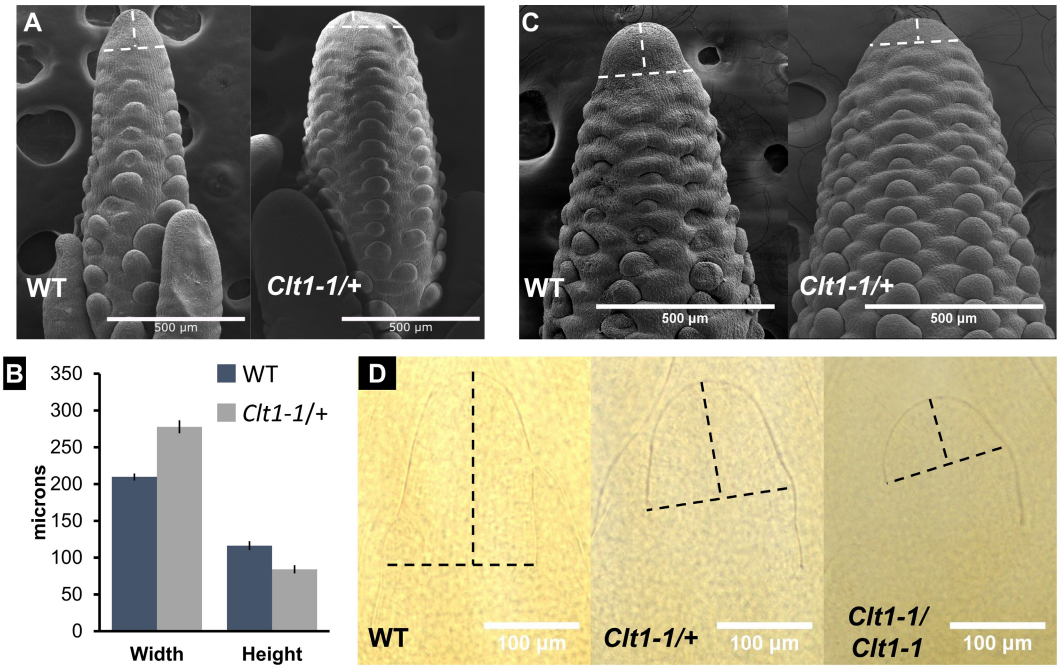

Figure 2.4 Meristem phenotype of *Clt1-1*.

(A) SEM of ~2 mm long tassel primordia. (B) Mean width and height of tassel meristem measured from SEM images as indicated by the dotted lines in (A) (n = 11; ± standard error; Welch's t-test, p = 5.56E-06 for width, p = 0.00074 for height). (C) SEM of ~2 mm long ear primordia. (D) FAA-fixed and methyl salicylate-cleared SAMs from 2 week old seedlings.

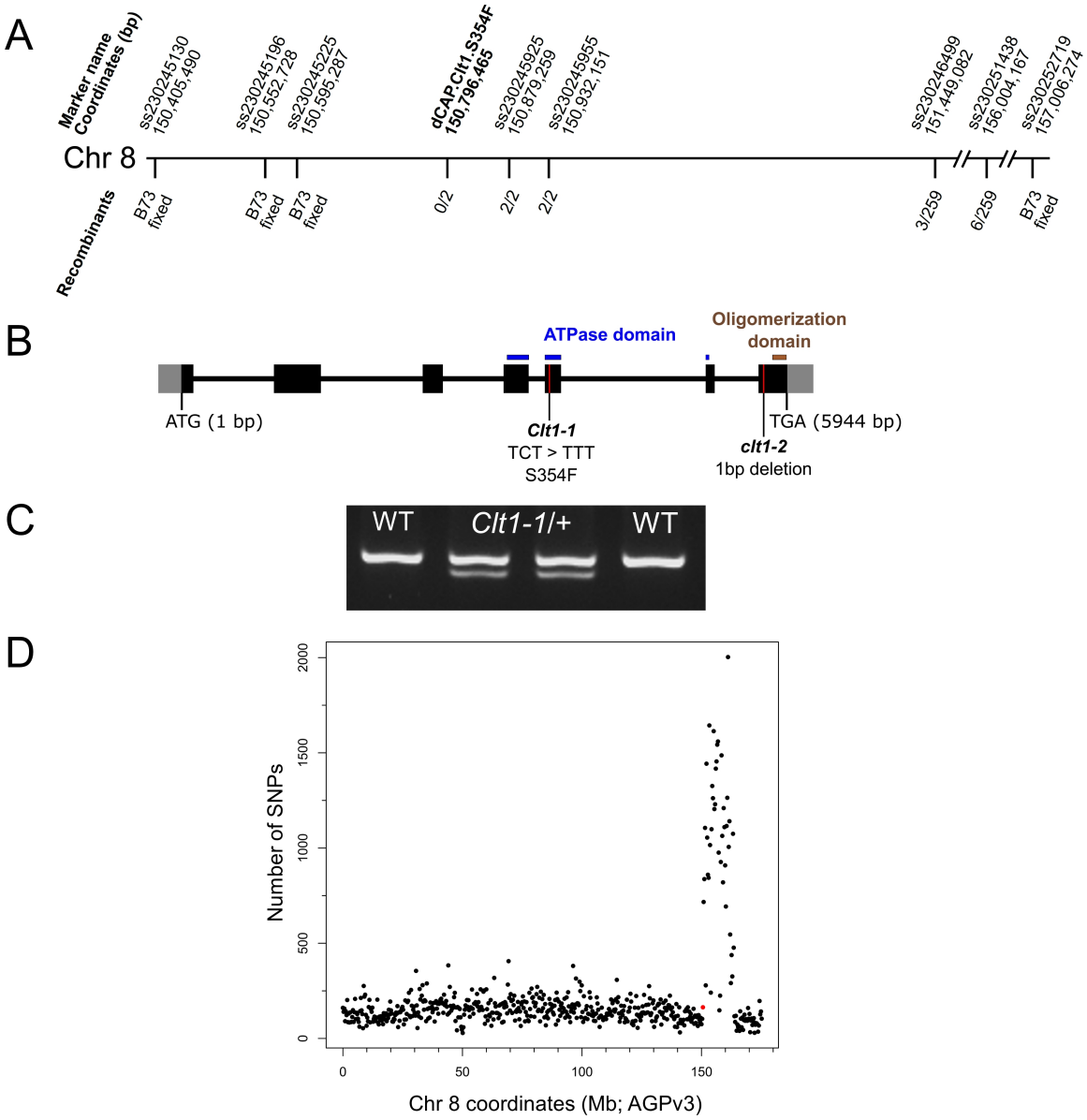

Figure 2.5 Mapping of *Clt1* to the maize ortholog of *KTN1* on Chr 8.

(A) Physical locations (B73 AGPv3) of markers used to genotype individuals from a B73 x *Clt1*/+ mapping population and the number of recombinants observed at each marker. Where the number of individuals tested was only 2 instead of 259, only the plants recombinant for the outer markers were tested. (B) Gene model for *clt1* (GRMZM2G017305) indicating locations of *Clt1-1* and *clt1-2*. Locations of protein domains were determined by searching CLT1 protein sequence against the Pfam database (Finn et al., 2015). (C) A dCAP assay directly interrogating the putative causative C to T lesion in *clt1*. (D) Density of SNPs called from whole-genome sequencing of *Clt1* homozygotes, in 300 kb non-overlapping windows with the window containing *clt1* indicated (red).

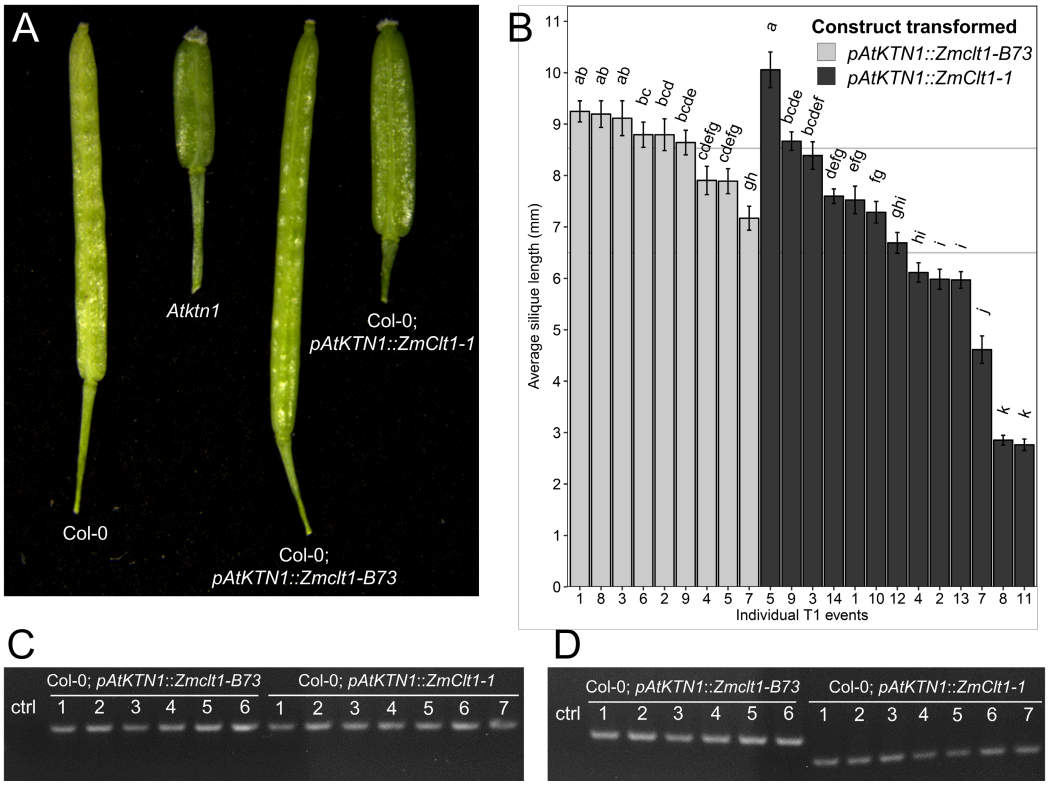

Figure 2.6 Heterologous expression of *Clt1-1* causes shorter and wider siliques in wildtype Col-0 *Arabidopsis*.

(A) Comparison of representative siliques from untransformed Col-0, the *ktn1-lue1* *Arabidopsis* mutant, Col-0 transformed with maize *clt1-B73* and Col-0 transformed with maize *Clt1-1* (left to right). (B) Average silique lengths of T1 plants transformed with *clt1-B73* or *Clt1-1*. ($n \geq 38$ siliques for each plant; ± standard error; letters represent Tukey groups at 0.05 significance level). (C,D) Genotypic verification of the transformed constructs in each T1 plant. (C) Before and (D) after digest of PCR product with DraI. The first lanes are a negative control, corresponding to amplification from untransformed Col-0. Cut fragments correspond to the *Clt1-1* allele. ID numbers correspond to those in (B). All plants in (B) were genotyped but not all are shown. All plants genotyped as expected, but event #8 for *Clt1-1* did not amplify likely due to PCR failure. Event #6 for *Clt1-1* was not phenotyped because it produced much fewer siliques than the other events.

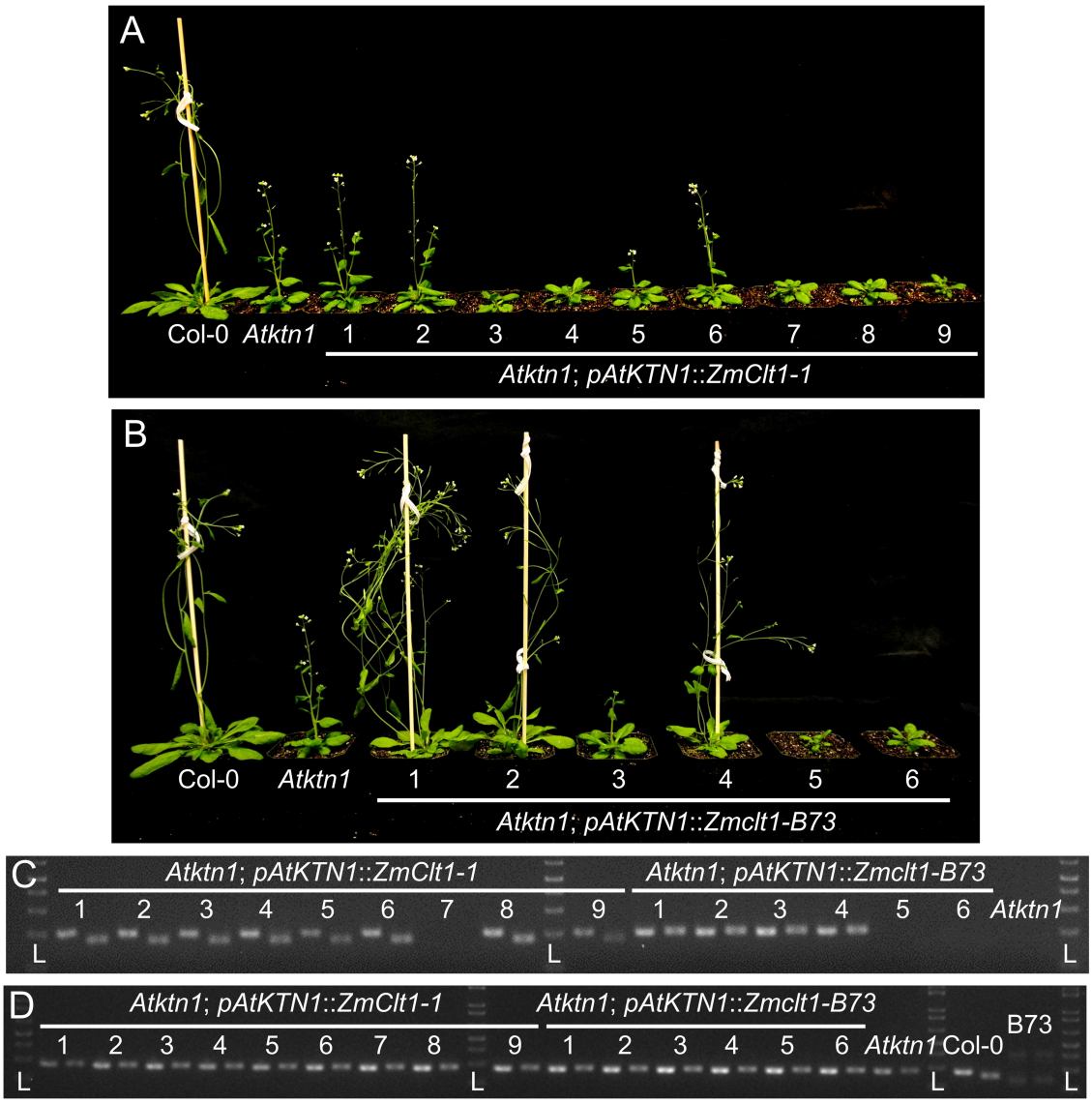

Figure 2.7 The maize allele *Clt1-1* has lost normal function.

T1 generation plants from transformations of *ktn1-lue1 Arabidopsis* mutants with maize (A) *Clt1-1* or (B) *clt1-B73*. (C,D) Results from genotyping using dCAPS markers. Samples were each loaded with the undigested PCR product on the left and the digested product in an adjacent well on the right. (C) Genotyping to confirm the presence and genotype of the transgenic construct. Cleaved allele corresponds to *Clt1-1*. (D) Genotyping to confirm all plants were *ktn1-lue1* homozygous. Cleaved allele corresponds to the wildtype Col-0 allele. L, molecular ladder.

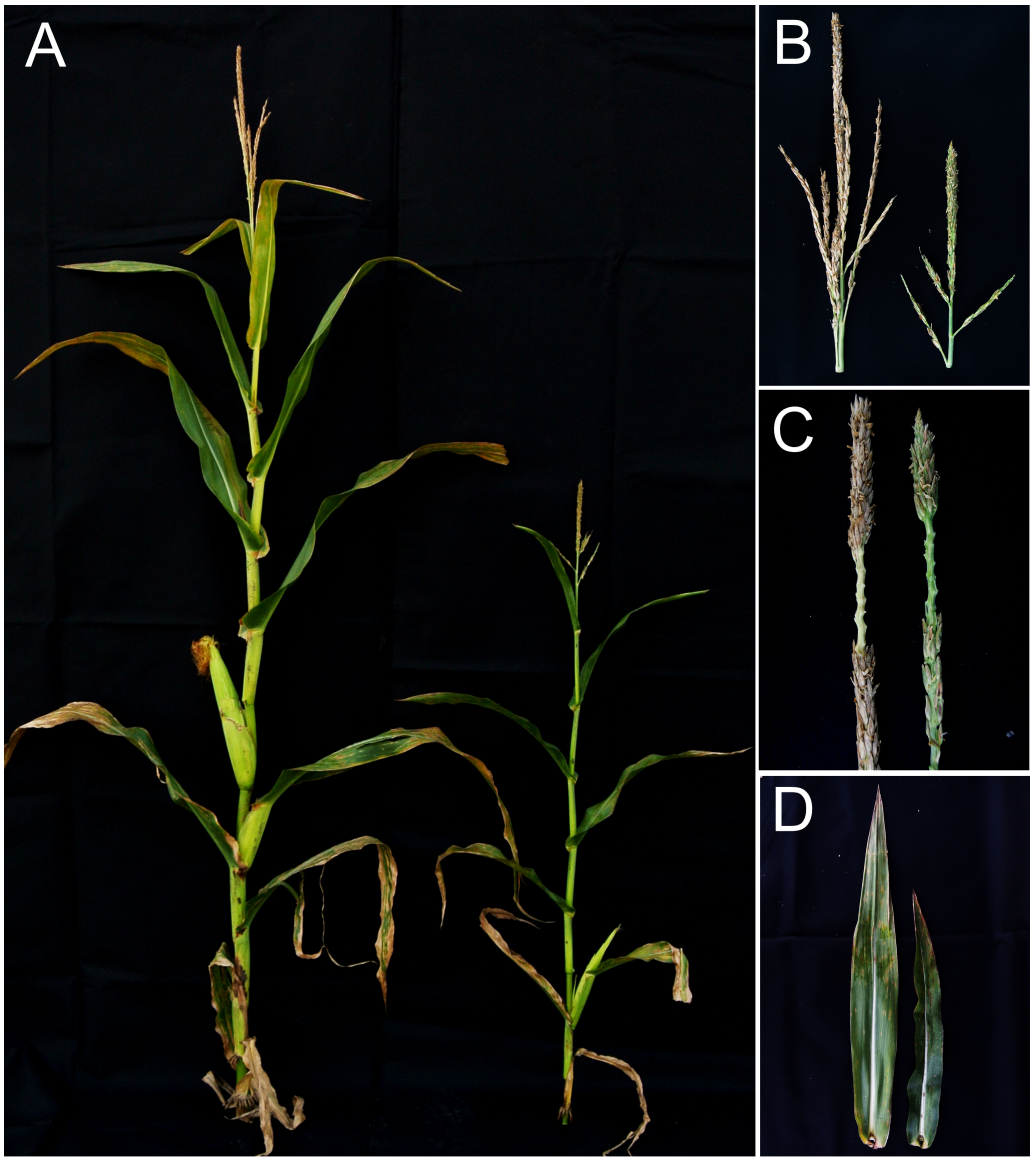

Figure 2.8 Phenotype of the *dcd3* mutant, which is homozygous for *clt1-2* on Chr 8 and a Chr 3 locus that includes the other KTN1 ortholog.

(A-D) Comparisons of (left) B73 with (right) the *dcd3* mutant, backcrossed 4 times with B73. (A) Whole plants. (B) Tassels. (C) Close-up of the central spike shown in panel (B). (D) Third leaf from the tassel. (E) Alignment of predicted protein sequence showing the effect of the *clt1-2* 1 bp deletion. Highlighted residues correspond to the C-terminal oligomerization domain.

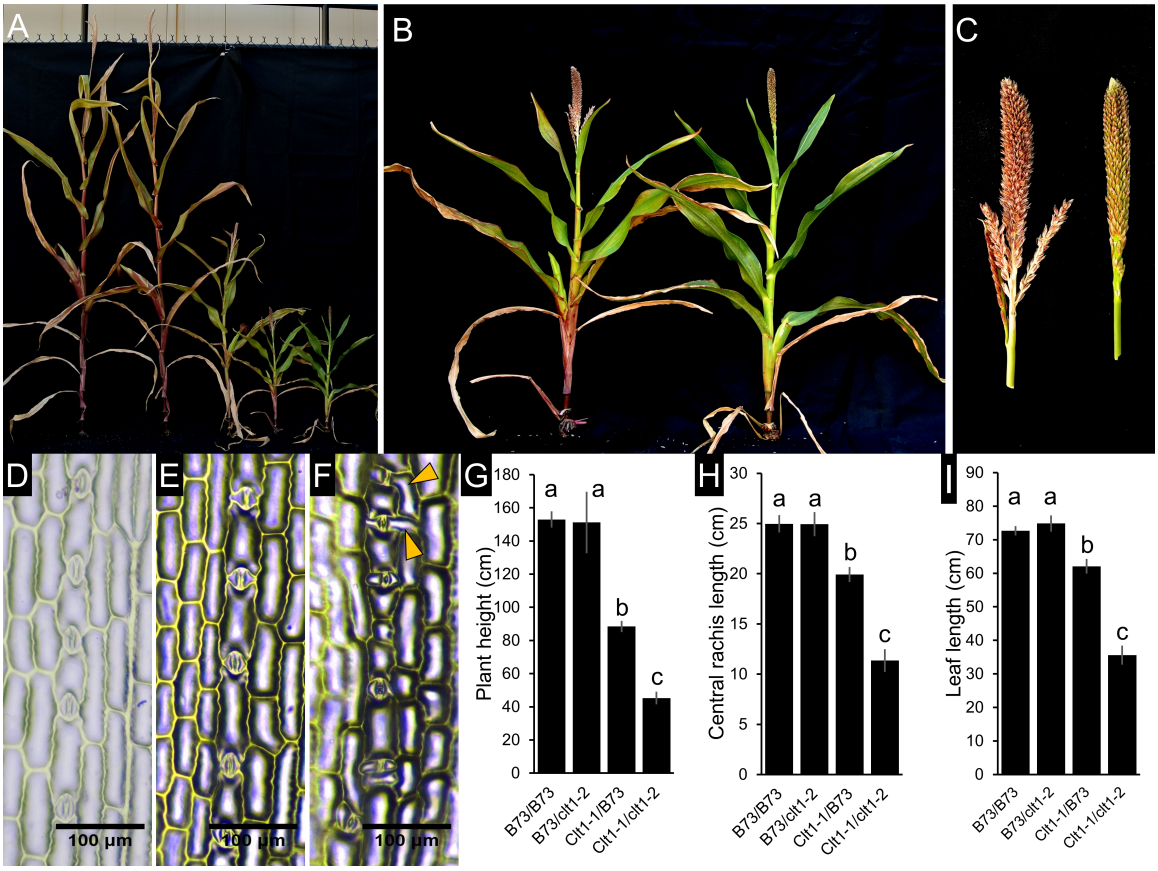

Figure 2.9 *Clt1-1* and *clt1-2* interact synergistically to produce a phenotype resembling *Clt1-1* homozygotes.

(A) Comparison of +/+, *clt1-2*/+, *Clt1-1*/+, *Clt1-1*/*clt1-2* and *Clt1-1*/*Clt1-1* whole plants (left to right). (B,C) Close-up of (left) *Clt1-1*/*clt1-2* and (right) *Clt1-1*/*Clt1-1* from panel (A), for (B) whole plants and (C) tassels. (D,E,F) Leaf impressions of (D) *clt1-2*/+, (E) *Clt1-1*/+ and (F) *Clt1-1*/*clt1-2*, taken from the third leaf. Arrowheads indicate malformed stomatal subsidiary cells. (G,H,I) Quantitative comparisons of +/+, *clt1-2*/+, *Clt1-1*/+ and *Clt1-1*/*clt1-2* segregating in a single family, for (G) plant height, (H) central rachis length and (I) length of the 5th leaf from the tassel. Letters represent Tukey groups calculated at the 0.05 significance level. Errors bars are ± standard error. n ≥ 6 of each genotype.

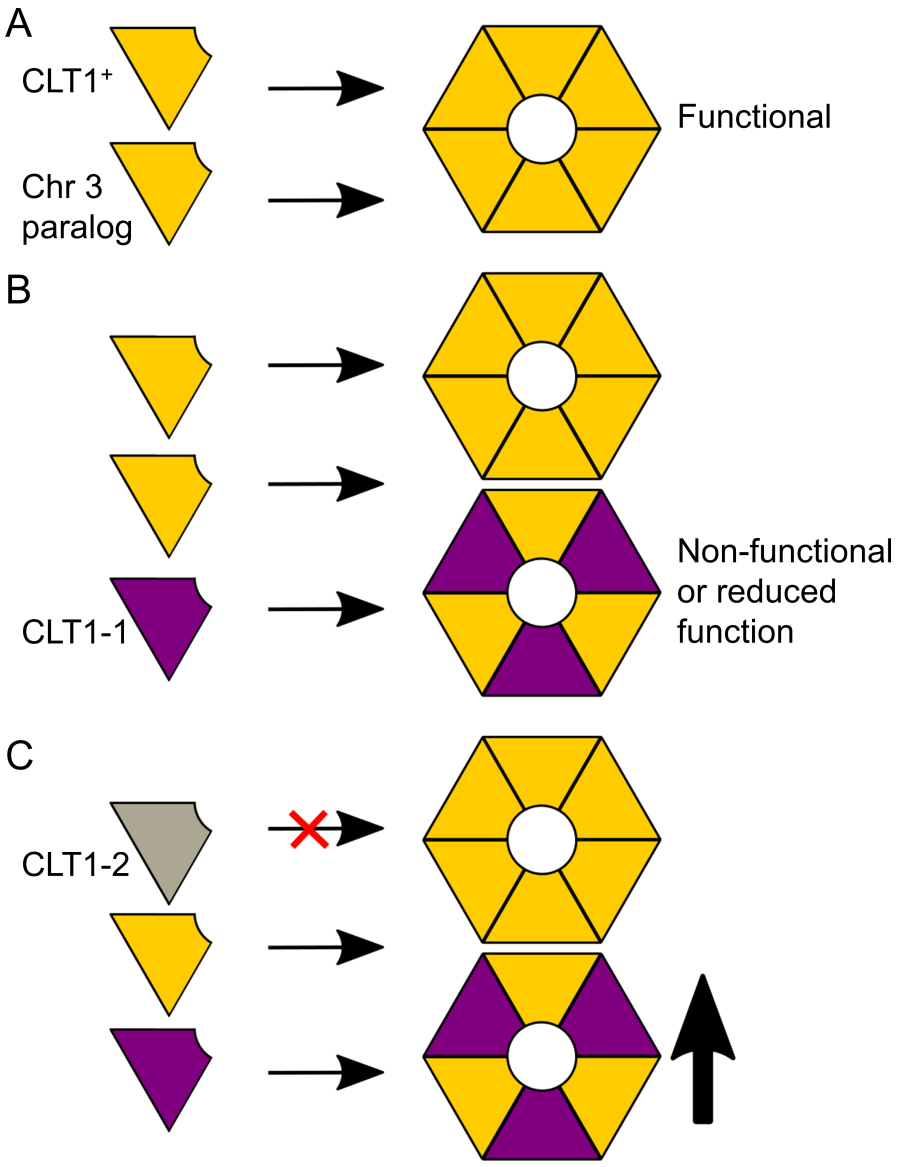

Figure 2.10 Model for the mechanisms of *Clt1-1* and *clt1-2*.

(A-C) The hypothetical pools of katanin monomers (left) and hexamers (right) in (A) a wildtype maize plant (B) a *Clt1-1*/+ heterozygote (C) a *Clt1-1*/*clt1-2* heterozygote. Yellow represents functional subunits encoded by wildtype alleles of *clt1* or the duplicate gene on Chr 3. Purple subunits are encoded by *Clt1-1* and, in this model, incorporate into and 'poison' katanin hexamers. Gray subunits are encoded by *clt1-2* and, in this model, cannot oligomerize or does so at a reduced efficiency, thereby reducing the number of functional CLT1 subunits and, in effect, increasing the proportion of complexes 'poisoned' by *Clt1-1*.

Table 2.1 SNPs and flanking sequences used to design KASP assays for mapping *Clt1-1*.

Marker name	SNP and flanking sequences
	Initial markers for delineating non-B73 linkage block in a B73-introgressed *Clt1-1* stock
ss230232973	GATCACATCGGCAGATTCGATGCTTCAGTCTGCAGAATTGAATAATCACC[C/G]GCTTTATCAGAGTACCAGGACTGACGCTACCTACGCCGCGTCCGGCCGGC
ss230234139	TAGTGCATGCGCGGCAGCAGCGGCGTCGTGTACGTGGCCCACGTGTCCGG[T/G]AGCTGCGCCGGAGACGAGAACCGCACGGCGAGCTGCACCTCGCCCATCTT
ss230235988	ACGTGATTTTGGGGAGCTCCATGATACACTTCTACTGTAAGGTTGGCTTG[G/A]TGGAGGCTGCCGAGGCAGTGTTTGAGCAGATGGAAGGGAGAGATGCTGTG
ss230237099	GCCTCACGGATCGCCTTGCTGGTCCGGGTGATGCCCACGGGGTACACGCA[A/G]TTGCCGTAGTAGCCGTCCACCGACGGCAGCACGCCGTGGAGGAGGTGCCG
ss230237767	GCTGGGCCTGGGGCGGGTCCTGTTCCTGTACTCCTGTCCTTCATTACTCA[C/G]CGACAGTAAGCACTGGCACTCCGGCTGAAGCAAGGGACCCGATTCTCAGA
ss230241506	GCGCGCGGGGACGCCGGGACCGGGAGAGGCAATCACCGCCGTCTTCCCCG[T/C]GTCCGGCTCACGACGCGCCGGTGGATTCGAGCGCACGGCCACCACCGTTG
ss230242504	CCTTGAGCCCCTGCACGAGCTTCCTCGCGGACGCCGGCACGGGCCCCGAC[T/G]GCCCCCTGGCTCCCCCTCCGCCGCTGCCGCTGCCGCTGCCGCTCATCCTC
ss230243736	AAGCTTGTCCCTGTTAAAAGCTACCGGCCGCTTGGTGCGCGGCGCTACCT[T/C]CCGTCTCTCGCTGGGAGAACAGACCAAGAAAATCGATCGCCACTAGTACC
ss230245130	GCGGGAAGGTTGAGACGGCGGGGGCTGGAGGTGGTGTGCGAGGCCACGAC[C/T]GGGCGGCGGCCGGACTCGGTTAAGAAGAGGGAGCGCCAGAACGACAAGCA
ss230246499	TGCGGGGGCTAGCTGAAGCTACTGGCGCAACGCAACTGGTGCGTGCTCTG[T/G]TGACTGCGAAAATACGAAGGGTCGGTTCAGGACTTACTCGATGGTTTGCA
ss230247863	TGGGGGCAGACAGGCAGGCAGATAGGCAGGTCGCGCTCTCGGAGGTGTGG[C/A]TTGGGGCCAAACCCTGCCCGATCGGCTCAAGCTCCCCCGCCGCTGCCGAA
ss230251438	CCCATCTAGCATATTAGGCCCATCTAGCCTCCCACGCCTTCAGGCTCAAG[C/T]GCAGTGCAGGCTGCTGATACGCTCCGACCACAGCCGTCCTCCGCCAGGCA

ss230252719	CCAGGCGCAGGGCGTCGTCGCGTCCGACCCCGTCCACGTG GCCAGCGCGC[T/C]GGTCGGGTCGGACAGCGCCGACTTGAA CACCACCAGCCCCAGCACCTCCT
ss230255326	AGGCTTGTCCTCCACATCGTCCCCAATTCATGCGTGCGAGC TGCTAGGTG[T/C]GGCGGATGGAGCACAACAGGGAGGTGA GACGTGCCAGAAAGAAAAACAGC
ss230257712	AGGTAGTAGCAATCGTTCGGGCTTTATGCAGGAGCTGCAG GAACAACATA[G/A]CATTCTCAGAAACTCCATCGAACAACT TAAAGTGTCAGAATCACTCAGGG
	Additional markers
ss230245196	TCTCGTTCTTCTTACGCCGAGAGGTGGATCCATTGGATGGA TTACTGGCG[G/C]TCATGCGTCTGCTATTGCTGCCTTCTGAT TTGAAGTACTGGAGTTTGTGA
ss230245225	CCTCACCTGACCGCGCACTCTCCTCACCTCACCTCGCCAAT GCTCTCCAC[T/C]ACCTCCCCGGTCCCACTCCTCGACACGCC GGCGCCCTCGACGGACGCCGA
ss230245925	TAGTACACTGCTGCTGCATAGCTAGAGTAAGGCTGACTCAC TGATAGTGC[T/A]AATTAATCATCCGTGCAGTGTCTCAGTCT CTACTACACACATGCGTCGCT
ss230245955	TGTCAACACAAACCAAGCTTCCTGATTTATGCATGTTTTTTT TCGAACGT[A/G]CAATTCATGCGCTTTGCTTCGAAGTTCCAG CTGCATGCAGTTTCTGTAGA

SNPs were identified and named in HapMap1 (Gore et al., 2009).

Table 2.2 Chromosomal coordinates, genotypes in B73 and positive control inbreds, and whether there was polymorphism between non-recombinant *Clt1-1*/+ and wildtype siblings (in the B73 introgression) for SNP markers used to map *Clt1-1*.

Marker name	Chr 8 location (AGPv3)	Genotype identified in **HapMap1** (Gore et al., 2009)			Polymorphism between *Clt1-1* and WT sibs
		B73	**CML333**	**MS71**	
Initial markers for delineating non-B73 linkage block containing *Clt1-1*					
ss230232973	138,395,238	C	G	N	no
ss230234139	139,540,935	T	G	G	no
ss230235988	141,761,055	G	A	A	no
ss230237099	142,812,210	A	G	G	no
ss230237767	144,028,268	C	G	G	no
ss230241506	147,254,535	T	C	C	no
ss230242504	148,211,452	T	G	G	no
ss230243736	149,343,351	T	C	C	no
ss230245130	150,405,490	C	T	T	no
ss230246499	151,449,082	T	G	G	YES
ss230247863	152,495,182	C	A	A	YES
ss230251438	156,004,167	C	T	T	YES
ss230252719	157,006,274	T	C	C	no
ss230255326	159,039,565	T	C	C	no
ss230257712	160,151,376	G	A	A	no
Additional markers used for fine-mapping					
*ss230245196	150,552,728	G	C	C	no
*ss230245225	150,595,287	T	C	C	no
ss230245925	150,879,259	T	A	A	YES
ss230245955	150,932,151	A	N	G	YES

*these markers were tested in an unsuccessful attempt to find a polymorphic left-flanking marker.

Table 2.3 Primers used to sequence *Clt1-1* gDNA and *clt1* transgenic constructs.

Primer name	Sequence (5'-3')
	Primers for sequencing *Clt1-1* gDNA
CLT1_seq_1F	GTACCAGACGGATGGTGGAC
CLT1_seq_1R	TCGTACGAATCAGAGCATCG
CLT1_seq_2F	TGAAGCAGCTGTATTCTTTAATGC
CLT1_seq_2R	TGTCTTCAAGATTTGATTGTTTGAG
CLT1_seq_3F	CCTTTTAAATTAGTCCCTTCTCAGTG
CLT1_seq_3R	TGGCACCCCTAGATACAAGC
CLT1_seq_4F	CTACGCTGTCCCTTATTGGTTC
CLT1_seq_4R	CCTCTGACGTTGACAGTATCCA
CLT1_seq_5F	TCATTCTGCTAGACAACAGAAAATG
CLT1_seq_5R	CAAAGGAACTGCAATGAGCA
CLT1_seq_6F	CAGCGGGAGTAGCCTAATGA
CLT1_seq_6R	GGTCTTGCCTGCTATCTTGC
CLT1_seq_6Rext	CAACCAAACACGGAGCATCT
	Primers for sequencing *clt1* transgenic constructs
CLT1constr_seq_1R	CAGCACAGATTGGGATGTTG
CLT1constr_seq_2F	ATTGTTGCGTTGAGGGAGAC
CLT1constr_seq_2R	**GGATTCGCCAT**TTCCTCTTT
CLT1constr_seq_3F	GATGGGCCCGAATCTAAAAT
CLT1constr_seq_3R	**TCACCCTTCTTGACGACTCA**
CLT1constr_seq_4F	**CAGGCACGGGAAAGACTC**
CLT1constr_seq_4R	ATTGAGGAGGGAGCCCAAC
CLT1constr_seq_5F	CCAGCAAAGAATCACCTTGG
CLT1constr_seq_5R	ACGTTTTCTGGCAGCAATTC
CLT1constr_seq_6F	TTTGGCTTGTTATGTGGCATT

CLT1constr_seq_1R and CLT1constr_seq_6F were used to sequence plasmid DNA directly so there are no corresponding forward and reverse primers respectively. Bolded CLT1constr_seq primer sequences bind to maize CDS and non-bolded sequences bind to *Arabidopsis KTN1* promoter, and 5' and 3' UTR.

Table 2.4 Phenotypes of different *clt1* genotypes segregating in a single family in a B73 background, grown in the field.

***clt1* genotype**	+/+	***Clt1-1*/+**	***Clt1-1* /*Clt1-1***
Plant height (cm)	184.59 (1.81; 20; a)	140.95 (1.93; 20; b)	48 (3.58; 8; c)
Leaf length (cm)	74.44 (1.17; 20; a)	54.65 (1.04; 19; b)	24.89 (1.08; 8; c)
Leaf width (cm)	9.22 (0.17; 19; a)	7.41 (0.25; 19; b)	3.8 (0.24; 8; c)
Central spike length (cm)	22.66 (0.66; 20)	15.64 (0.38; 20; ***)	NA
Tassel length (cm)	31.18 (0.56; 20)	22.14 (0.5; 20; ***)	NA
Primary tassel branches	7.05 (0.29; 20)	7.45 (0.39; 20; ns)	NA
Spikelet density on main rachis (/cm)	12.46 (0.23; 20)	19.57 (0.59; 20; ***)	NA
Rachis diameter (mm)	2.81 (0.09; 20)	3 (0.07; 20; ns)	NA
Estimated total spikelets	282.25 (9.56; 20)	308.47 (14.31; 20; ns)	NA

Values are means with the standard error and sample size in parentheses. Letters indicate Tukey groups at a 0.05 significance level. *** indicates P-value < 0.0001 and ns is not significant as determined by Welch's t-test. Total spikelets estimated by multiplying central spike length by spikelet density on the main rachis. Tassel traits could not be measured for *Clt1-1*/*Clt1-1* because the tassel did not develop properly (Figure 2.3B).

2.5 References

Andorf, C.M. et al. (2016). MaizeGDB update: new tools, data and interface for the maize model organism database. Nucleic Acids Res. **44**: D1195–201.

Van der Auwera, G.A. et al. (2013). UNIT 11.10 From FastQ Data to High-Confidence Variant Calls: The Genome Analysis Toolkit Best Practices Pipeline A. Bateman, W.R. Pearson, L.D. Stein, G.D. Stormo, and J.R. Yates, eds (John Wiley & Sons, Inc.: Hoboken, NJ, USA).

Babst, M., Sato, T.K., Banta, L.M., and Emr, S.D. (1997). Endosomal transport function in yeast requires a novel AAA-type ATPase, Vps4p. EMBO J. **16**: 1820–31.

Bichet, A., Desnos, T., Turner, S., Grandjean, O., Hofte, H., and Höfte, H. (2001). BOTERO1 is required for normal orientation of cortical microtubules and anisotropic cell expansion in Arabidopsis. Plant J **25**: 137–148.

Bolger, A.M., Lohse, M., and Usadel, B. (2014). Trimmomatic: A flexible trimmer for Illumina sequence data. Bioinformatics **30**: 2114–2120.

Bommert, P., Je, B.I., Goldshmidt, A., and Jackson, D. (2013). The maize Galpha gene COMPACT PLANT2 functions in CLAVATA signalling to control shoot meristem size. Nature **502**: 555–558.

Bommert, P., Lunde, C., Nardmann, J., Vollbrecht, E., Running, M., Jackson, D., Hake, S., and Werr, W. (2005). thick tassel dwarf1 encodes a putative maize ortholog of the Arabidopsis CLAVATA1 leucine-rich repeat receptor-like kinase. Development **132**: 1235–1245.

Bouquin, T., Mattsson, O., Naested, H., Foster, R., and Mundy, J. (2003). The Arabidopsis lue1 mutant defines a katanin p60 ortholog involved in hormonal control of microtubule orientation during cell growth. J Cell Sci **116**: 791–801.

Burk, D.H., Liu, B., Zhong, R., Morrison, W.H., and Ye, Z.-H.H. (2001). A katanin-like protein regulates normal cell wall biosynthesis and cell elongation. Plant Cell **13**: 807–827.

Chia, J.-M. et al. (2012). Maize HapMap2 identifies extant variation from a genome in flux. Nat. Genet. **44**: 803–7.

Cingolani, P., Platts, A., Wang, L.L., Coon, M., Nguyen, T., Wang, L., Land, S.J., Lu, X., and Ruden, D.M. (2012). A program for annotating and predicting the effects of single nucleotide polymorphisms, SnpEff: SNPs in the genome of Drosophila melanogaster strain w1118; iso-2; iso-3. Fly (Austin). **6**: 80–92.

Clough, S.J. and Bent, A.F. (1998). Floral dip: a simplified method forAgrobacterium-mediated transformation ofArabidopsis thaliana. Plant J. **16**: 735–743.

Confalonieri, F. and Duguet, M. (1995). A 200-amino acid ATPase module in search of a basic function. BioEssays **17**: 639–50.

DePristo, M.A. et al. (2011). A framework for variation discovery and genotyping using next-generation DNA sequencing data. Nat. Genet. **43**: 491–8.

Edgar, R.C. (2004). MUSCLE: multiple sequence alignment with high accuracy and high throughput. Nucleic Acids Res. **32**: 1792–7.

Finn, R.D. et al. (2015). The Pfam protein families database: towards a more sustainable future. Nucleic Acids Res. **44**: D279–D285.

Goodstein, D.M., Shu, S., Howson, R., Neupane, R., Hayes, R.D., Fazo, J., Mitros, T., Dirks, W., Hellsten, U., Putnam, N., and Rokhsar, D.S. (2012). Phytozome: a comparative platform for green plant genomics. Nucleic Acids Res. **40**: D1178–86.

Gore, M.A., Chia, J.M., Elshire, R.J., Sun, Q., Ersoz, E.S., Hurwitz, B.L., Peiffer, J.A., McMullen, M.D., Grills, G.S., Ross-Ibarra, J., Ware, D.H., and Buckler, E.S. (2009). A First-Generation Haplotype Map of Maize. Science (80-.). **326**: 1115–1117.

Green, P.B. (1962). Mechanism for Plant Cellular Morphogenesis. Science **138**: 1404–5.

Hartman, J.J., Mahr, J., McNally, K., Okawa, K., Iwamatsu, A., Thomas, S., Cheesman, S., Heuser, J., Vale, R.D., and McNally, F.J. (1998). Katanin, a Microtubule-Severing Protein, Is a Novel AAA ATPase that Targets to the Centrosome Using a WD40-Containing Subunit. Cell **93**: 277–287.

Hartman, J.J. and Vale, R.D. (1999). Microtubule disassembly by ATP-dependent oligomerization of the AAA enzyme katanin. Science (80-.). **286**: 782–785.

Heckman, K.L. and Pease, L.R. (2007). Gene splicing and mutagenesis by PCR-driven overlap extension. Nat. Protoc. **2**: 924–32.

Höfgen, R. and Willmitzer, L. (1988). Storage of competent cells for Agrobacterium transformation. Nucleic Acids Res. **16**: 9877.

Jackson, D. and Hake, S. (1999). Control of phyllotaxy in maize by the abphyl1 gene. Development **126**: 315–323.

Jackson, D., Veit, B., and Hake, S. (1994). Expression of maize KNOTTED1 related homeobox genes in the shoot apical meristem predicts patterns of morphogenesis in the vegetative shoot. Development **120**: 405–413.

Komorisono, M., Ueguchi-Tanaka, M., Aichi, I., Hasegawa, Y., Ashikari, M., Kitano, H., Matsuoka, M., and Sazuka, T. (2005). Analysis of the rice mutant dwarf and gladius leaf 1. Aberrant katanin-mediated microtubule organization causes up-regulation of gibberellin biosynthetic genes independently of gibberellin signaling. Plant Physiol. **138**: 1982–93.

Kumar, S., Stecher, G., and Tamura, K. (2016). MEGA7: Molecular Evolutionary Genetics Analysis Version 7.0 for Bigger Datasets. Mol. Biol. Evol. **33**: 1870–1874.

Li, H. (2013). Aligning sequence reads, clone sequences and assembly contigs with BWA-MEM. arXiv:1303.3997.

Lyons, E., Pedersen, B., Kane, J., and Freeling, M. (2008). The Value of Nonmodel Genomes and an Example Using SynMap Within CoGe to Dissect the Hexaploidy that Predates the Rosids. Trop. Plant Biol. **1**: 181–190.

McKenna, A., Hanna, M., Banks, E., Sivachenko, A., Cibulskis, K., Kernytsky, A., Garimella, K., Altshuler, D., Gabriel, S., Daly, M., and DePristo, M.A. (2010). The Genome Analysis Toolkit: a MapReduce framework for analyzing next-generation DNA sequencing data. Genome Res. **20**: 1297–303.

McNally, K.P., Bazirgan, O.A., and McNally, F.J. (2000). Two domains of p80 katanin regulate microtubule severing and spindle pole targeting by p60 katanin. J. Cell Sci. **113 (Pt 9**: 1623–33.

Mohr, S.E., Smith, J.A., Shamu, C.E., Neumüller, R.A., and Perrimon, N. (2014). RNAi screening comes of age: improved techniques and complementary approaches. Nat. Rev. Mol. Cell Biol. **15**: 591–600.

Neff, M.M., Turk, E., and Kalishman, M. (2002). Web-based primer design for single nucleotide polymorphism analysis. Trends Genet. **18**: 613–615.

Ng, P.C. and Henikoff, S. (2001). Predicting deleterious amino acid substitutions. Genome Res. **11**: 863–74.

Ng, P.C. and Henikoff, S. (2003). SIFT: Predicting amino acid changes that affect protein function. Nucleic Acids Res. **31**: 3812–4.

Panteris, E., Adamakis, I.-D.S., Voulgari, G., and Papadopoulou, G. (2011). A role for katanin in plant cell division: microtubule organization in dividing root cells of fra2 and lue1Arabidopsis thaliana mutants. Cytoskeleton (Hoboken). **68**: 401–13.

Paredez, A.R., Somerville, C.R., and Ehrhardt, D.W. (2006). Visualization of cellulose synthase demonstrates functional association with microtubules. Science **312**: 1491–5.

Pautler, M., Tanaka, W., Hirano, H.Y., and Jackson, D. (2013). Grass meristems I: shoot apical meristem maintenance, axillary meristem determinacy and the floral transition. Plant Cell Physiol **54**: 302–312.

Ray, P.M., Green, P.B., and Cleland, R. (1972). Role of Turgor in Plant Cell Growth. Nature **239**: 163–164.

Sassi, M. et al. (2014). An auxin-mediated shift toward growth isotropy promotes organ formation at the shoot meristem in Arabidopsis. Curr. Biol. **24**: 2335–42.

Schnable, J.C., Springer, N.M., and Freeling, M. (2011). Differentiation of the maize subgenomes by genome dominance and both ancient and ongoing gene loss. Proc. Natl. Acad. Sci. U. S. A. **108**: 4069–74.

Taguchi-Shiobara, F., Yuan, Z., Hake, S., and Jackson, D. (2001). The fasciated ear2 gene encodes a leucine-rich repeat receptor-like protein that regulates shoot meristem proliferation in maize. Genes Dev **15**: 2755–2766.

Tamura, K. and Nei, M. (1993). Estimation of the number of nucleotide substitutions in the control region of mitochondrial DNA in humans and chimpanzees. Mol. Biol. Evol. **10**: 512–26.

Uyttewaal, M., Burian, A., Alim, K., Landrein, B., Borowska-Wykręt, D., Dedieu, A., Peaucelle, A., Ludynia, M., Traas, J., Boudaoud, A., Kwiatkowska, D., and Hamant, O. (2012). Mechanical stress acts via katanin to amplify differences in growth rate between adjacent cells in Arabidopsis. Cell **149**: 439–51.

Vajjhala, P.R., Wong, J.S., To, H.-Y., and Munn, A.L. (2006). The beta domain is required for Vps4p oligomerization into a functionally active ATPase. FEBS J. **273**: 2357–73.

Weigel, D. and Glazebrook, J. (2002). Arabidopsis: A laboratory manual (Cold Spring Harbor Laboratory Press: New York).

Wightman, R. and Turner, S.R. (2007). Severing at sites of microtubule crossover contributes to microtubule alignment in cortical arrays. Plant J. **52**: 742–51.

Xiang, C., Han, P., Lutziger, I., Wang, K., and Oliver, D.J. (1999). A mini binary vector series for plant transformation. Plant Mol. Biol. **40**: 711–717.

Yang, F., Bui, H.T., Pautler, M., Llaca, V., Johnston, R., Lee, B., Kolbe, A., Sakai, H., and Jackson, D. (2015). A maize glutaredoxin gene, abphyl2, regulates shoot meristem size and phyllotaxy. Plant Cell **27**: 121–31.

Zhang, G. et al. (2012). Genome sequence of foxtail millet (Setaria italica) provides insights into grass evolution and biofuel potential. Nat. Biotechnol. **30**: 549–554.

Zhang, Q., Fishel, E., Bertroche, T., and Dixit, R. (2013). Microtubule severing at crossover sites by katanin generates ordered cortical microtubule arrays in Arabidopsis. Curr. Biol. **23**: 2191–5.

CHAPTER 3. NATURALLY-OCCURRING ALLELES OF *KTN1B* MODIFY THE PHENOTYPE OF *CLT1-1*

3.1 Introduction

Geneticists have long observed that mutations can have dramatically different effects depending on the genetic background of the mutant (reviewed in Nadeau, 2001). The specific genes responsible for altering the expression of a phenotype are called modifiers; identifying modifiers that either enhance or suppress a mutant phenotype helps both to elucidate the function of the initial gene and to reveal additional genetic components controlling a particular trait. Enhancer/suppressor screens (reviewed in Page and Grossniklaus, 2002) are conducted by observing a mutant in diverse genetic contexts and looking for altered expression of the mutant phenotype. Induced genetic variation (e.g. treatment with mutagens such as ethyl methanesulfonate (EMS)), is often used to create modifier alleles. However, natural variation provides an alternate source of genetic variation and should, presumably, be especially fruitful in genetically diverse species such as maize, an outcrossing crop.

Utilization of natural variation as a source for modifier alleles allows the discovery of genetic variants caused by more diverse structural changes compared with changes caused by commonly used mutagens. For example, EMS typically causes G/C to A/T transitions and transposon-tagging strategies would, by definition, cause insertion mutations. On the other hand, modifier alleles discovered from natural variation should reflect more diverse mechanisms. Another advantage of identifying natural genetic variants is that understanding why the causal variant has persisted over many generations may shed light on the evolutionary relationship between the interacting genes.

The highly conserved, microtubule-severing protein, katanin, was first discovered in sea urchin (McNally and Vale, 1993). The p60 component of katanin, which is

responsible for the microtubule-severing activity, is encoded by *KATANIN1* (*KTN1*) in *Arabidopsis thaliana* and by the ortholog, *dwarf and gladius leaf1* (*dgl1*), in rice (*Oryza sativa*). Mutants of this gene in both species have a short stature and more compact organs that are thought to be caused by defective cell growth anisotropy (Bichet et al., 2001; Burk et al., 2001; Komorisono et al., 2005). Formation of cell shape is guided by rigid cellulose microfibrils (CMFs) in the cell wall that can organize into transverse rings to make elongation biased towards the longitudinal axis (Green, 1962; Ray et al., 1972). These patterns of CMFs are templated by a network of cortical microtubules (CMTs) in the cell cortex, a layer directly below the plasma membrane (Paredez et al., 2006). KTN1 is required for uniform, transverse CMTs and thus facilitates the organization of CMFs into transverse arrays that promote cell elongation (Burk et al., 2001). In addition, KTN1 has been implicated in other roles that involve the rearrangement of microtubules, such as during mitosis (Panteris et al., 2011), and in growth responses to phytohormones like gibberellins and auxins (Bouquin et al., 2003; Komorisono et al., 2005; Xu et al., 2010; Sassi et al., 2014).

In Chapter 2, results were presented indicating that the partially dominant *Clt1-1* allele in maize is caused by a missense mutation affecting the ATPase domain of one of the two *KTN1* co-orthologs in maize (GRMZM2G017305). To better understand the function of the *clt1* gene in maize, a screen was conducted for naturally occurring genetic modifiers. To this end, the mutant *Clt1-1* was crossed to the Nested Association Mapping (NAM) population founder lines, a panel of maize inbred lines selected to maximize genetic variation between each line (Yu et al., 2008; McMullen et al., 2009). Several NAM lines were found to harbor modifiers of *Clt1-1*, causing a novel phenotype where *Clt1-1*/+ plants became even shorter and had upper internodes that were especially compressed. Data discussed in this work suggest that the modifiers in these lines are alleles of *ktn1b* (GRMZM2G054715), the homoeolog of *clt1*. Previous work with *KTN1* in *Arabidopsis* and *dgl1* in rice, show no closely related paralogs in these species (see Chapter 2). The identification of *ktn1b* alleles as modifiers of *Clt1-1* in maize provides tools to understand *KTN1*-like function in a system where there are two closely related homoeologs of this gene due to a recent whole-genome duplication (WGD) (Schnable et

al., 2011). In addition, we discuss the phenotype of *Clt1-1*/+; *ktn1b*/*ktn1b* double mutants, the characterization of different naturally occurring *ktn1b* alleles, sequence divergence between *clt1* and *ktn1b*, and a hypothetical model for how *clt1* and *ktn1b* work together to control internode elongation in maize.

3.2 Materials and Methods

3.2.1 Growth conditions

Experiments involving mature plants were grown in the field in West Lafayette (WL), IN during the summer. Experiments involving seedlings were grown under greenhouse conditions as described in Chapter 2.

3.2.2 Screening for modifier genes of *Clt1-1* using the NAM founder lines

Over the course of 3 field seasons, the 26 NAM founder lines (Yu et al., 2008) were crossed by *Clt1-1*/+ (backcrossed at least 8 times into B73), and F2 families were created by sib-mating wildtype and mutant F1 plants. As crosses for the different lines were made, the F2 families were visually screened for modified phenotypes in *Clt1-1*/+ plants.

3.2.3 Bulked segregant analysis (BSA) to map the modifier gene of *Clt1-1*

Twenty modified *Clt1-1*/+ plants, identified by reduced upper internodes and shorter plant height, and 20 normal *Clt1-1*/+ plants were selected from an F2 family derived from a sib-mating of F1 plants of the cross between inbred line Ki11 and *Clt1-1*/+ (BC8 to B73). Equal numbers of leaf discs were collected from each individual and pooled independently for modified plants and normal plants. DNA was extracted from each pool, and also from the inbreds B73 and Ki11. Samples were sent to DNA Landmarks (Quebec, Canada) for genotyping on the MaizeSNP50 BeadChip (Illumina, CA, USA) that interrogated approximately 50,000 SNPs distributed throughout the maize genome. The data returned consisted of a frequency of the reference allele (B73) for each SNP.

Based on the genotyping results of the B73 and Ki11 samples submitted, markers that were not polymorphic between B73 and Ki11 were discarded, along with markers with heterozygous genotypes. For each of the 24,383 remaining markers, the differences between the allele frequencies of the pool of modified *Clt1-1*/+ plants versus the pool of normal *Clt1-1*/+ plants, inbred Ki11 versus the modified *Clt1-1*/+ pool, and inbred Ki11 versus the normal *Clt1-1*/+ pool were calculated and plotted against the physical location of each marker.

3.2.4 Genotyping of *ktn1b* and *clt1*

For experiments where the genotype of the modifier locus or its putative causative gene, *ktn1b*, is described, plants were genotyped because variation in expressivity made it difficult to classify all plants visually. KASP assays (LGC genomics; formerly KBioscience) were designed and made for two SNPs. The first is ss229806741 (AGCTCCCGTTTCCTTGGGACGGAGGCGATATTGCCACGCACCGGCGCCGA[G/A]TTGTACACGCGGAAACGGATTTGAGGGCGATGATGTGGCGTGGCAGCTGC), chosen from maize HapMap data (Gore et al., 2009) and located at Chr 3: 207,101,563 bp, about 1 Mb away from *ktn1b*. The second is kat3_Ki11_in5 (ACGTAGGAGAAAGCATAAGGAACTACAATTTGAATAGAGGGAATATGTTA[G/C]TAACTTACTAYTGTTCACATTAATGTGCATTATGTTGACTTCTAAATTGC), chosen based on sequencing of a part of the *ktn1b* genomic region in Ki11 (Appendix B) and located at Chr 3: 208,123,562, which is in intron 5 of *ktn1b*. The marker kat3_Ki11_in5 was used except in Figure 3.2A, and the CML333 and M37w backgrounds in Figure 3.4B due to kat3_Ki11_in5 not yet being available at the time or lack of polymorphism with B73 respectively. KASP assays were run according to manufacturer instructions, on a Roche LightCycler 480.

In mature plants, the genotype of *Clt1-1* plants was determined by the phenotype, but the DraI dCAP marker described in Chapter 2 was utilized for Figure 3.3 because the *Clt1-1* phenotype can be ambiguous at the seedling stage.

3.2.5 Shoot apical meristem dissections

Seedlings were genotyped for both *clt1* and *ktn1b* as soon as enough leaf tissue emerged (approximately V1). Shoot apical meristems (SAM) were dissected from seedlings 14 days after planting (DAP), fixed in formalin–acetic acid–alcohol (FAA) and cleared by methyl salicylate as described in Chapter 2.

3.2.6 Sequencing and RT-PCR for *ktn1b* in different NAM inbreds

To better understand the *ktn1b* alleles in the different NAM lines examined in this work, we initially attempted to sequence genomic DNA (gDNA) for the *ktn1b* region. Portions of Ki11 and to a lesser extent, Mo18w, were successfully sequenced by running BigDye (Applied Biosystems) reactions on PCR products from primers that amplified ~1 kb fragments spanning the *ktn1b* region (Table 3.1). Ultimately, a cDNA approach was pursued because many gDNA primers did not amplify. Some primer pairs amplified only with B73 template suggesting sequence divergence between inbreds at those primer sites, but some primer pairs selected using the B73 reference genome sequence did not amplify even with B73 template DNA, suggesting that those regions of *ktn1b* may have physical constraints that inhibit efficient PCR.

Total RNA was extracted from individual mesocotyls of newly emergent seedlings for each inbred line using TRIzol reagent according to manufacturer instructions (Invitrogen). cDNA was produced using an oligo-dT primer and SuperScript III reverse transcriptase (Invitrogen) according to manufacturer instructions. For initial assessment and sequencing, amplification was done with primers binding the 5’ and 3’ untranslated regions (UTR) (Table 3.1) using Phusion high-fidelity polymerase (Thermo Fisher Scientific). Gel fragments were purified for each line, cloned into pGEM-T Easy vectors (Promega), and sequenced using BigDye and the cloning primers. For verification of splice variants and clarification of the exons/introns involved, primers flanking sub-sections of the *ktn1b* cDNA (Table 3.1) were used for amplification using ExTaq polymerase (Takara).

RNA from CML333, and B73 as a control, were also amplified using a 3’ Rapid Amplification of cDNA Ends (3’ RACE) approach to investigate premature termination

of CML333 *ktn1b* transcripts. The procedure was adapted from an existing protocol (Scotto-Lavino et al., 2006). Briefly, reverse transcription was carried out as before but with a modified oligo-dT primer, Q_t (Table 3.1), designed to bind to the 5' end of the poly-A tail and add an adapter for subsequent amplification. Next, primer Q_o, which binds to the adapter added by the Q_t primer, was used together with the 5' UTR primer to amplify the cDNA using Q5 high-fidelity polymerase (NEB). Gel fragments were purified, cloned and sequenced as described above.

3.2.7 Comparisons with *KTN1* orthologs in sorghum and rice

Phylogenetic analysis (Figure 2.1A) revealed two predicted genes in sorghum (*Sorghum bicolor*) and one in rice (*Oryza sativa* L. ssp. *Japonica*) that are highly related to *KTN1* (AT1G80350) from *Arabidopsis*. Out of the two *KTN1* homologs in sorghum, Sobic.003G259400 has been shown to be orthologous to maize *clt1* and *ktn1b* via synteny of neighboring genes (Schnable et al., 2011) and Sobic.010G114200 may be undergoing pseudogenization according to expression data discussed below, so Sobic.003G259400 was considered to best represent functional, orthologous sequence in sorghum. For rice, LOC Os01g49000 was taken as the putative ortholog because it was the only highly related homolog as identified by the phylogenetic analysis; also the rice *dgl1* mutant is caused by mutations in this gene and its phenotype strongly resembles *ktn1* in *Arabidopsis* (Komorisono et al., 2005).

3.2.8 Analysis of HapMap3 data

To identify polymorphisms in *clt1* and *ktn1b* among diverse maize lines, the maize HapMap3 dataset was utilized (Bukowski et al., 2015). This dataset consists of whole-genome sequencing of approximately one thousand maize varieties and one *Tripsacum* line, aligned to the B73 AGPv3 reference genome. A variant call format (VCF) file containing genotypes, including imputations, was downloaded from the CyVerse Data Store according to the instructions on Panzea (http://www.panzea.org/).

Calculations of nucleotide diversity (π; Nei, 1987) among the HapMap3 lines for *clt1* and *ktn1b* were conducted using only SNPs, excluding indels. First, *ktn1b* sequences

were re-constructed for each maize line by substituting the HapMap3 SNPs into the B73 reference sequence using the GATK tool, FASTAAlternateReferenceMaker (McKenna et al., 2010). The sequences were aligned with the MUSCLE algorithm (Edgar, 2004) and analyzed with DnaSP v5 (Librado and Rozas, 2009) to determine π for synonymous and nonsynonymous sites.

Effects for each polymorphism were predicted using SnpEff (Cingolani et al., 2012) with reference gene models from the B73 AGPv3 genome. Heterozygous genotypes were assumed to be genotyping errors and were not considered.

3.3 Results

3.3.1 A modifier gene in the inbred Ki11 causes a novel *Clt1-1*/+ phenotype

To better understand the genetic interactions that underlie *clt1* function in maize, *Clt1-1* was crossed with the NAM founder lines to screen for modifier genes. A novel phenotype of *Clt1-1*/+ plants was observed in the F2 with Ki11, where *Clt1-1*/+ plants were even shorter, with internode shortening that was more severe in the upper internodes (Figure 3.1A, B). In addition, these modified *Clt1-1*/+ plants tended to make non-functional and under-developed tassels (Figure 3.1C), and ears were never observed.

In order to map the gene causing this modification of the *Clt1-1*/+ phenotype, a bulked segregant analysis (BSA) approach was used by genotyping separate pools of normal *Clt1-1*/+ and modified *Clt1-1*/+ plants segregating within an F2 family of a cross with Ki11 using a SNP array that interrogates ~50,000 SNPs across the maize genome. For each pool of DNA, a SNP index was obtained for each SNP on the array, ranging from 0 to 1, with the maximum and minimum values corresponding to homozygous genotypes of the two possible alleles. In a plot of the difference in allele frequencies between the two pools of DNA at each SNP, the region containing the modifier gene would be expected to peak at 0.66, while other regions should be close to 0. The BSA results for the *Clt1-1* modifier gene revealed such a peak on the long arm of Chr 3 (208,122,523-208,133,257 bp), a region that contains *ktn1b*, the duplicate gene of *clt1* (Figure 3.1D). The location of this peak was corroborated by plotting the differences in

allele frequencies between the Ki11 inbred parent and the modified *Clt1-1*/+ pool, which indicated strong enrichment for Ki11 genotypes at the same region (Figure 3.1E). Plots of the differences in allele frequencies between Ki11, and either modified or normal *Clt1-1*/+ pools both show a peak on Chr 8 with a maximum of around 0.75 that corresponds to *clt1* and reflects the fact that *Clt1-1* had been introgressed into B73 prior to crossing with Ki11 (Figure 3.1E, F). This serves as genotypic confirmation that the modified plants were indeed *Clt1-1*/+ plants despite the atypical phenotypes.

3.3.2 Interaction between *clt1* and the modifier gene

Because the expressivity of the modified phenotype varied, it was difficult to identify with complete certainty by phenotype which plants were homozygous for the Ki11 modifier gene. Information about the location of the modifier gene from the BSA results allowed markers to be designed to identify plants by genotype and quantify traits for each genotypic class.

To characterize internode shortening without having to remove leaves, the length of an internode was approximated using the distance between the ligules of flanking leaves. Using this proxy, the ratio of the lengths of the 2nd and 8th internodes (counting downwards from the tassel) was reduced by the Ki11 allele of the Chr 3 modifier gene in an additive manner, but only in the *Clt1-1*/+ plants (Figure 3.2A). In contrast, the Chr 3 modifier gene from Ki11 had no effect in sibling plants that did not carry a *Clt1-1* mutation, indicating that interaction between *Clt1-1* and the Ki11 modifier gene creates the compressed upper internodes of the modified plants. Within the modified *Clt1-1*/+ plants, the top three internodes were comparably short (Figure 3.2B). As expected, the lower internodes, assayed by the 7th to 9th internodes from the tassel, were substantially longer but became progressively shortened going upwards, suggesting that the compression of upper internodes is caused by a somewhat gradual change as opposed to a sudden transition (Figure 3.2B). Similar to upper internode length, plant height also showed an interaction between *Clt1-1* and the modifier gene. But, this effect was not additive, with the B73 allele being incompletely dominant over the Ki11 allele (Figure 3.2C). Finally, both SAM height and width were decreased in *Clt1-1*/+ plants that were

homozygous for the Ki11 modifier allele (Figure 3.3A, B). However, these changes in meristem shape are unlikely to be the direct cause of the shortened internodes because internode elongation is mainly driven by the elongation of cells created from intercalary meristems at the bases of elongating internodes (Nemoto et al., 2004).

3.3.3 Ki11 has low *ktn1b* expression and other low-expressing NAM lines also modify *Clt1-1*/+

Because *ktn1a* was already suspected to be the causative gene of *Clt1-1* (see Chapter 1), *ktn1b* became a gene of interest when BSA results mapped the Ki11 modifier to its region on Chr 3. Interestingly, publicly available RNA-seq data (QTeller) for seedling shoot apex tissue indicated that Ki11 is a low-expressing line of *ktn1b* compared to other NAM founder lines while B73 is a high-expressing line (Figure 3.4A). Other NAM founder lines ranged from low-level *ktn1b* expression, comparable with Ki11, to substantially higher expression similar to B73. Thus, we hypothesized that the modified phenotype of *Clt1-1*/+ plants involved reduced expression of *ktn1b* and that the other low-expressing lines would also modify the phenotype of *Clt1-1*/+ in a manner similar to Ki11.

To test this hypothesis, four low *ktn1b* lines and two high *ktn1b* lines were chosen for closer examination (Figure 3.4A). Note that Mo18w was chosen for this experiment based on output from an older version of QTeller which indicated an expression level that was more similar to the other low *ktn1b* lines, but output from an updated version of QTeller (using a newer version of Cufflinks) indicated moderately high *ktn1b* transcript levels for Mo18w relative to the other lines (Figure 3.4A). *Clt1-1*/+ plants from the F2 of crosses between *Clt1-1*/+ (B73) and these 6 lines were genotyped for *ktn1b*, and plant heights were measured to quantify the modified phenotype. Consistent with our hypothesis, homozygotes of the alleles from the high *ktn1b* lines were the same height as sibling plants homozygous for the B73 allele (Figure 3.4B). However, low *ktn1b* expression was not a good predictor for modification of the *Clt1-1*/+ phenotype. Mo18w had a strong reduction in plant height despite having moderately high *ktn1b* expression and CML228 behaved like a weak *ktn1b* allele, producing a significant but weaker

reduction in plant height compared to other low *ktn1b* lines. Thus, expression level of *ktn1b* alone cannot explain the modification of the *Clt1-1*/+ phenotype, suggesting other molecular defects are present in the *ktn1b* alleles of the lines that modify *Clt1-1*/+, and these are discussed below.

Importantly, the modified *Clt1-1*/+ plants from these lines also had relatively compressed upper internodes (Figure 3.5) similar to the modified plants in the Ki11 F2 and consistent with a shared genetic mechanism for modifying the *Clt1-1*/+ phenotype. In order to provide more support that the same gene was causing the modified phenotypes in these different NAM lines, each of the founder lines selected above was crossed by an F1 *Clt1-1*/+ plant from a cross between Ki11 and *Clt1-1*/+, producing progeny that were heterozygous with the allele from the NAM line that the F1 was crossed to and either the Ki11 or the B73 allele of the modifier gene. Short plants with compressed upper internodes could be recapitulated only in plants that were heterozygous for the Ki11 modifier allele and a modifier allele from another line that can modify *Clt1-1*/+ (Figure 3.6) and these plants were more strongly reduced in plant height than for corresponding plants in crosses with lines that do not modify *Clt1-1*/+ (Figure 3.7). Note that these differences in the effect of the Ki11 modifier allele compared to the B73 allele (Figure 3.7) were not tested statistically due to insufficient seed for planting replicates of each background.

3.3.4 Other defects in *ktn1b* in the NAM lines that modify *Clt1-1*/+ besides low expression

In an effort to understand the *ktn1b* alleles in inbred lines that produce modified *Clt1-1*/+ plants, we attempted to sequence *ktn1b* from the gDNA of the lines examined above. Parts of Ki11 and Mo18w *ktn1b* were sequenced (Appendix B), but many of the primer pairs did not produce amplicons and ultimately cDNA was sequenced instead, leading to several surprising findings. Amplification using the Ext_F and Ext_R primers that bind to the 5'UTR and the 3'UTR respectively produced a major product at the expected size of 1.7 kb only in the lines that either weakly modified *Clt1-1*/+ plants or did not modify *Clt1-1*/+ at all, namely CML228, B73, M37w and NC358 (Figure 3.8A,

B). *ktn1b* cDNAs showed a variety of defects in the lines that modified *Clt1-1*/+ (Figure 3.8A, B). In CML333, there appeared to be no amplification at any size. In Ki3 and Ki11, there were amplicons of various sizes of comparable band intensities indicating frequent alternative splicing. In Mo18w, there was a major product a few hundred base pairs less than the expected length.

Sequencing clones of the cDNA amplicons revealed different splicing and transcription patterns in these inbred lines (Appendix C). The Mo18w transcript was missing exon 2, a 466 bp fragment (Figure 3.8C). Excision of exon 2 removes most of the MT-binding domain-encoding portion of *ktn1b* and produces a brief frameshift that is restored to the correct frame by a nearby downstream 7 bp insertion (Figure 3.9). Assuming there are no indels in exon 2 (partially sequenced from gDNA, Appendix B), this 7 bp insertion causes a premature stop codon in transcripts where exon 2 does not get excised (Figure 3.9). Sequencing intron 1 in Mo18w gDNA showed that the splicing donor and acceptor sites were intact and were not responsible for the excision of exon 2 (Appendix B).

Sequencing Ki3 and Ki11 revealed an 8 bp deletion towards the 3' end of the gene, which causes a frameshift that alters a predicted C-terminal oligomerization domain (Figure 3.8D; Figure 3.9) and begins only 10 residues downstream of the first affected residue in an *Arabidopsis ktn1* allele that conditions a strong mutant phenotype (Burk et al., 2001). Sequencing Ki3 and Ki11 also revealed the sequences of three of the six spliceforms indicated by the Ext_F/Ext_R amplification (Figure 3.8D-F; Figure 3.9). In the first two spliceforms, a portion of intron 1 containing an in-frame stop codon is retained and exon 3 is excised. In one of these spliceforms, exon 3 is replaced by a novel 54 bp sequence containing another in-frame stop codon and sharing homology with a Prem1 Gypsy retroelement (50/54 nt identical, e-value = 4.2e-16; Wessler et al., 2009). In the other spliceform, exons 2 and 4 are directly spliced together. In the third spliceform, exons 2-5 are excised, removing 2/3 of the predicted protein sequence including most of the ATPase domain. Importantly, there was substantial product that appeared to be the correct size, in addition to the aberrant spliceforms (Figure 3.8E, F). Nonetheless, the combination of the deletion at the 3' end, weakened expression and the likely

nonfunctional isoforms should be highly deleterious. Note that the spliceform containing the 54 bp sequence was identified by sequencing in Ki3 cDNA only, while the other two spliceforms were identified only in Ki11 sequences, but PCR results support the presence of all three spliceforms in both lines (Figure 3.8E, F). Partial sequence of Ki11 gDNA showed that the splicing acceptor site was intact for intron 3, and both donor and acceptor sites were intact for introns 4-6 (Appendix B). Other donor and acceptor sites were not sequenced successfully.

Although no product was obtained for CML333 cDNA using the Ext_F-Ext_R primers initially (Figure 3.8B), increasing the number of PCR cycles produced a weakly amplified product, probably facilitated by residual amounts of the oligo-dT primer used for cDNA synthesis acting as a reverse primer (not shown). This product was cloned and sequenced, and showed two different spliceforms that both terminate after exon 5, but that differ in the part of intron 5 retained (Figure 3.8G), leading to loss of approximately the last 25% of the protein (Figure 3.9). This premature transcript termination was confirmed using 3' RACE (Figure 3.8H), which adds an adapter to the 3' end of transcripts via a modified oligo-dT primer. Sequencing the product from 3'RACE revealed a third spliceform, in which the beginning of the retained intron 5 was identical with one of the previous spliceforms, but the transcript was terminated 46 nucleotides earlier (Figure 3.8G).

Overall patterns of gel bands (Figure 3.8 B, E, F, H) were reproduced when the same PCRs were repeated with two separate tissue samples for each NAM line (Appendix D), indicating that the transcription defects described above are consistent in each line. Among the NAM lines that either did not modify *Clt1-1*/+ plants or did so only weakly, and that produced *ktn1b* transcript of the correct size, several missense mutations were found in CML228 and NC358 although there were no obvious deleterious polymorphisms (Figure 3.9). M37w *ktn1b* cDNA was 100% identical to B73.

3.3.5 Expression patterns of *ktn1b* and *clt1*

The lack of obvious defects in *clt1-2* homozygotes (Chapter 2) or NAM inbreds that are homozygous for deleterious *ktn1b* alleles suggests functional redundancy

between *clt1* and *ktn1b*, and this idea is supported by the 97.48% amino acid identity between KTN1B and CLT1 predicted proteins (Figure 3.10A). Among the NAM inbreds, lower *ktn1b* expression was not compensated by elevated *clt1* expression (Qteller; Figure 3.10B). In fact, there was substantially less variation in *clt1* expression at the shoot apex among the NAM lines than for *ktn1b*, with roughly 2-fold and 5-fold differences between the lowest and highest NAM lines for *clt1* and *ktn1b* respectively. In a separate published RNA-seq dataset for B73 only (Sekhon et al., 2013; Stelpflug et al., 2015), *clt1* is expressed at consistent levels in most tissue types tested while *ktn1b* expression fluctuates dramatically (Figure 3.11). Overall, *ktn1b* expression was comparable to *clt1* in tissue expected to have high cell growth and division activity but was substantially lower in tissue expected to have low cell growth and division. For example, *ktn1b* expression was comparable to *clt1* at the base of leaves but much lower at leaf tips, comparable to *clt1* in developing leaves but lower in mature leaves, and comparable to *clt1* in developing internodes but lower in fully grown internodes.

3.3.6 Divergence of gene structure between *ktn1b* and *clt1*

Based on the B73 reference genome, introns in *ktn1b* are substantially larger than those in *clt1*, causing an increase in gene size of about 4 kb (Figure 3.12A). Furthermore, comparisons with two closely-related homologs in sorghum (see Chapter 2) suggest these larger *ktn1b* introns are a result of *ktn1b*-specific intron expansion (Figure 3.12A). Interestingly, BLASTn searches against a maize transposable element database (Wessler et al., 2009) suggest that *ktn1b*-unique regions in introns 3 and 5 are at least partially derived from transposable elements (Figure 3.12A).

In the promoter region, an approximately 80 bp region is homologous between *clt1* and Sobic.003G259400, but only partially conserved in Sobic.010G114200 and not conserved in *ktn1b* (Figure 3.12A, B). Importantly, Sobic.010G114200 appears to be in the process of being pseudogenized with public RNA-seq data indicating transcript levels two to three orders of magnitude weaker than Sobic.003G259400 in all tissues examined, suggesting that Sobic.003G259400 best represents the functional sequence for sorghum (Table 3.2).

These data suggest that potentially regulatory sequences in maize *ktn1b* have diverged from *clt1* and this may explain the expression differences between these two genes in 'mature' tissues, as described above (Figure 3.11).

3.3.7 Deleterious polymorphisms are more common in *ktn1b* than *clt1* among natural variation represented by the maize HapMap3

The combination of *Clt1-1* and a loss-of-function allele, *clt1-2*, leads to a severe, distinctive phenotype resembling *Clt1-1* homozygotes (see Chapter 2). Assuming this phenotype is representative of the interaction between *Clt1-1* and loss-of-function *clt1* alleles in general, strong loss-of-function *clt1* alleles likely do not exist among the NAM founder lines because such a phenotype was not observed in any of the crosses between *Clt1-1*/+ and the NAM founders during the modifier screen (not shown). This suggests a preferential loss of *ktn1b* function and retention of *clt1* function among the NAM founder lines.

To test this idea further, the maize HapMap3 (Bukowski et al., 2015) dataset was utilized to reconstruct approximate *clt1* and *ktn1b* sequences for each HapMap3 line to estimate sequence diversity in *clt1* and *ktn1b*. Using this method, the coding sequence of *ktn1b* had a substantially higher ratio of nucleotide diversity between nonsynonymous and synonymous sites compared with *clt1*, suggesting that purifying selection is stronger for *clt1* (Figure 3.13A). To assess the prevalence of potentially deleterious polymorphisms in *ktn1b* and *clt1*, the biological impact of each variant was predicted using SnpEff (Cingolani et al., 2012). "Moderate" polymorphisms include missense changes, codon insertions or deletions that do not affect the reading frame and modifications to the 5' and 3' UTR. "High" impact changes are those that affect the reading frame or cause large changes to the CDS, including gain or loss of start or stop codons, frameshift mutations and loss of splicing donor or acceptor sites. For *clt1*, 13 polymorphisms with "moderate" or "high" impact were identified, while 35 such variants were found for *ktn1b* (Figure 3.13B). Within the *clt1* variants, only one was "high" impact and was found in only one line, Hi27. On the other hand, six "high" impact variants were found for *ktn1b*, with one of these corresponding to the short deletion

identified in the cDNA sequences of Ki3 and Ki11 in this work (Figure 3.8D). Note that the sixth "high" impact variant for *ktn1b* was manually added because the sequence of the Mo18w insertion causing a frameshift under normal splicing (Figure 3.8C) was not included in its annotation in the HapMap data; as a result, its frameshift effect was not detected by SnpEff. Despite the prevalence of splicing defects as documented in this work, no variants were identified in splice donor or acceptor sites for any *ktn1b* introns among the NAM founders.

3.4 Discussion

3.4.1 Loss of *ktn1b* function happened multiple times among NAM founder lines

The results in this work indicate that defects in the homoeolog of *clt1* in maize, *ktn1b*, modify the phenotype of *Clt1-1* mutants and cause *Clt1-1*/+ plants to become even shorter with compressed upper internodes. At least 3 different deleterious alleles of *ktn1b* were identified, one each from CML333 and Mo18w, and one that appears to be shared between Ki3 and Ki11. A weak allele may exist in CML228. The unique natures of the *ktn1b* alleles in Ki3/Ki11, Mo18w and CML333 suggest that these alleles arose independently and this idea is supported by the phylogenetic relationships of these lines, calculated from 21 million SNPs (Hufford et al., 2012). NC358, which has no transcript defects and does not modify *Clt1-1*, is in a sister clade of the clade containing Ki3 and Ki11. Other lines with deleterious *ktn1b* alleles, Mo18w and CML333, are in two more basal clades that both branch off before the divergence of NC358 and Ki3/Ki11, consistent with the Ki3/Ki11 allele forming independently from those in Mo18w and CML333. The likely independent formation of these deleterious *ktn1b* alleles bolsters the idea that *ktn1b*—and not a different, tightly linked gene—is the causative gene of the modified *Clt1-1* phenotype.

3.4.2 A model for *clt1* and *ktn1b* function in maize internode elongation

No obvious phenotypic consequences were observed in the NAM founder lines that were homozygous for deleterious *ktn1b* alleles but homozygous wildtype for *clt1*

(not shown). Because there are only two *KTN1* orthologs in maize (see Chapter 2), *clt1* function likely compensates for loss of *ktn1b* in these inbred lines. This is consistent with the two genes sharing 95.16% and 97.48% identity at the coding sequence and protein level respectively. Addition of a *Clt1-1* allele to plants homozygous for deleterious *ktn1b* alleles revealed cryptic effects of *ktn1b*, presumably by hindering the compensatory effects of *clt1*.

However, *Clt1-1*/*Clt1-1* homozygotes and modified *Clt1-1*/+ phenotypes are distinct from each other, with upper internodes exceptionally compressed in the modified *Clt1-1*/+ plants but uniformly reduced in the *Clt1-1* homozygotes, suggesting that *clt1* and *ktn1b* functions are not identical. We propose an expression-based model (Figure 3.14) to explain the difference in phenotypes between *Clt1-1* homozygotes and modified *Clt1-1*/+ plants. In this model, *clt1* expression is high in lower internodes but decreased in upper internodes. In NAM inbreds with deleterious *ktn1b* alleles, *clt1* activity is sufficient for normal upper and lower internodes. On the other hand, addition of a *Clt1-1* allele reduces CLT1 function and this is especially impactful in the upper internodes where *clt1* expression is lower in the first place, leading to dramatically shortened upper internodes. In *Clt1-1* homozygotes, katanin activity is reduced uniformly along the plant leading to comparable reduction in all internodes. In future studies, qRT-PCR or RNA-seq using tissue from upper and lower elongating internodes will clarify the expression patterns of *clt1* and *ktn1b*. Alternatively, a similar model can be proposed where the decline in *clt1* function in upper internodes is caused by a mechanism that is post-translational instead of transcriptional. A study by Loughlin et al. (2011) found that differences in katanin microtubule-severing activity in two different species of frogs were caused by a single SNP that increased phosphorylation of katanin p60 in the species with less active katanin. If future qRT-PCR results do not support the proposed weakening of *clt1* expression in upper internodes, it would be interesting to test for reduced microtubule-severing activity in protein extracts from upper internodes compared with that of lower internodes in the modified *Clt1-1*/+ plants that could result, for example, from increased phosphorylation of CLT1 in upper internodes.

A second interesting observation is that *Clt1-1*/+; *ktn1b*$^{-}$/*ktn1b*$^{+}$ plants (Figure 3.2C; Figure 3.4B; Figure 3.5) have a relatively mild effect compared with *Clt1-1*/*clt1-2* (see Chapter 2) even though two out of the four *KTN1* homologs are functional in both cases, suggesting that *clt1* is more important than *ktn1b* for proper development. Publicly available RNA-seq data indicate that *ktn1b* expression fluctuates more than *clt1*, with expression sharply suppressed in certain tissues (Figure 3.11). Thus, it is possible that loss of one *clt1* homolog has a larger effect than losing one *ktn1b* homolog because *clt1* accounts for a larger proportion of KTN1 molecules in certain tissues. On the other hand, the tissues with low *ktn1b* expression seem to be mature tissue that are expected to have low cell division and elongation rates, such as leaf tips versus leaf bases, younger leaves versus older leaves, while expression in more developmentally important tissues such as the shoot apex and elongating internode (at V9) were comparable to *clt1* (Figure 3.11). Thus, we postulate that the difference between *clt1* and *ktn1b* is that *clt1*-encoded katanin p60 is more biochemically active than the *ktn1b* version and thus loss of one copy of *clt1* has a larger impact than losing one copy of *ktn1b* (Figure 3.14). Several amino acid substitutions are present between CLT1 and KTN1B (Figure 3.10A). The polymorphism in the ATPase domain is between amino acids with similar R groups, but more drastic amino acid substitutions occur in the predicted microtubule-binding domain and in the oligomerization domain that could conceivably decrease the microtubule-binding or oligomerization efficiencies of KTN1B respectively. *In vitro* microtubule-severing and ATPase assays (as described in Hartman et al., 1998) could test this hypothesis that *ktn1b*-encoded protein is less active than *clt1*-encoded protein.

3.4.3 Maize *ktn1b* is diverging from its homoeolog, *clt1*

Both introns and the predicted promoter region in *ktn1b* appear to have diverged from *clt1* when using sorghum orthologs for comparison (Figure 3.12). The introns in *ktn1b* have expanded considerably, at least partially due to transposon insertions. In the promoter region, there is a sequence of ~80 bp that is conserved between *clt1* and Sobic.003G259400, the dominant paralog in sorghum, but not in *ktn1b*. These changes to

potentially regulatory regions may have caused the differences in the expression profiles of *ktn1b* and *clt1* in 'mature' tissues (Figure 3.11).

Accumulation of nonsynonymous and deleterious mutations among the HapMap3 lines is also increased in *ktn1b* compared with *clt1*, suggesting that *clt1* function is preferentially retained (Figure 3.13). The hypothesis that *clt1* provides more katanin function in maize than *ktn1b*, as discussed above, is consistent with this idea. However, it is puzzling that *clt1-2* homozygotes are not obviously different from wildtype plants (Chapter 2). Why would *clt1* be preferentially retained if losing it has no effect? One possible explanation is that *clt1-2* may not be a null allele and possesses sufficient residual activity for a wildtype phenotype. High-confidence null *clt1* alleles will be needed to test this idea and could be obtained relatively easily using a targeted approach with clustered regularly interspaced short palindromic repeats (CRISPR)/CRISPR-associated (Cas) technology (Jinek et al., 2012), which has been adopted successfully for maize recently (Liang et al., 2014).

3.4.4 Connection between low expression and molecular defects in *ktn1b*?

The molecular characterization of *ktn1b* from Ki3, Ki11 and CML333 suggest a possible association between low *ktn1b* expression (Figure 3.4A), and defects such as aberrant spliceforms, premature transcript termination and indels (Figure 3.8). This relationship, if present, is not absolute because CML228 has no detectable molecular defect, while Mo18w has both defective splicing and an exonic insertion even though it has moderately high *ktn1b* transcript levels. The reduced *ktn1b* expression in Ki3, Ki11 and CML333 could be an artifact of the alternative splicing and premature transcription termination. The shorter mRNA molecules resulting from the alternate isoforms probably contributes to lower RNAseq signals simply because less reads would align to these reduced isoforms. Additionally, the alternate isoforms may produce sequence reads that are difficult to align and may not get attributed to *ktn1b* expression. To rule out these potential technical issues, qRT-PCR could be done using primers that amplify within the 5' UTR and the first exon of *ktn1b,* which are present in all the isoforms sequenced.

In the case of Ki3 and Ki11, lower expression of *ktn1b* may involve nonsense mediated decay (NMD; reviewed in Shaul, 2015). This process curbs the production of potentially harmful partial proteins by degrading transcripts containing premature stop codons, such as those in the alternative isoforms of Ki3 and Ki11. In *Arabidopsis*, NMD of specific genes can be confirmed by observation of increased expression level in mutants where NMD is impaired (Hori and Watanabe, 2005; Yoine et al., 2006), but such mutants have not yet been identified for maize and testing of potential NMD targets will be hampered until such tools are available.

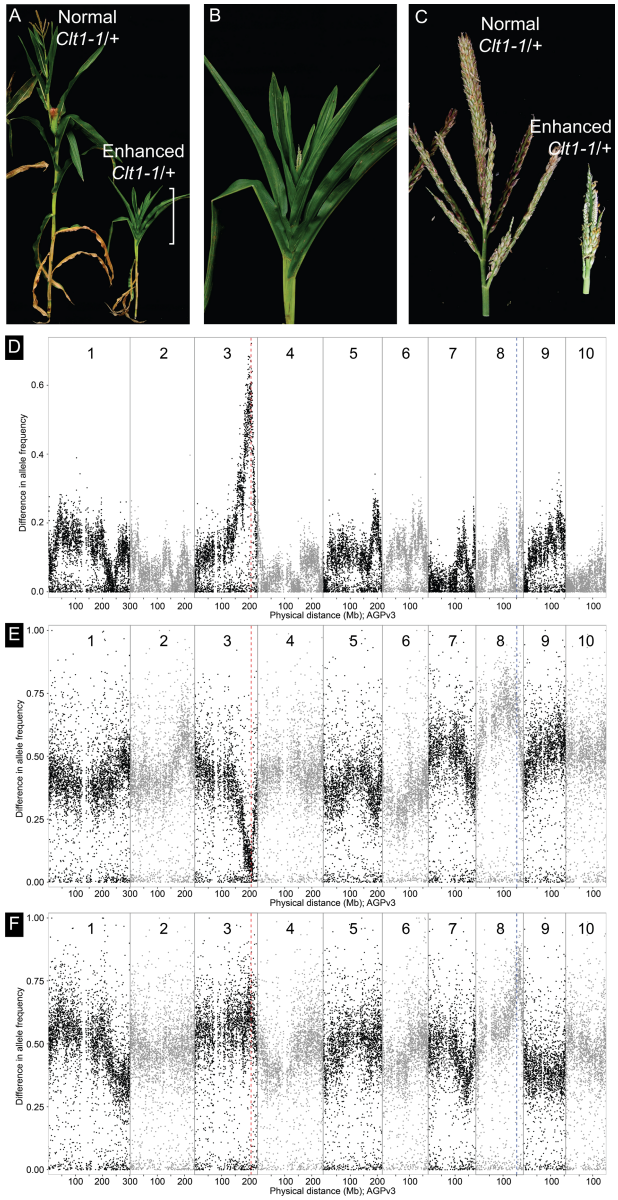

Figure 3.1 The inbred Ki11 harbors a modifier gene, of the mutant *Clt1-1*, that maps to a region on Chr 3 containing *ktn1b*, the homoeolog of *clt1*.

(A) Comparison of a typical *Clt1-1*/+ mutant with a modified *Clt1-1*/+ plant segregating in an F2 family derived from a cross between *Clt1-1*/+ and Ki11. The bracket indicates the compressed upper internodes observed in the modified *Clt1-1*/+ plants. (B) Close-up of the compressed upper internodes in the modified plant shown in panel (A). (C) Close-up of the tassels from the plants shown in panel (A), highlighting the reduced tassel size and poor spikelet development in the modified *Clt1-1*/+ plant. (D) BSA results calculated from the difference in allele frequencies between the normal and modified *Clt1-1*/+ DNA pools. The dotted lines indicate the location of *ktn1b* (red) and *clt1* (blue). (E, F) Difference in allele frequencies between the inbred Ki11, and (E) the modified *Clt1-1*/+ pool or (F) the normal *Clt1-1*/+ pool.

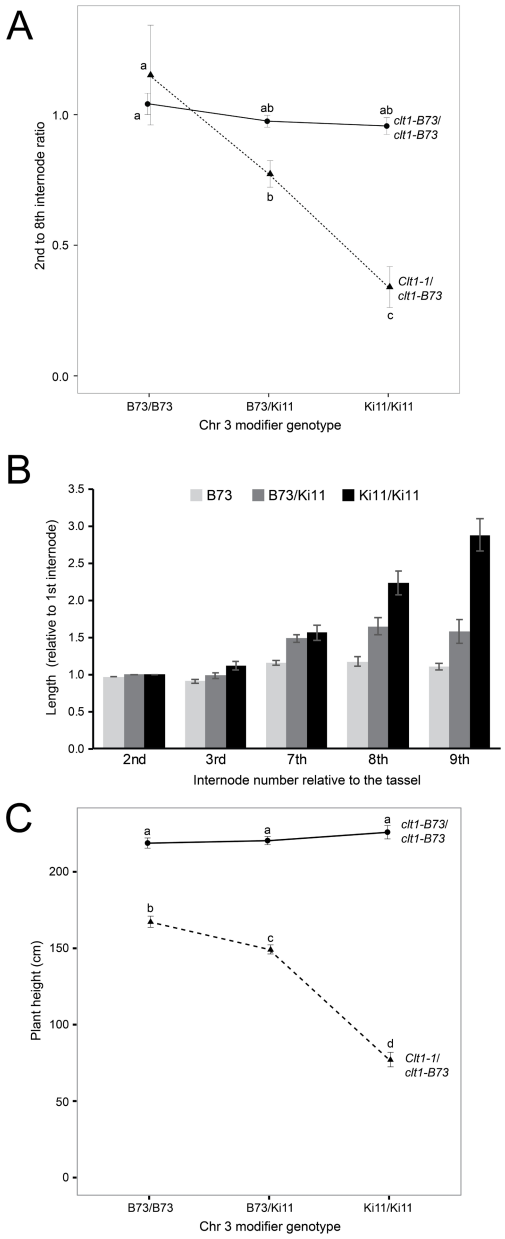

Figure 3.2 In *Clt1-1*/+ plants, the Ki11 modifier gene causes preferential reduction of upper internodes and shorter plant height.

F2 plants derived from sib-mating mutant with wildtype at the F1 of a cross between Ki11 and *Clt1-1*/+ (B73), and grown in (A) WL 2014 or (B, C) WL 2015. (A, B) Internode lengths proxied by distance between ligules of successive leaves. (A) Mean ratio of internode lengths of the 2nd and 8th internodes from the tassel for different *clt1* and *ktn1b* genotypes (n $\geqslant$ 12). (B) Mean internode lengths normalized to the first internode of *Clt1-1*/+ plants with different *ktn1b* genotypes (n $\geqslant$ 15). (C) Mean plant height for different *clt1* and *ktn1b* genotypes (n $\geqslant$ 19). For all panels, error bars indicate SEM and letters indicate Tukey groups at the 0.05 significance level.

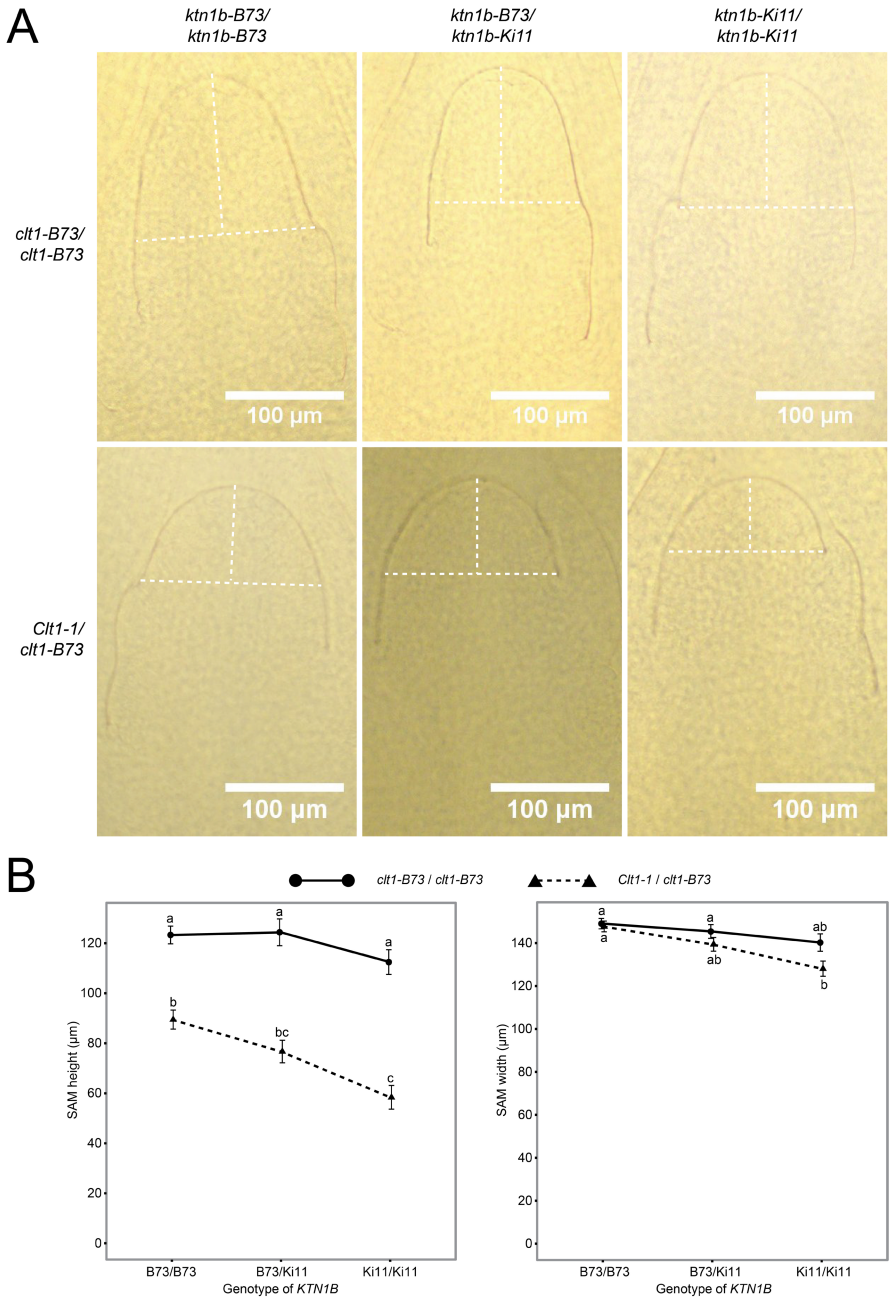

Figure 3.3 In *Clt1-1*/+ plants, the Ki11 modifier gene causes shorter and narrower SAMs.

SAMs from 14 DAP F2 seedlings derived from sib-mating mutant with wildtype at the F1 of a cross between Ki11 and *Clt1-1*/+ (B73). (A) Representative cleared SAMs from different *clt1* and *ktn1b* genotypes. Dotted lines indicate where SAM height and width were measured. (B) Mean (left) SAM height and (right) width for different *clt1* and *ktn1b* genotypes (n ≥ 11). Error bars indicate SEM and letters indicate Tukey groups at the 0.05 significance level.

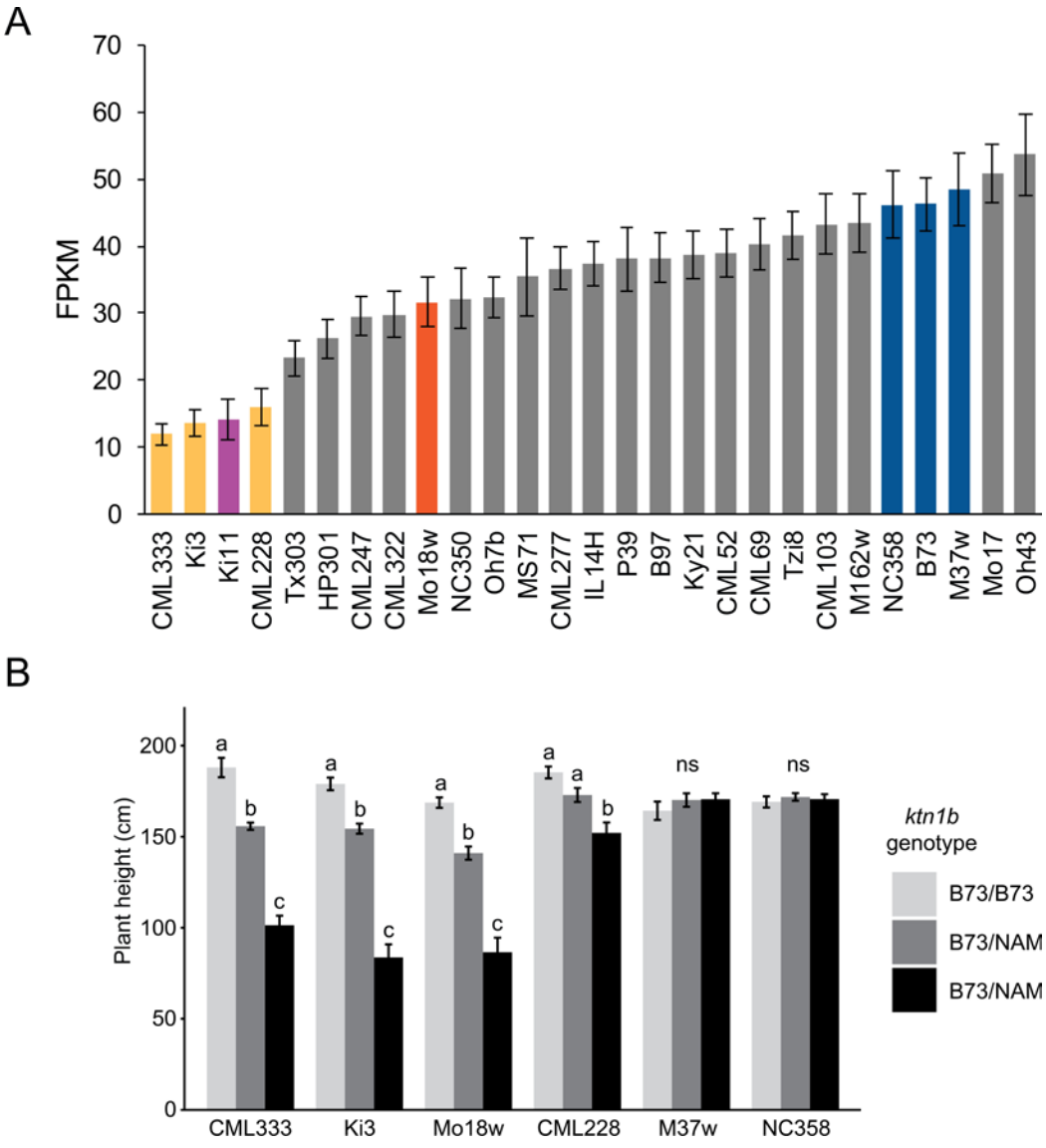

Figure 3.4 Expression of *ktn1b* and the ability to modify *Clt1-1* among different NAM lines.

(A) Expression of *ktn1b* at the shoot apex of 14-day old dark-grown seedlings among the NAM founder lines assessed by RNA-seq read abundance. Bar colors indicate Ki11 (pink), low *ktn1b* lines (yellow), Mo18w (orange), high *ktn1b* lines (blue) and backgrounds not examined in this work (gray). Data produced by Li et al. (2012) and analyzed by QTeller (www.qteller.com). FPKM, Fragments per kilobase of transcript per million mapped reads. Error bars indicate 95% confidence intervals. (B) Mean plant heights of F2 *Clt1-1*/+ individuals with different *ktn1b* genotypes ($n \geq 16$). Plants were derived from sib-mating mutants with wildtypes at the F1 of a cross between each NAM line and *Clt1-1*/+ (B73). Error bars indicate SEM and letters indicate Tukey groups at the 0.05 significance level for *ktn1b* genotypes comparing within each NAM background.

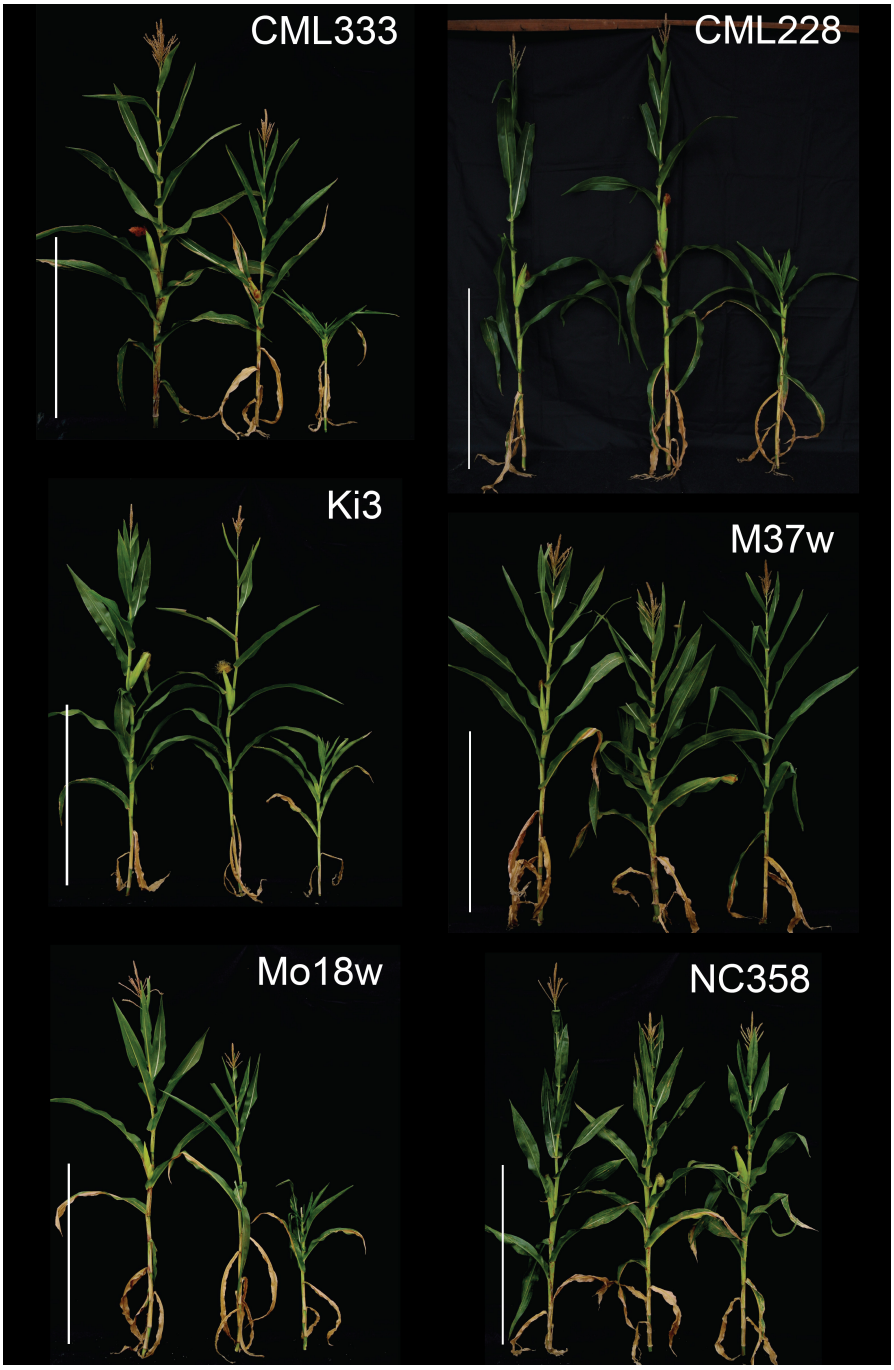

Figure 3.5 Comparison of plant morphology in representative *Clt1-1*/+ plants segregating in F2 families derived from crosses of different NAM lines and *Clt1-1*/+.

In each panel, three *Clt1-1*/+ plants are shown with *ktn1b* genotypes of (left to right) B73/B73, B73/NAM or NAM/NAM. Plants were derived from sib-mating mutants with wildtypes at the F1 of a cross between each NAM line and *Clt1-1*/+ (B73). Panels are adjusted to approximately the same scale. Scale bars indicate 100 cm.

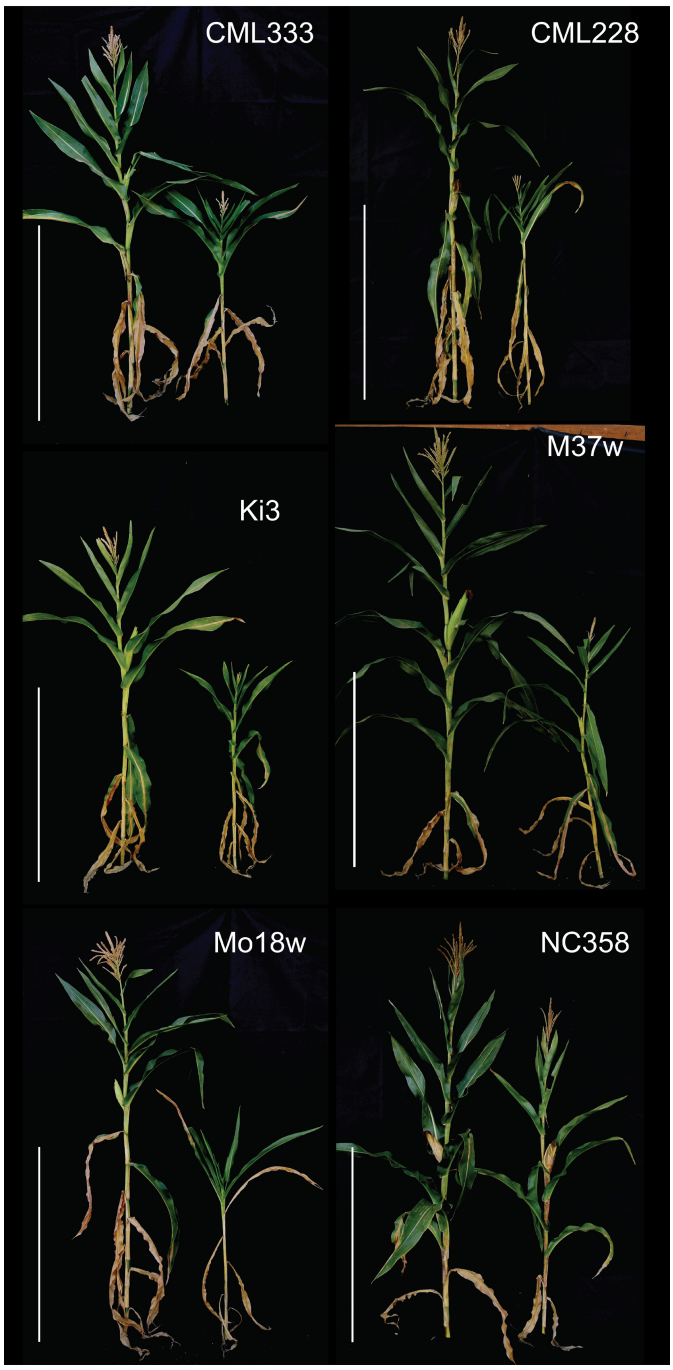

Figure 3.6 Combining *ktn1b-Ki11* with *ktn1b* alleles from NAM lines that modify *Clt1-1*/+ recapitulates the modified *Clt1-1*/+ phenotype

In each panel, two *Clt1-1*/+ plants are shown with *ktn1b* genotypes of (left to right) B73/NAM or Ki11/NAM. Plants were derived from crosses between the respective NAM inbreds and F1 mutants from Ki11 x *Clt1-1*/+ (B73). Panels are adjusted to approximately the same scale. Scale bars indicate 100 cm.

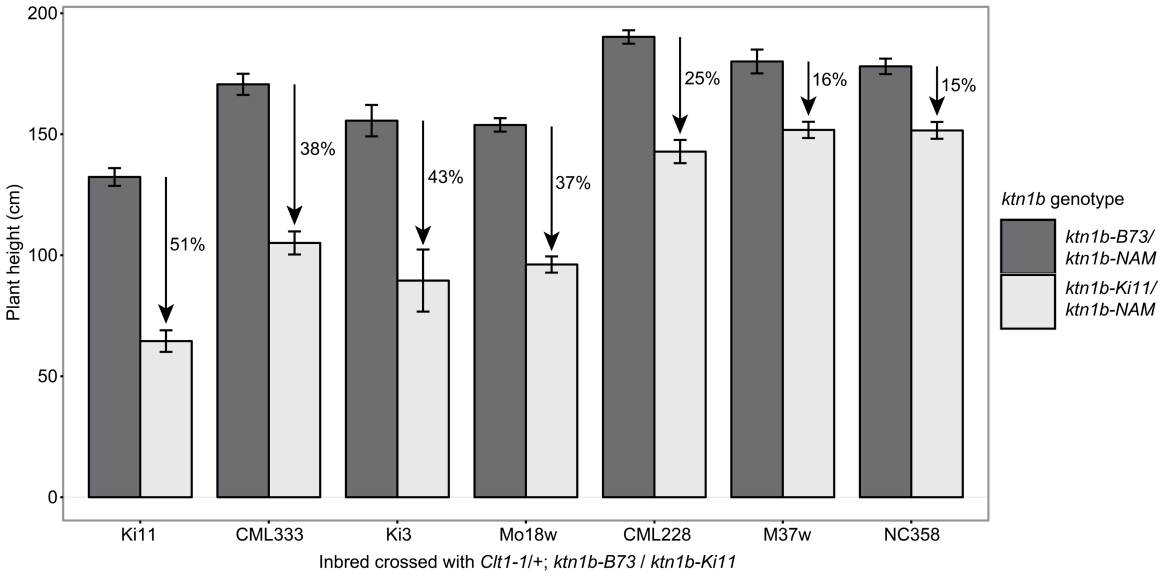

Figure 3.7 In *Clt1-1*/+ plants, combining *ktn1b-Ki11* with a *ktn1b* allele from NAM lines that modify *Clt1-1*/+ reduces plant height more than for NAM lines that do not modify *Clt1-1*/+.

Plants derived from crosses between the respective NAM inbreds and F1 mutants from Ki11 x *Clt1-1*/+ (B73). Mean plant heights of F2 *Clt1-1*/+ individuals with different *ktn1b* genotypes (n = 6 and 8 for Ki11/Ki3 and Ki11/Ki11 respectively; n ≥ 15 for all other genotypes). Error bars indicate SEM and the percent reduction in mean height caused by replacing *ktn1b-B73* with *ktn1b-Ki11* for each background are indicated.

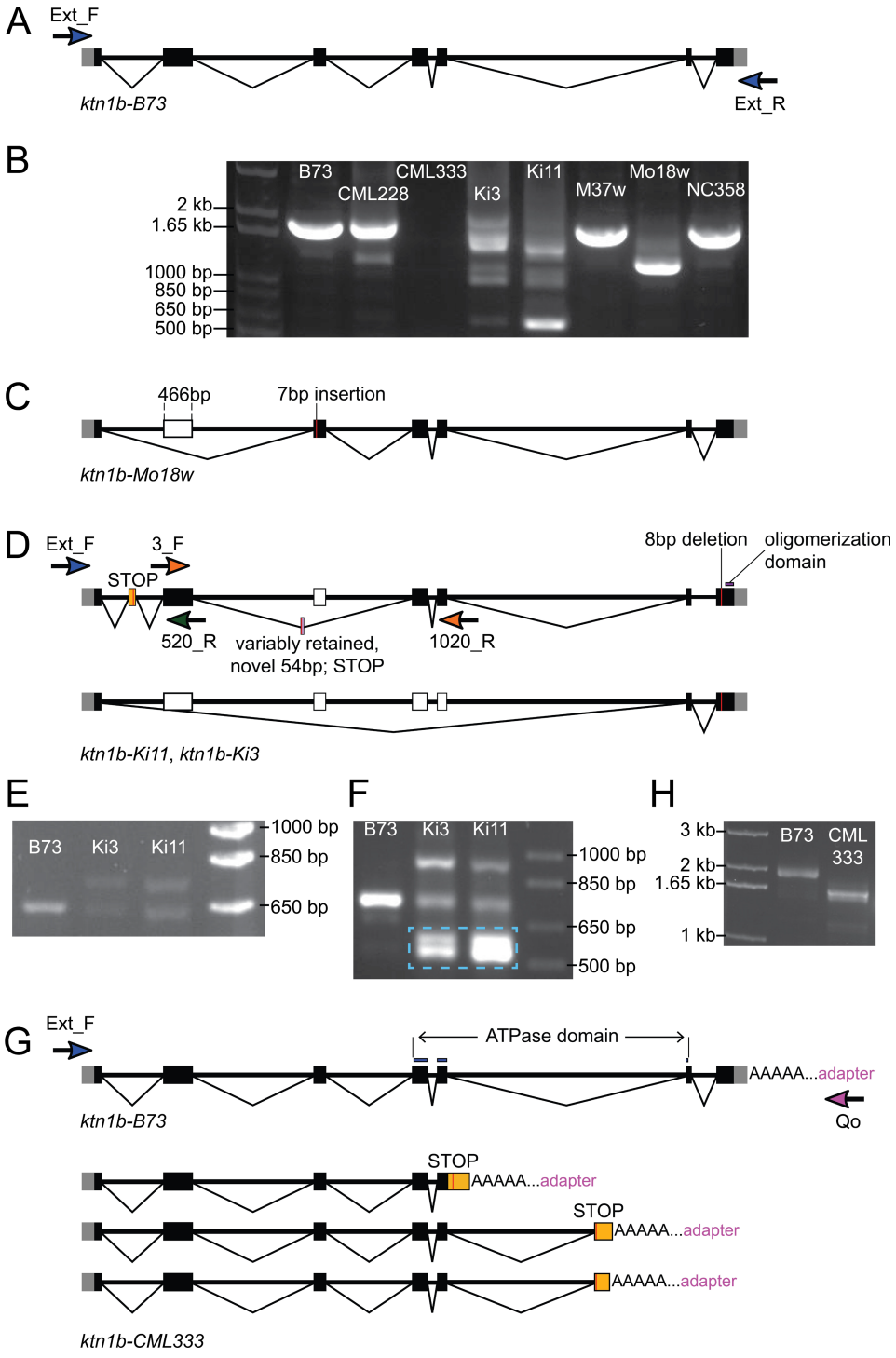

Figure 3.8 Alternative splicing and indels in *ktn1b* of different NAM inbreds.

(A) Gene model of *ktn1b* in B73. Blue arrows indicate PCR primers, binding to the 5' and 3' UTRs, that were used to amplify the products shown in panel (B). (B)

Amplification of *ktn1b* cDNA from different NAM inbreds using the primers indicated in panel (A). Purified gel slices were cloned and sequenced as described in the text. (C) Alternative spliceform of *ktn1b* transcript from Mo18w identified by sequencing. The 7 bp insertion (red bar) corrects the frameshift caused by excision of exon 2. (D) Alternative spliceforms of *ktn1b* transcript from Ki3 and Ki11 identified by sequencing. Note that the 54 bp (pink) was identified by sequencing in Ki3 sequence only while the spliceform missing exons 2-5 (bottom) was identified by sequencing in Ki11 only but in both cases, PCR suggests that the features are present in both Ki3 and Ki11. In-frame stop codons caused by the partial retention of intron 1 and the 54 bp sequence are indicated. An 8 bp deletion occurs in the final exon in both lines causing a frameshifted sequence in the oligomerization domain. (E,F) Amplification of *ktn1b* cDNA using primers (E) Ext_F-520_R and (F) 3_F-1020_R indicated in panel (D) corroborate aberrant spliceforms shown in panel (B). (F) The blue dashed box indicates products corresponding to excision of exon 3 and variable retention of the 54 bp novel sequence. (G) *ktn1b* transcript isoforms in CML333 revealed by sequencing of PCR products resulting from increasing the number of cycles of the PCR in panel (B) and from (H) 3' RACE. The earliest in-frame stop codons in the retained portions of intron 5 are indicated. (H) Amplification of CML333 *ktn1b* cDNA from 3' RACE using the primers indicated in panel (G).

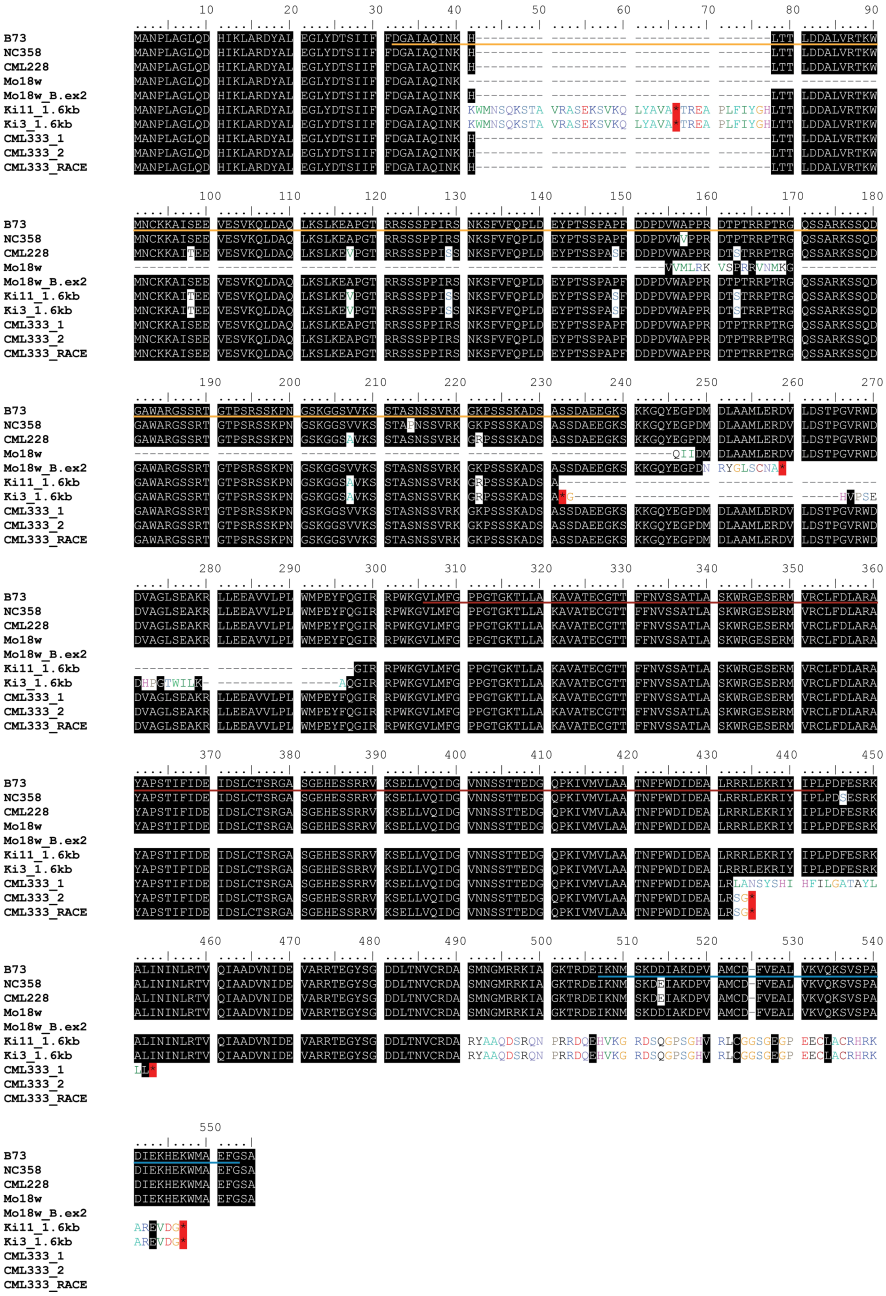

Figure 3.9 Multiple sequence alignment of predicted amino acid sequences based on the cDNA sequences from different NAM founder lines.

Black highlighted residues are identical to B73. Red highlighted asterisks indicate stop codons. Underlined residues correspond to the microtubule-binding domain (yellow), the ATPase domain (red) and the oligomerization domain (blue). Mo18w_B.ex2 is Mo18w cDNA sequence with B73 exon 2 sequence manually added to show the predicted effect of the 7 bp insertion in transcripts where exon 2 is not excised. M37w *ktn1b* cDNA was 100% identical to B73 and was not included in this alignment. CLUSTALW algorithm (Thompson et al., 1994) within BioEdit (Hall, 1999).

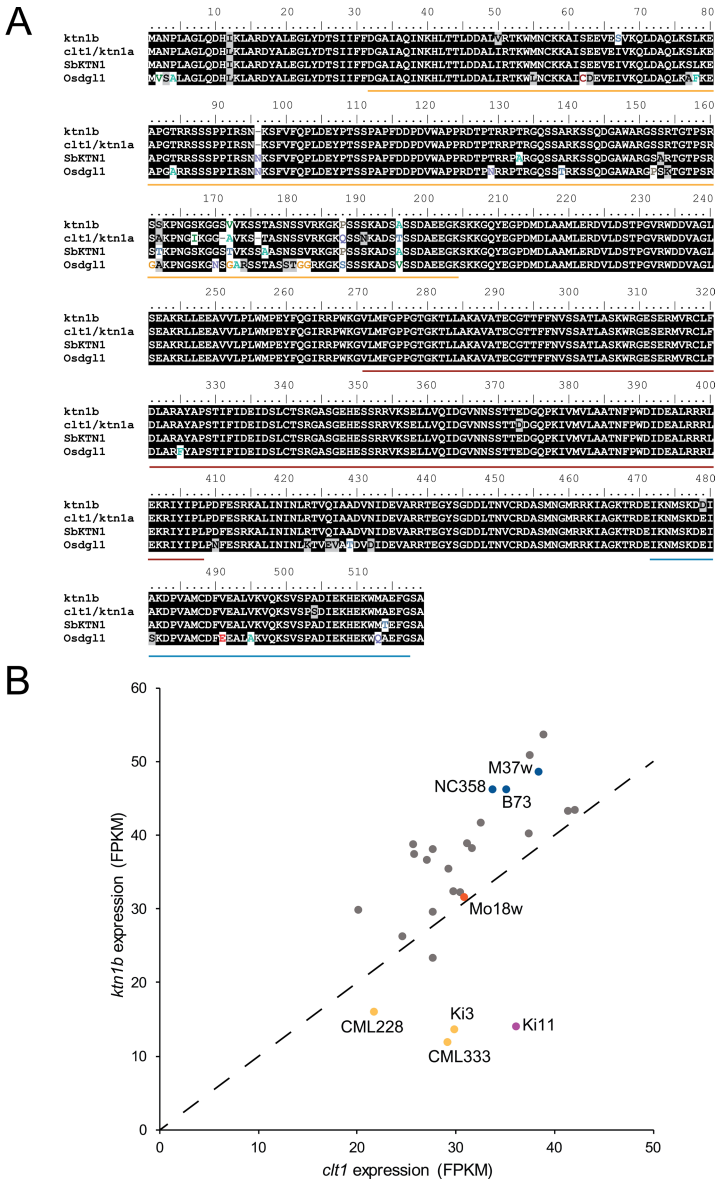

Figure 3.10 Comparison of predicted protein sequence and expression at the shoot apex of *ktn1b* versus *clt1*.

(A) Alignment of predicted protein sequence of maize KTN1B and CLT1, and orthologs in sorghum (Sobic.003G259400) and rice (LOC Os01g49000). Identical residues between the two paralogs are indicated (black highlighting). Underlined residues correspond to the microtubule-binding domain (yellow), the ATPase domain (red) or the oligomerization domain (blue). CLUSTALW algorithm (Thompson et al., 1994) within BioEdit (Hall, 1999). (B) RNA-seq read abundance (analyzed by www.qteller.com) in the shoot apex of 14-day old dark-grown seedlings among the NAM founder lines (Li et al., 2012). Data point colors indicate Ki11 (pink) and low (yellow), moderate (orange) or high (blue) *ktn1b*-expressing lines. The diagonal line represents 1:1 expression of *ktn1b* and *clt1*. FPKM, Fragments Per Kilobase of transcript per Million mapped reads.

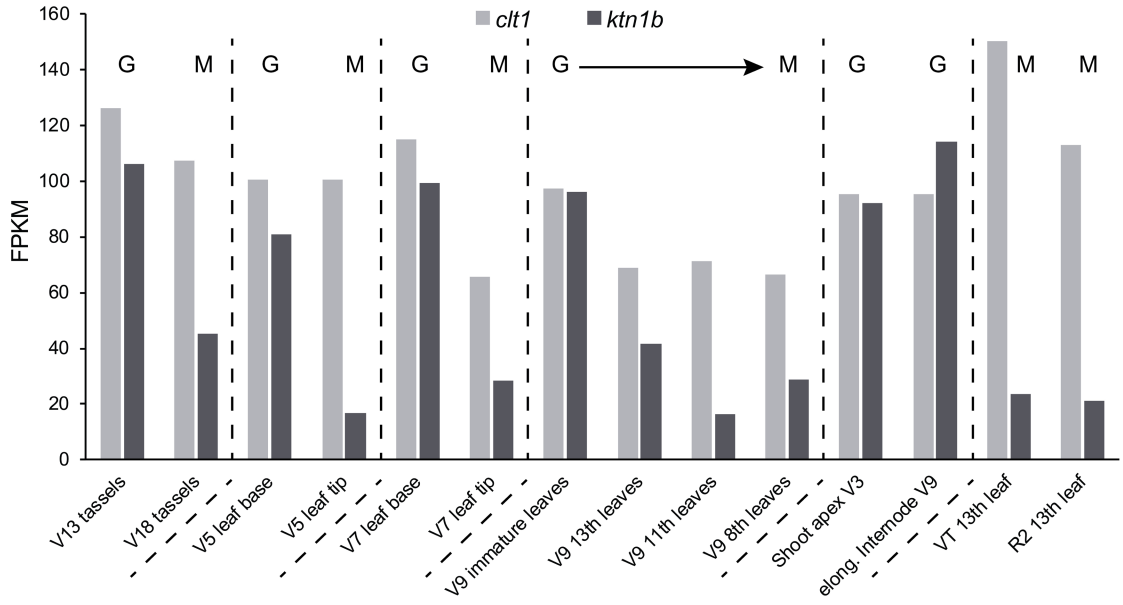

Figure 3.11 Expression of *clt1* and *ktn1b* in different tissues in B73.

Published RNA-seq data (Sekhon et al., 2013; Stelpflug et al., 2015) obtained from MaizeGDB (Lawrence et al., 2004). *ktn1b* expression is higher in tissue expected to have high cell division and growth (G), compared with mature tissue (M). "Elong. Internode V9", an elongating internode in a V9 plant. Note that the 13th leaf is fully extended by VT. FPKM, Fragments Per Kilobase of transcript per Million mapped reads.

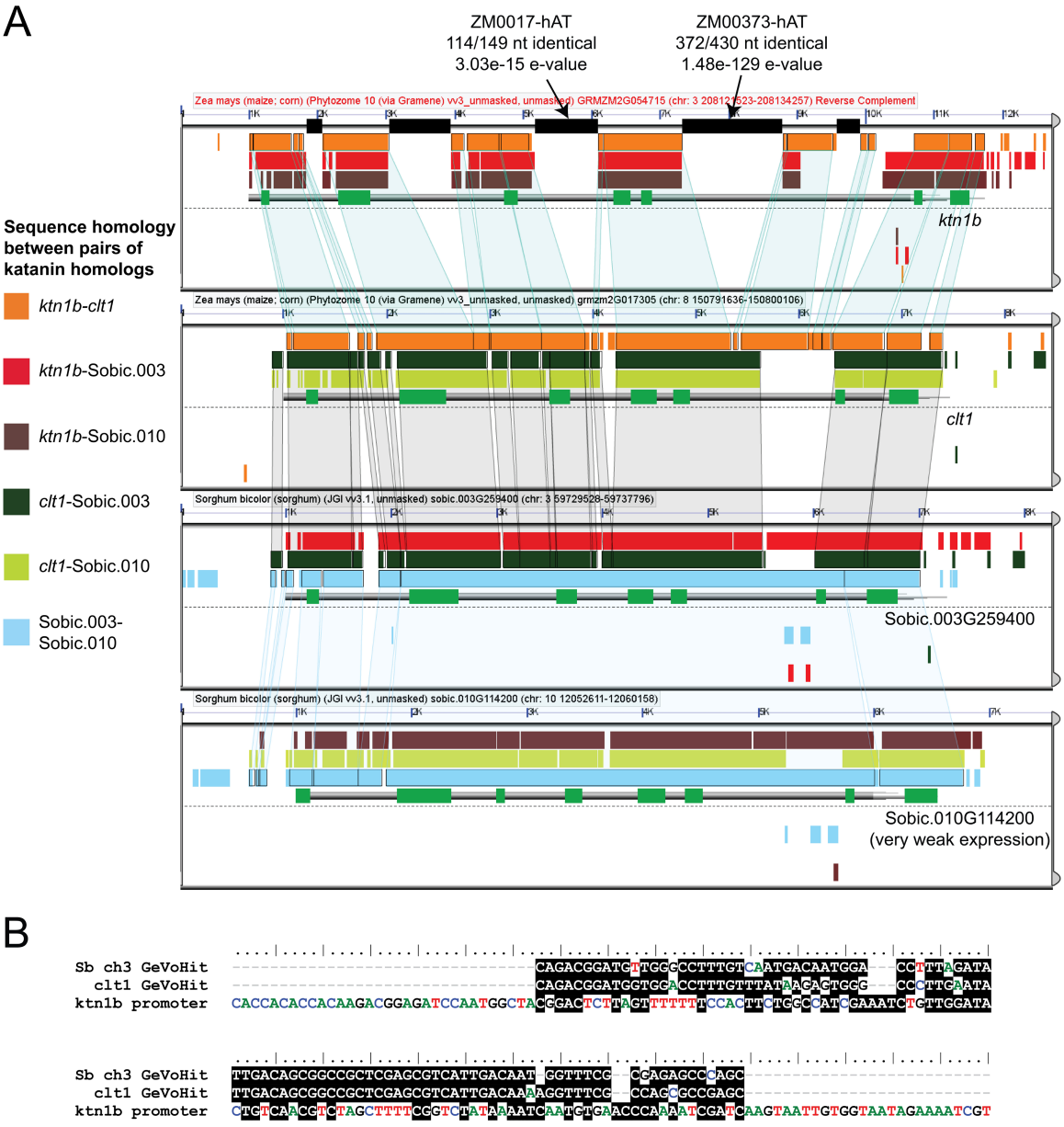

Figure 3.12 Comparison of genomic regions of katanin p60 genes in maize and sorghum.

(A) Comparison of genomic regions of *ktn1b*, *clt1*, Sobic.003G259400 and Sobic.010G114200. Exons (green) and non-coding regions (gray), including UTRs and introns are represented. The pointed ends of each gene indicate the direction of the reading frame. Similar regions between pairs of genes, as indicated in the legend, are represented by the rectangles above the gene models. For clarity, translucent wedges indicating corresponding homologous regions are drawn only for genes adjacent to each other in the diagram. Intron sequences unique to *ktn1b* are indicated (black rectangles); arrows indicate two such *ktn1b*-unique sequences with partial homology (BLASTn) to

the indicated transposable elements (Wessler et al., 2009). Note that exon annotations were manually added. Generated with CoGe GEvo tool (Lyons and Freeling, 2008). (B) ClustalW alignment of the homologous sequences in the putative promoters of Sobic.003G259400 and *clt1* indicated in panel A, and the first 600 bp of the putative promoter (sequence immediately upstream of the predicted 5' UTR) of *ktn1b*. Only the portion of the *ktn1b* promoter that aligned with the Sobic.003G259400 and *clt1* sequences is shown.

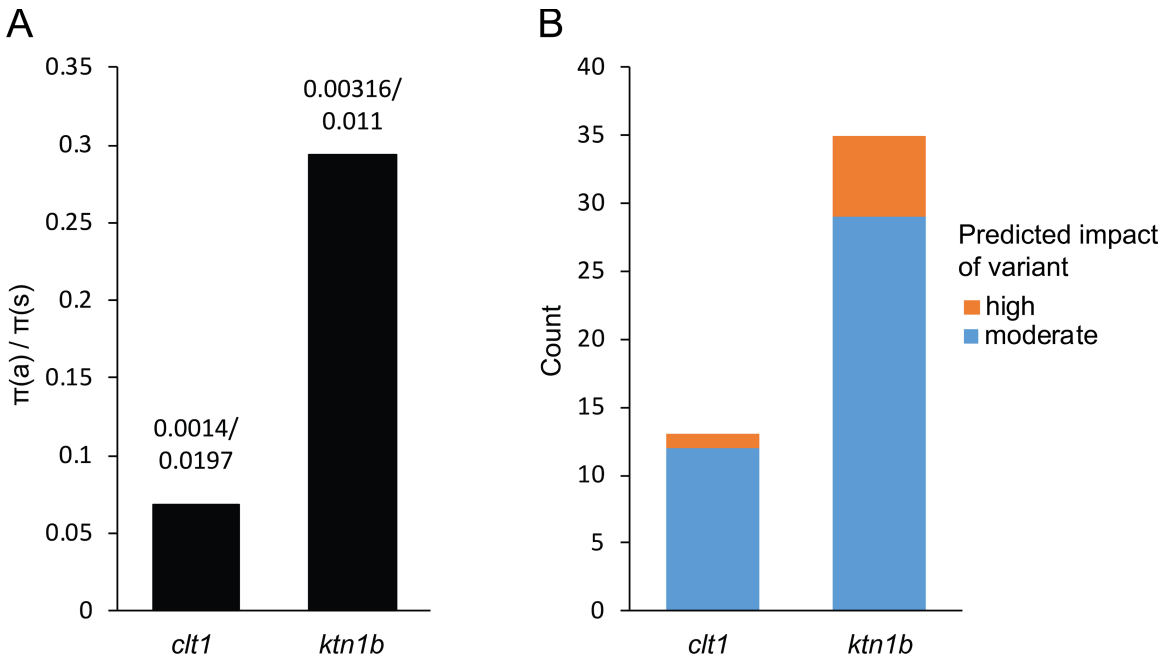

Figure 3.13 Sequence polymorphism in *clt1* and *ktn1b* according to HapMap3 data.

(A) Ratio of nucleotide diversity in nonsynonymous sites (π_a) versus synonymous sites (π_s) in *clt1* and *ktn1b* among the HapMap3 lines. The actual values of π_a and π_s are written above each bar. (B) Number of different variants in the HapMap3 dataset that were predicted by SnpEff to have either "moderate" or "high" impact. See text for explanation of classification of predicted impact.

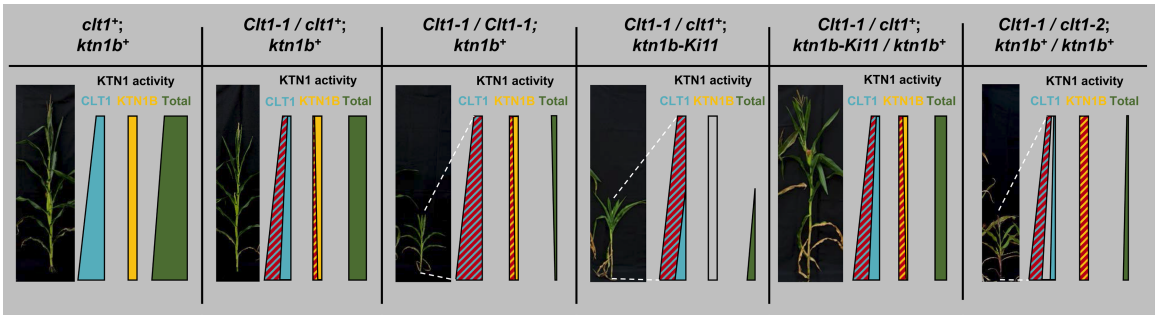

Figure 3.14 A hypothetical model based on differences in expression timing and biochemical activities of CLT1 and KTN1B that explains the different phenotypes between *Clt1-1* homozygotes and modified *Clt1-1*/+ plants, and between *Clt1-1*/*clt1-2* and *Clt1-1*/+; *ktn1b*$^{-}$/*ktn1b*$^{+}$.

The blue bars represent CLT1 activity which decreases in upper internodes due to lower transcription. The yellow bars represent KTN1B activity which does not change between lower and upper internodes, but are lower than CLT1 due to hypothetical differences in biochemical (microtubule-severing) activity. The green bars represent the overall KTN1 activity due to the combined effects of CLT1 and KTN1B. The red cross-hatching represents the dominant-negative effect of CLT1-1.

Table 3.1 Primer sequences for sequencing and amplifying *ktn1b* gDNA and cDNA.

Primer name	Sequence (5'-3')	Comment
Ext_F	CGTTCTCTCCATCGAACTGGC	Figure 3.8 B, E, H; sequencing Mo18w gDNA
Ext_R	CAGCGGTCAGCGGATATCAA	Figure 3.8B
520_R	GTTAGAGGCAGTTGATGATTTAACC	Figure 3.8E; sequencing Mo18w gDNA
3_F	AACCGTTGGACGAGTATCCA	Figure 3.8F
1020_R	GACTCATGTTCACCAGATGCT	Figure 3.8F
Q_t	CCAGTGAGCAGAGTGACGAGGACTCG AGCTCAAGCTTTTTTTTTTTTTTTTVN	cDNA synthesis for 3' RACE
Q_o	CCAGTGAGCAGAGTGACG	Amplifies from Q_t-derived adapters; Figure 3.8H
Enh_6F	CAACATGGCCAAAATGTCAATA	sequencing Ki11 gDNA (primers with the same number were amplified as a pair)
Enh_6R	ATCTTCAGTGGTGGAGCTATTGTT	
Enh_7F	GCATGGTTCGTTGTTTATTTGAT	
Enh_7R	ACCCAAGAAGACCCACAATGTA	
Enh_9F	CTCCTTTAGCCTCTGGAAGTCAG	
Enh_9R	AAGGCTGAAGAAGGGTCTATCC	
Enh_10F	CCTAAAACCCACACCCTTACAG	
Enh_10R	AAAATCAATTTGTTCGCAATGA	
Enh_11F	GAGAAGTCTAACGTAGGAGAAAGCA	
Enh_11R	TTGCCACGGCTAATTGATG	

Table 3.2 Publicly available expression levels of Sobic.003G259400 and Sobic.010G114200 in different tissues and conditions based on RNA-seq.

Tissue and growth condition	Sobic.003G259400	Sobic.010G114200
Shoot.control water	12.864	0.032
Root bottom.vegetative	11.528	0.016
Root bottom.anthesis	11.456	0.022
Root.nitrate	11.325	0.019
Root.ammonia	11.161	0.023
Root bottom.grain maturity	11.095	0.022
Root.control water	11.053	0.05
Root.urea	10.949	0.024
Root top.vegetative	10.881	0.017
Seed imbibed.grain maturity	10.835	0.032
Panicle upper.anthesis	10.826	0.205
Root bottom.floral initiation	10.25	0.023
Panicle.floral initiation	10.047	0.02
Root bottom.juvenile	9.936	0.011
Shoot.ammonia	9.462	0.036
Root.control fertilized	9.435	0.029
Peduncle.floral initiation	9.362	0.03
Shoot.nitrate	9.309	0.023
Shoot.control fertilized	9.28	0.038
Shoot.urea	8.846	0.066
Panicle lower.anthesis	8.676	0.349
Root top.juvenile	8.48	0.024
leaf flag 1 internode.grain maturity	8.327	0.029
Stem 1cm.vegetative	8.218	0.022
Stem 2mm.juvenile	8.115	0.027
leaf flag 1 internode.anthesis	7.977	0.024
Stem mid internode.anthesis	7.807	0.035
Root middle.floral initiation	7.62	0.015
Stem mid internode.grain maturity	7.413	0.038
Leaf lower whorl.vegetative	7.256	0.026
Seed dry.grain maturity	7.255	0.015
Internode growing upper.floral initiation	6.962	0.025
Leaf sheath growing.grain maturity	6.813	0.017
Internode growing.floral initiation	6.163	0.009
Leaf blade.juvenile	6.155	0.006
Leaf upper growing.anthesis	6.037	0.026
Internode mature.floral initiation	5.933	0.013
Leaf lower.juvenile	5.451	0.011
Leaf sheath growing.anthesis	5.422	0
Leaf lower growing.floral initiation	5.212	0.004

Leaf upper growing.floral initiation	5.091	0.004
Leaf lower growing.grain maturity	4.55	0.008
Leaf sheath growing.floral initiation	4.536	0.008
Leaf lower growing.anthesis	4.335	0.054
Leaf middle whorl.vegetative	3.627	0.013
Leaf upper.juvenile	3.427	0.007
Leaf upper whorl.vegetative	3.191	0.007

Expression levels in FPKM, Fragments Per Kilobase of transcript per Million mapped reads. Data retrieved from the GeneAtlas on Phytozome (Goodstein et al., 2012).

3.5 References

Bichet, A., Desnos, T., Turner, S., Grandjean, O., Hofte, H., and Höfte, H. (2001). BOTERO1 is required for normal orientation of cortical microtubules and anisotropic cell expansion in Arabidopsis. Plant J **25**: 137–148.

Bouquin, T., Mattsson, O., Naested, H., Foster, R., and Mundy, J. (2003). The Arabidopsis lue1 mutant defines a katanin p60 ortholog involved in hormonal control of microtubule orientation during cell growth. J Cell Sci **116**: 791–801.

Bukowski, R. et al. (2015). Construction of the third generation Zea mays haplotype map (Cold Spring Harbor Labs Journals).

Burk, D.H., Liu, B., Zhong, R., Morrison, W.H., and Ye, Z.-H.H. (2001). A katanin-like protein regulates normal cell wall biosynthesis and cell elongation. Plant Cell **13**: 807–827.

Cingolani, P., Platts, A., Wang, L.L., Coon, M., Nguyen, T., Wang, L., Land, S.J., Lu, X., and Ruden, D.M. (2012). A program for annotating and predicting the effects of single nucleotide polymorphisms, SnpEff: SNPs in the genome of Drosophila melanogaster strain w1118; iso-2; iso-3. Fly (Austin). **6**: 80–92.

Edgar, R.C. (2004). MUSCLE: multiple sequence alignment with high accuracy and high throughput. Nucleic Acids Res. **32**: 1792–7.

Goodstein, D.M., Shu, S., Howson, R., Neupane, R., Hayes, R.D., Fazo, J., Mitros, T., Dirks, W., Hellsten, U., Putnam, N., and Rokhsar, D.S. (2012). Phytozome: a comparative platform for green plant genomics. Nucleic Acids Res. **40**: D1178–86.

Gore, M.A., Chia, J.M., Elshire, R.J., Sun, Q., Ersoz, E.S., Hurwitz, B.L., Peiffer, J.A., McMullen, M.D., Grills, G.S., Ross-Ibarra, J., Ware, D.H., and Buckler, E.S. (2009). A First-Generation Haplotype Map of Maize. Science (80-.). **326**: 1115–1117.

Green, P.B. (1962). Mechanism for Plant Cellular Morphogenesis. Science **138**: 1404–5.

Hall, T.A. (1999). BioEdit: a user-friendly biological sequence alignment editor and analysis program for Windows 95/98/NT. Nucleic Acids Symp. Ser. **41**: 95–98.

Hartman, J.J., Mahr, J., McNally, K., Okawa, K., Iwamatsu, A., Thomas, S., Cheesman, S., Heuser, J., Vale, R.D., and McNally, F.J. (1998). Katanin, a Microtubule-Severing Protein, Is a Novel AAA ATPase that Targets to the Centrosome Using a WD40-Containing Subunit. Cell **93**: 277–287.

Hori, K. and Watanabe, Y. (2005). UPF3 suppresses aberrant spliced mRNA in Arabidopsis. Plant J. **43**: 530–40.

Hufford, M.B. et al. (2012). Comparative population genomics of maize domestication and improvement. Nat. Genet. **44**: 808–811.

Jinek, M., Chylinski, K., Fonfara, I., Hauer, M., Doudna, J.A., and Charpentier, E. (2012). A programmable dual-RNA-guided DNA endonuclease in adaptive bacterial immunity. Science **337**: 816–21.

Komorisono, M., Ueguchi-Tanaka, M., Aichi, I., Hasegawa, Y., Ashikari, M., Kitano, H., Matsuoka, M., and Sazuka, T. (2005). Analysis of the rice mutant dwarf and gladius leaf 1. Aberrant katanin-mediated microtubule organization causes up-regulation of gibberellin biosynthetic genes independently of gibberellin signaling. Plant Physiol. **138**: 1982–93.

Lawrence, C.J., Dong, Q., Polacco, M.L., Seigfried, T.E., and Brendel, V. (2004). MaizeGDB, the community database for maize genetics and genomics. Nucleic Acids Res. **32**: D393–7.

Li, X. et al. (2012). Genic and nongenic contributions to natural variation of quantitative traits in maize. Genome Res. **22**: 2436–44.

Liang, Z., Zhang, K., Chen, K., and Gao, C. (2014). Targeted mutagenesis in Zea mays using TALENs and the CRISPR/Cas system. J. Genet. Genomics **41**: 63–8.

Librado, P. and Rozas, J. (2009). DnaSP v5: a software for comprehensive analysis of DNA polymorphism data. Bioinformatics **25**: 1451–2.

Loughlin, R., Wilbur, J.D., McNally, F.J., Nédélec, F.J., and Heald, R. (2011). Katanin Contributes to Interspecies Spindle Length Scaling in Xenopus. Cell **147**: 1397–1407.

Lyons, E. and Freeling, M. (2008). How to usefully compare homologous plant genes and chromosomes as DNA sequences. Plant J. **53**: 661–673.

McKenna, A., Hanna, M., Banks, E., Sivachenko, A., Cibulskis, K., Kernytsky, A., Garimella, K., Altshuler, D., Gabriel, S., Daly, M., and DePristo, M.A. (2010). The Genome Analysis Toolkit: a MapReduce framework for analyzing next-generation DNA sequencing data. Genome Res. **20**: 1297–303.

McMullen, M.D. et al. (2009). Genetic properties of the maize nested association mapping population. Science **325**: 737–40.

McNally, F.J. and Vale, R.D. (1993). Identification of katanin, an ATPase that severs and disassembles stable microtubules. Cell **75**: 419–429.

Nadeau, J.H. (2001). Modifier genes in mice and humans. Nat. Rev. Genet. **2**: 165–74.

Nei, M. (1987). Molecular Evolutionary Genetics (Columbia University Press).

Nemoto, K., Nagano, I., Hogetsu, T., and Miyamoto, N. (2004). Dynamics of cortical microtubules in developing maize internodes. New Phytol. **162**: 95–103.

Page, D.R. and Grossniklaus, U. (2002). The art and design of genetic screens: Arabidopsis thaliana. Nat. Rev. Genet. **3**: 124–36.

Panteris, E., Adamakis, I.-D.S., Voulgari, G., and Papadopoulou, G. (2011). A role for katanin in plant cell division: microtubule organization in dividing root cells of fra2 and lue1Arabidopsis thaliana mutants. Cytoskeleton (Hoboken). **68**: 401–13.

Paredez, A.R., Somerville, C.R., and Ehrhardt, D.W. (2006). Visualization of cellulose synthase demonstrates functional association with microtubules. Science **312**: 1491–5.

Ray, P.M., Green, P.B., and Cleland, R. (1972). Role of Turgor in Plant Cell Growth. Nature **239**: 163–164.

Sassi, M. et al. (2014). An auxin-mediated shift toward growth isotropy promotes organ formation at the shoot meristem in Arabidopsis. Curr. Biol. **24**: 2335–42.

Schnable, J.C., Springer, N.M., and Freeling, M. (2011). Differentiation of the maize subgenomes by genome dominance and both ancient and ongoing gene loss. Proc. Natl. Acad. Sci. U. S. A. **108**: 4069–74.

Scotto-Lavino, E., Du, G., and Frohman, M.A. (2006). 3’ end cDNA amplification using classic RACE. Nat. Protoc. **1**: 2742–5.

Sekhon, R.S., Briskine, R., Hirsch, C.N., Myers, C.L., Springer, N.M., Buell, C.R., de Leon, N., and Kaeppler, S.M. (2013). Maize gene atlas developed by RNA sequencing and comparative evaluation of transcriptomes based on RNA sequencing and microarrays. PLoS One **8**: e61005.

Shaul, O. (2015). Unique Aspects of Plant Nonsense-Mediated mRNA Decay. Trends Plant Sci. **20**: 767–79.

Stelpflug, S., Sekhon, R., Vaillancourt, B., Hirsch, C., Buell, C., de Leon, N., and Kaeppler, S. (2015). An Expanded Maize Gene Expression Atlas based on RNA Sequencing and its Use to Explore Root Development. Plant Genome **9**.

Thompson, J.D., Higgins, D.G., and Gibson, T.J. (1994). CLUSTAL W: improving the sensitivity of progressive multiple sequence alignment through sequence weighting, position-specific gap penalties and weight matrix choice. Nucleic Acids Res. **22**: 4673–4680.

Wessler, S., Bennetzen, J., Dawe, K., Jiang, N., SanMiguel, P., and Freeman, B. (2009). Maize transposable element database.

Xu, T., Wen, M., Nagawa, S., Fu, Y., Chen, J.-G., Wu, M.-J., Perrot-Rechenmann, C., Friml, J., Jones, A.M., and Yang, Z. (2010). Cell surface- and rho GTPase-based auxin signaling controls cellular interdigitation in Arabidopsis. Cell **143**: 99–110.

Yoine, M., Ohto, M., Onai, K., Mita, S., and Nakamura, K. (2006). The lba1 mutation of UPF1 RNA helicase involved in nonsense-mediated mRNA decay causes pleiotropic phenotypic changes and altered sugar signalling in Arabidopsis. Plant J. **47**: 49–62.

Yu, J., Holland, J.B., McMullen, M.D., and Buckler, E.S. (2008). Genetic design and statistical power of nested association mapping in maize. Genetics **178**: 539–51.

APPENDICES

Appendix A Contiguous sequence of *Clt1-1* from Sanger sequencing

N, C > T putative causative lesion.

>Clt1_sangerseq_contig
ATATTGACAGCGGCCGCTCGAGCGTCATTGACAAAAGGTTTCGCCAGCGCCG
AGCCTCATCATCAGCCACCCGTCCACCACCACCCAGCCCATTTCTCGTCCCCA
AAATTTCGAGTTTCGAAACCAAACCAAACGAAGCGACACTGCACGTGTACGA
ACCTACGACAGCTCTCTACTTCCCTCGCGTCCTCTCCATCGAGAGCTGCTCCT
GCTCGTCTCCTCCCACACCGCGCAATTCGTCGGGATTCGGGAACCCTAGCGCC
GGATCTCCGCGGCAGCGGCGGAAATGGCGAATCCCCTAGCGGGGCTGCAGG
ACCACCTCAAGCTCGCGCGGGACTACGCGCTCGAGGGCCTCTACGACACCTC
CATCATCTTCTTCGACGGCGCCATCGCCCAGATCAACAAGTGAGCTTCTTATA
ATCCCCTGACCCCGGTTCTCCAGTTGCCCTATTACGCCGTGGATTCGATGGCT
ATATCAGTCTACTACGGCGAATTGGCGATGAGTCGGTGTGAATCGCGCGTCC
TGCCTGTGCGGATCTGCGGGTTTGGCCACACGGCGACGGTTTTCATTTCGGCT
GCTGCTTTTAGTTGGTTGGCAGTTGTAGTTTTGCTCTTTTGCGCTTTCTGCTGA
AACACTGGTGTTAGGTCTATCCCTATTTTTAGTTTGCATTTTTTTTTTGAAATG
AGAAAAAGTGAAAAATATATTAGGACAAATGGTTTACATTCTTTTTCATTTAG
TAATCAACTTTATGTAGGATAAATGATATGGTAATTGTTGAATATACATTAGG
TGGGAAGATATTTAAAAGCTTAAAAATGCATTTTCCTTCTACTTAATGTTATC
ATAGATAAACTGTGCATGCATCTGGCTACTTTATTTGATCCTCTGATTCACAC
AAAATGGATGAACTCTCAGAGCTATGAGCAAAGAAGTAATAAAACTGTGAA
GCAGCTGTATTCTTTAATGCTTTATTTTAGTCTTGCAAGTTTCAGGATAGTATG
TGGTGTGTTTTCAATAGAACAGTGGAATCATGTCAAAGTTACTGTTCGACAGA
TAATAGCTTTGAAGCACTGTCCCAAAGGGGGAAATTCAGATTCTTTCTTATTG
ATAAAATATCTAGGAAAGACACTTAAAAGCCTAGATAATGTCGTTTCCTCGTT
TTCCATGTTATTAAGGTTCATCTTAACCATACAGGCATCTAACTACTTTGGAC
GATGCTCTGATTCGTACGAAATGGATGAACTGCAAGAAAGCAATCTCTGAAG
AAGTGGAAATTGTGAAACAGTTGGATGCTCAATTAAAGTCCCTTAAAGAAGC
TCCTGGGACAAGGCGGTCATCATCACCTCCTATTCGGTCTAATAAATCATTTG
TTTTCCAACCGTTGGATGAGTATCCAACATCTTCACCAGCACCCTTTGATGAT
CCTGATGTGTGGGCTCCACCAAGGGATACACCAACCCGAAGACCAACAAGA
GGTCAATCTAGTGCAAGGAAGTCCTCCCAAGATGGAGCCTGGGCACGTGGTT
CATCAAGGACTGGAACACCTAGTCGAAGCGCAAAACCTAATGGGATTAAAG
GAGGTGCTGTTAAATCAACTGCCTCTAACAGTTCTGTAAGGAAAGGGAAACA
AAGTTCAAACAAGGCTGATTCAACGGTAATTTTATCAAATAAGTGTTTACATA
CCTTAATCTTTTGTTTCTGAAAAATATGATGTGTATTCATTCTAATTTCCATTG
TGCACATTGGCATAGGCAAAAAATGTGACCCTAACCGATGTACTAGTAACTT
GTTTTTTGTTTTTGGAAGTATATCTATGTGTCAATCTTCATAGTAGAAAACAA
TATTTCGATAAAGGCATCTAGAATATGCACTTCTCTTACAATTAGTTCTCATG
TGTATATACATTGCAGAATGTGTCTCTACCTTTTAAATTAGTCCCTTCTCAGTG
TACACAGAATTTGAGGAAACATATTTCTTTGGGATATTGCTCAATCAATCGTT
TATTGCCACTTACCCCCCTGTGCTCTCTAGAAGGTGTCTCTAGTTAAAGTGTA

GAATCATGATCTTCAACATCATCGTCATCATCTATCCCTTGTGTACCTGTGTCC
GGGGAGGCTGCCAAGTATACAGTCATGCTTAACATGTTGTCTTGGTCGGGAT
CCAGATGCCTAGGCGCTGTGGTGGCAACCTGGTCCAGGGCACTCAAACAATC
AAATCTTGAAGACAAGATAACACTTAATCAAATCACAACTTAAGCAAACAAA
CATAATGAAGTTTCTTATCTATGTTGATATACTCACAATCACATTTACTATTTA
TCTCCTCCATACCTGGATTGTCTGCATATCTTGTAGGCATAGTATGAAGTGTA
CTAGACAAAAAATGACATTTAGATGGCAAAAGGACATCACATAAAACCATGT
TGAAACTGTAGTGCCTATCATTAAGTTCTGAATCAGGATACTGGAATATGCAC
GTGTACAATCATACCCCCCTTGTTATCACCCTTCTGCTAAGATAGGCAATTGC
CAGTTACTTATTTTTTTGTGAGCAAATTGCCAGTTATTTTTTTGTGAGCAAATT
GCCAGTTACTGAATTGCTTCTAATGATATTTTTTTTTGAAAAATCTTCTTTTTC
CAACTCTGTTTTCCAGAGTAGTGATGCTGAGGAAGGTAAGTCCAAGAAGGGT
CAGTATGAAGGGCCAGATATGGACTTAGCTGCAATGCTTGAAAGGGATGTTC
TGGATTCTACTCCAGGAGTAAGATGGGATGATGTTGCCGGACTTAGTGAGGC
CAAACGACTCCTCGAGGAAGCAGTTGTGCTTCCTCTCTGGATGCCTGAATATT
TTCAGGTAATAGTCTATATTCTTCTACGCTGTCCCTTATTGGTTCAAACTAAGC
ACTGTAAAGTATCTGAAAAATGTCTATTTGTTCTTGGCACTAACACATTTTAC
AGGCGCATATCGATGGGAATGATATGGCATTTTTGGTGCTCTACCATGGACAT
AGTCTAAGATATGCATAGTTACTACGTACTGGTTTTTTATACAACTCTTTTATG
TTTATGGCTGTCAACATGATATGGCATGAAACTGGTGTTTCCTTTGTTTGGTG
CCACTGACGTTTTCTTGATGCTTGTATCTAGGGGTGCCAATGGGCTCTAAATT
TTACACTATAAAATTTAAGGATCAGATCGAATTAGGATCAGACTCTATTTCTA
TTCATTTTTGAACTAAAATTTATTTAGTGCCCTAAGAAATTAAGAAGCATTTG
GATCACGATCTATTACCACCCCTACTTGTATATGTTTTCTTAATTGCCATACTG
ATTTGGATTATGCTGTTCTTGAATGATCATGAACCCAACCAATCTTTTCTCTCT
TGTAGCCTTTTTCATCTGGTCTAAACTTGATACATAGTGGCTAATTATGTCCA
CTTTTCCTTATCAGGGTATTCGTCGACCTTGGAAAGGAGTTCTTATGTTTGGTC
CACCAGGCACGGGAAAGACTCTTTTGGCAAAGGCAGTGGCCACCGAATGTGG
AACAACATTCTTTAATGTTTCCTCTGCAACACTGGCCTCTAAATGGCGTGGCG
AGAGTGAGCGCATGGTCCGTTGCTTATTTGATCTTGCGAGGGCCTATGCTCCA
AGTACAATTTTCATTGATGAAATTGACTCCTTATGCACGTCGCGCGGGTATGT
GGAGTTAATTTTCCTAGATGTTGCTCGTGTCTACAAGTCAATGAAAAATTCCT
CAATATTTTGCACTATAAGCAAGAATGTATCATTCTGCTAGACAACAGAAAA
TGTACCTATATGTTTAATGTATTTATCCATTTTCTTTCTTAATATCAGTGCCTC
CGGCGAACATGAGTCGTCAAGAAGGGTGAAGTTTGAACTTCTAGTGCAAATT
GATGGTGTAAACAATAGCTCCACCACTGATGATGGCCAGCCAAAAATTGTTA
TGGTTCTGGCTGCTACAAATTTTCCATGGGATATTGATGAGGCACTGAGGTTG
GCAAACTCTTATTCTTATATTTACTTCATTTTATGTACTGCTGTCTACTTACGA
ATAGGGGTTGATACCTGGAATATGCATAGGTTCACATAAACCGGTCATCAGT
AGAGCTTGATTACTGAGTGATGCTTCTAGTAGTGGATACTGTCAACGTCAGA
GGCAGTTTATTTGATTTTTCAAAACTTAGAGAATCTTTTGTCTCATTCATGCTC
CATTTATCACATCACTGACCACTGTTTATTTGGTAAGATAAGAAAACTATCAT
AGTTCATAACTGCAGTATGTGGAAGATGTAATTTACAACAGACAAATCTGCA
CTTTGTATAAGACATGTAGCCAACACAATATGTAAGCACAGATACTTCTATG
AGGATTATAGGTGTTCATGGGCGAGGCTGAAAAGAATAGTGCTAGCCAATCA

AATTCACACTATATCCCCCCTAGGACAGAATCAGCACCCAGCCACCCACTAC
AGCTGCAGCAGGCCAATCAGACCAGCCAGTGATGCAGGCATCCATACTTGAG
TGTTTGATCGGAGGATACTCCCACTGCTGCCATGTGCCATGACATATAAATAT
GTTAAACTTACCTAATGTGTATCTTCTATCTTGGTGATATTTTTTCTTAGAACC
TCAACTCAATTGATTGTTGCATATGTTGTATCCCTGACAATGAGCCCTCAATG
TGTACACGGTTTCCTAGACTTGGATATCGACCCCAAGTTGTCATGTCACCAAG
TCATCCTATGTTGCACTCATTTAATGTGCACAATACAATGCAGCGGGAGTAGC
CTAATGATCTCCCTCTTAAGAAATCATCAATCCATCTCCTTTGCCGCTCTCCTG
CTCAGCTCAGCTCATCAGTCATGGCTCATCCCTTCCTGGCCTTTTGCAGGCCA
GGTTGATCACCATAGTCCAGAGTACTGGTGACCGAGGCCAAGGCCACTTGGT
CCTGTATTTATGTCATTTATATTTTTCAATGTATTCAGTTACATTTGTTCTAAA
CAAAACAAATCCACTAATTGCTCATTGCAGTTCCTTTGTAGTCCTTTACAGTT
CTTTGTGTTATTGCGTTTATAGTGTCTAGTTCTTTTCAGTTATGTAATTTCCTTC
AAGCAAAGCCCCCAATTTTGCAAAGATGTTATTTGTTCAAATAATACGGTTAG
TGTTTTAAAATTGATTCTTGAGTGAAACTACAAATAAAACTGAACTATTGATT
GCAAAATCATTGGTTATTTGACCAGGGAAAAGTAAATGGTTATTTTGGCAATT
TTTATAATAATAGACATTGCTGCAAATGAAAAGGCTATGCACCCTCCAATTGC
CTCGTTTTGTCCCAGATGTTTTTTTTGTTGAAATTAGAAGGGTGTATAATGCA
CTCATTTAATGTGCGTTATGTTGACTTTAATTGCCCAGGCGGAGGCTGGAGAA
GCGTATTTATATTCCACTTCCAGATTTTGAAAGTAGAAAGGCACTTATCAACA
TTAATCTTAGAACAGTTCAGGTATGTATTGGAGATATCTTTCTAGATCATCTT
GTGTTATCTTTATCCTCTTCCCTTTGTTTCATTTTGGGTCTTTGTGAACACATTG
ATTTTATCAGGCATGCCATGATGAACATGTCAAAATTGTTGGCACTTTATTTT
CTGAAATCGCATGTACACGCCTGCATCATAACCATTATATATGTTGGCCTGCA
CTTTCTTATTCTGAATTTCTTGTTTTCCTAATGAAACGTAAATGCCCTTGACAA
TGGATACTTATCTAAGCACTGCACTGATGTTTTTTTTGTTGAACCAATTTGTTT
AATACTCTAATTCAGTACATTGAGGTTATCAATGATTGTGCCATATCTTCAGT
GGCTTCTTGTTATTGCCGTGCCTCCTTTTATATGACAGATAACGTTACTGCTCT
ACCTCCTTTTATATCTGACAGATAGCCGCAGATGTTAACATCGACGAGGTTGC
TCGGAGGACAGAAGGCTATAGTGGAGATGATCTGACAAACGTTTGCCGCGAT
GCCTCAATGAATGGCATGAGGCGCAAGATAGCAGGCAAGACCCGCGACGAG
ATCAAGAACATGTCAAAGGACGAGATAGCCAAGGACCCGGTGGCCATGTGC
GACTTTGTGGAGGCTCTGGTGAAGGTTCAGAAGAGTGTCTCGCCTTCAGACA
TAGAGAAGCATGAGAAGTGGATGGCTGAGTTTGGGTCTGCCTGAGACCTCGG
CCATCTGCTTGGGTCCTGTTCAAACATTCGTTTTGTGTGGGTTGACACGGCAT
TCCGTAGCAATGATACGGTGTTACCCGCCGGTGGTCTTGCTTCATATAGACCA
GAGGCACGAGCTATCTTGTCTGTTTCCAGTGATGCTAGGAATTGAGTTCACGA
TCGTTTCAGTTCTTGGTATATGCACTTTCTGCTGTCAAACGTATCTCATC

Appendix B Alignment of the B73 reference genomic sequence of *ktn1b* with contiguous sequences from Sanger sequencing of *ktn1b* gDNA from Ki11 and Mo18w

N, start codon; N, exon; N, stop codon. Exon numbers are indicated to the right of the alignment.

Ki11
-Parts 1 and 2 of Ki11 sequence are two non-overlapping contigs, separated by an un-sequenced gap in intron 5.

```
B73                     TATCAAGGGAAATACCAATCTCCCATAATACAAGTTGTAAGATGACATATCCATAATCTC  4560
Ki11genomickat3part1    ------------------------------------------------------CCATAATC  8
                                                                                *   **

B73                     ACAAGCACACAATCAACTAAAATGACAAGTTCTAAAATGACATCTAACAACCACATGCAC  4620
Ki11genomickat3part1    ACAAGCACACAATCAACTAAAATGACAAGTTCTAAAATGACATCTAACAACCACATGCAC  68
                        ************************************************************

B73                     ACAATCAACTAAAACGACATGCCCACAACCACAATGACACAAGCATCACTCTCAATCTCC  4680
Ki11genomickat3part1    ACAATCAACTAAAACGACATGCCCACAACCACAATGACACAAGCATCACTCTCAATCTCC  128
                        ************************************************************

B73                     CTTCTATCTATGATCTCTCAGGAACCATCATCCAAATCATGAGTATTAGTAACCAACATT  4740
Ki11genomickat3part1    CTTCTATCTATGATCTCTTAGGAACCAACATCCAAATCATGAATATTAGTAACCAACATT  188
                        ****************** ******** ************** ******************

B73                     TCAATCTCCCTTCCTTGCCGTGGCAGATGACAGGTGCAGAGGCGCAGAGGTGGCGG----  4796
Ki11genomickat3part1    TCAATCTCCCTTCCTTGCCGTGGCAGATGACAGGTGCAGAGGCGCAGAGGTGGTGGGCGG  248
                        ************************************************** **

B73                     GTGGATGGTGGATGACACCTGACAGGCTCGTTTTAGGGTGCACAATGATTCTCTCATGGG  4856
Ki11genomickat3part1    ATGGATGGTGGATGACACCTGACAGGCTCGTTTTAGGGTGCACAATGATTCTCTCATGGG  308
                         ************************************************************

B73                     CTGGGGCTGGAGCTGGACCTTCCTAAAGTGTTAAAGCGTCACTTTTCACGGCCCATAGCG  4916
Ki11genomickat3part1    CTGGGGCTGGAGCTGGACCTTCCTAAAGTGTTAAAGCGTCACTTTTCACGGCCCATAGCG  368
                        ************************************************************

B73                     TTTAAACGCCTAAAACTGGCGCTTAAAATTAGCT--GTAGCGCCTAAAACGAGCGCTTTA  4974
Ki11genomickat3part1    TTTAAACGTCTAAAACTGGCGCTTAAAATTAGCGTTGTAGCGCCTAAAACGAGTGCTTTA  428
                        ******** ************************   ***************** ******

B73                     CGCTTTTTTGTGAAACGTTCTAGCGCTTTAGGCACTTAGTAGCGTTTTGGTGCTTAAAAG  5034
Ki11genomickat3part1    CACTTTTTTGTGAAATGTTCTAGCGCTTTAGGCACTTAGTAGCGTTTTGGTGCTTAAAAG  488
                        * ************* ******************************************

B73                     GCATTTAAAAGGCGTTTAAAAGGCGCTTAAGCGACTTTTTAATAACCATGCTGGGCCTGC  5094
Ki11genomickat3part1    GCGTTTAAA-----------AGGCGCTTAAGCGACTTTTTAATAACCATGCTGGGCCTGC  537
                        ** ******           ************************************

B73                     CTGCTTTTTTTATATGTTTATGGCTGTGGACATGGCATGGCATGAAACTGGTGGTTCCTT  5154
Ki11genomickat3part1    CTTCT-TTTTTATATGTTTATGGCTGTGGATATGACATGGCATGAAACTGGTGGTTCCTT  596
                        ** ** ********************** *** ************************

B73                     TATTTTCCATGGGTGGTTTCTGGATACTTGTATTTGTTTTCTTAATTGTGATACCAATTT  5214
Ki11genomickat3part1    TATTTTCCATGGGTGGTTTCTGGATACTTGTATTTGTTTTCTTATTTGTGATACCAATTT  656
                        ****************************************** ***************

B73                     GGATCATGTTATTCTTTAATGGTCATGAACCCAACTAATCTATTCTCTCTTGTAGCCTTT  5274
Ki11genomickat3part1    GGATCATGTTATTCTTTAATGGTCATGAACCCAACTAATCTATTCTCTCTTGTAGCCTTT  716
                        ************************************************************

B73                     CTCAT-TTAGTCTAAACTCTATACATAGTGGCTAATTATGTCCACTCTTCTTTATCAGGG  5333
Ki11genomickat3part1    CTCATTTTAGTCTAAACTCTATACATAGTGGCTAATTATGTCCACTCTTCTTTATCAGGG  776
                        ***** ********************************************************
```

```
B73                 TATTCGTCGACCTTGGAAAGGAGTTCTTATGTTTGGTCCACCAGGCACGGGAAAGACTCT 5393
Ki11genomickat3part1 TATTCGTCGACCTTGGAAAGGAGTTCTTATGTTTGGTCCACCAGGCACGGGAAAGACTCT 836
                    ************************************************************

B73                 TTTGGCAAAGGCAGTGGCTACAGAATGTGGAACAACATTCTTCAATGTTTCCTCTGCAAC 5453
Ki11genomickat3part1 TTTGGCAAAGGCAGTGGCTACAGAATGTGGAACAACGTTCTTCAATGTTTCCTCTGCAAC 896
                    ********************************** ********************** 4

B73                 ATTGGCCTCTAAATGGCGCGGCGAAAGTGAGCGCATGGTTCGTTGTTTATTTGATCTTGC 5513
Ki11genomickat3part1 ATTGGCCTCTAAATGGCGCGGCGAAAGTGAGCGCATGGTTCGTTGTTTATTTGATCTTGC 956
                    ************************************************************

B73                 GAGGGCCTATGCTCCAAGTACAATTTTCATTGATGAAATTGACTCCTTATGCACATCACG 5573
Ki11genomickat3part1 GAGGGCCTATGCTCCAAGTACAATTTTCATTGATGAAATCGACTCCTTATGCACATCACG 1016
                    ************************************ ********************

B73                 TGGGTATGTGAAGTCAAGTTTGCTAGTTGTTCATTTACTCGAGTCAATGAAAATTTCTTC 5633
Ki11genomickat3part1 TGGGTATGTGAAGTCAAGTTTGCTAGTTGTTCATTTACTCGAGTCAATGAAAATTTCTTC 1076
                    ************************************************************

B73                 AATATTTTGCACCATAAGCATGAATGTATCATTCTGCTGGACAAGAAAAAATGTACCTAT 5693
Ki11genomickat3part1 AATATTTTGCACCATAAGCATGAATGTATCATTCTGCTGGACAAGAA-AAATGTACCTAT 1135
                    ********************************************** ************

B73                 ATCGCCAGTTAATGTATTTGTCCATTTTTTCTACATATCAGAGCATCTGGTGAACATGAG 5753
Ki11genomickat3part1 ATCGCCAGTTAATGTATTTGTCCATTTTTTCTACATATCAGAGCATCTGGTGAACATGAG 1195
                    ************************************************************

B73                 TCGTCAAGAAGGGTGAAGTCTGAACTTCTAGTGCAAATTGATGGTGTAAACAATAGCTCC 5813
Ki11genomickat3part1 TCGTCAAGAAGGGTGAAGTCTGAACTTCTAGTGCAAATTGATGGTGTAAACAATAGCTCC 1255
                    ************************************************************ 5

B73                 ACCACTGAAGATGGTCAGCCAAAAATTGTTATGGTTCTAGCTGCAACAAATTTTCCATGG 5873
Ki11genomickat3part1 ACCACTGAAGATGGTCAGCCAAAAATTGTTATGGTTCTAGCTGCAACAAATTTTCCATGG 1315
                    ************************************************************

B73                 GATATTGATGAGGCACTGAGGTTGGCAAACTCTTATTCTCATATTCACTTCATTTTAGGT 5933
Ki11genomickat3part1 GATATTGATGAGGCACTGAGGTTGGCAAACTCTTATTCTCATATTCACTTCATTTTAGGT 1375
                    ************************************************************

B73                 GCTACTGCCTACTTATTATTATGAATAAGGGTTGGTACCTGGAAGATGCATATGATGGTT 5993
Ki11genomickat3part1 GCTATTGCCTACTTATGATTATGAATAAGGGTTGGTACCTGGAAGATGCATAGGATGGTT 1435
                    **** *********** ************************************ *******

B73                 CA--------CATAAACGGATAAACCTGTCATATTTTAGCAGTAGCACCTGATTGCTTGA 6045
Ki11genomickat3part1 CACAACTTCACATAAACGGATAAACCTGTCATACTTTAGCAGTAGCACCTGATTGCTTGA 1495
                    **        ********************** ************************

B73                 GTGGTGCTGCTAGTAGCGTTAGATACTGTCGAAGCCAGGGACAGTTTATTTGATTTCTCA 6105
Ki11genomickat3part1 GTGGTGCTGCTAGTAGTGTTAGATACTGTCGAAGTCAGGGACAGTTTATTTGATTTCTCA 1555
                    *************** ***************** ************************

B73                 AGACTTTTACAGAATCATTTTTTCTCAGTCATGCTGCATTGTCACACCACTGACCACTGT 6165
Ki11genomickat3part1 AGACTTTTACAGAATCATTTTCTCTCAGTCATGCTGCATTGTCACACCACTGACCACTGT 1615
                    ******************** ************************************

B73                 TTATTTGGTGAGACAAGAAACTATGGTAGTTCCTAACTTCAGTATGTGGAAGATGTAATT 6225
Ki11genomickat3part1 TTATTTGGTGAGACAAGAAACTATGGTAGTTCCTAACTGCAGTATGTGGAAGATGTAATT 1675
                    ************************************ *********************

B73                 TACCAGAGACAAACCAGCACCTTGTATAAGACATGTAGCCAACACAGTACGTAAACACGA 6285
Ki11genomickat3part1 TACCAGAGACAAACCAGCACCTTGTATAAGACATGTAGCCAACACAGTACGTAAACACGA 1735
                    ************************************************************

B73                 ACGCTTCTATGAGGATTAGAGGTGTTCACAGGTGAGGGTTTCTCGCCGAGGGTTGACCCT 6345
Ki11genomickat3part1 ACGCTTCTATGAGGATTATAGGTGTTCACAGGCGAGGGTTTCTCGCCGAGGGTTGACCCT 1795
                    ***************** ************* ************************

B73                 CCAACGGTGGGAGTGAAAGGGCCTCTATCTGAGTTAGTTAGGGTACTAAATCCGACTCCA 6405
Ki11genomickat3part1 CCAACGGTGGGAGTGAAAGGGCCTCTATCTGAGTTGGTTAGGGTACTGAATTCGACTCCA 1855
                    ********************************** *********** *** ********

B73                 TATGGGTGCGAATTTCAGGCTAGGGTTAAAAAATTCCCTCGTTTGCCCCACACCAAAGCA 6465
Ki11genomickat3part1 TATGGGTGCGAATTTCAGGCTAGGGTTAAAAAATTCCCTCGTTTGCCCCATACCAAAGCA 1915
                    ************************************************ *********

B73                 CAGGTCTAAGGTCCGTGCCAGTTGTGGTCATTCTCACATGGAGTCATGGACTATGGCGTT 6525
Ki11genomickat3part1 CAGGTCTAAGGTCCGTGCCAGTTGTGGTCATTCTCACATGGAGTCATGGACTATGGCGTT 1975
                    ************************************************************
```

```
B73                     GCTGCTTATGGATGGGGAAGGGTTCGGGGTTTTCTCAACATGCATTAGAAGGTCTTCCAG 6585
Ki11genomickat3part1    GCTGCGTATGGATGGGGAAGGGTTCGCGGTTTTCTCGACATGCATTAGAAAGTCTTCCAG 2035
                        ***** ******************** ********* ************* *********

B73                     GTTGAGTTTTTTAGACCTTCCAATAGTTGCATGGACACCGAGGCAATCAATAGTGTGGGT 6645
Ki11genomickat3part1    GTTGAGTTTTTTAGACCTTCCAATAGTTGCATGGACACAGAGGCAATCAATAGTGTGGGT 2095
                        ************************************ ********************

B73                     GGTGCCATACTAAATTTTCCTATTACTGTTACAGTGGTTCCCCTTTTATAGGGGTTGGGT 6705
Ki11genomickat3part1    GGTGCCATACTAAATTTTCCTATTACTGTTACAGTGGTTCCCCTTTTATAGGGGTTGGGT 2155
                        ************************************************************

B73                     AGATCTTTTCGCCTTCACGAGAATGCCCCCTACCTGGTACAGGATATTCCTAGGATCCCT 6765
Ki11genomickat3part1    AGATCTTTTCGTCTTCACGAGAATGCCCCCTACCTGCTACAGGATATTCCTAGGATCCCT 2215
                        *********** ********************** ***********************

B73                     ATCATCATAGGAACGGGGGTACGGAGGGACATTTCCACTCCAAACCGCCTTACATTGTGG 6825
Ki11genomickat3part1    ATCATCATAGACACGGGGGTAC----------------------------------- 2237
                        **********  **********

B73                     GTCTTCTTGGGTCTTTCCTAGGCTTCTCTTGTTTTGGGCTGTGTCTGTTGACTCCTTTGC 6885
Ki11genomickat3part1    ------------------------------------------------------------ 2237
```

```
B73                     TCCTTTAGCCTCTGGAAGTCAGAGGCTTTATACGAGGGCTTCTAGTTTTCTACACAAAGG    7680
ki11gdnakat3part2       ------------------------------------------------------------    0

B73                     CTTCCCTGGTATCCAGCCATCAGCTTGGTTCCTCAACTCCGCTTGGGGACACGATTCACA    7740
ki11gdnakat3part2       -------------------TCAGCTTGGTTCCTCAACTCCGCTTGGGGACACGATTCACA    41
                                           ****************************************

B73                     AAGAAGGGAGATGTTAGCTCAAGTGAACACCCAAGGCTGGGGCTTCACCTCAACACTAGC    7800
ki11gdnakat3part2       AAGAAGGGAGATGTTAGCTCAAGTGAACCCCCAAGGCCGGGGCTTCACCTCAACACTAGC    101
                        *************************** ******** ***********************

B73                     CATCGCAAATTCACATTATATCTTCCCTAGTACAAAAATCACGCACCCACGACAGCAGCC    7860
ki11gdnakat3part2       CATCACAAATTCACATTATATCTTCCCTAGTACAAAAATCATGCACCCACGACAGCAGCC    161
                        **** ********************************** ******************

B73                     AGCAGGCCGACCAGCCAGTGATGCAGGCATCCAGGCTTGAGATGTGTTCGTGTTTGATTG    7920
ki11gdnakat3part2       AGCAGGCCGACCAGTCAGTGATGCAGGCTTCCAGACTTGAGATGTGTTCGTGTTTGATTG    221
                        ************** ************* ***** *************************

B73                     GAGGCTACTCCCAATGCTGCAATGTGCCATGTCATAAGAATACAAATATGATAAAATTTA    7980
ki11gdnakat3part2       GAGGCTACTCCCAATGCTGCAATGTGCCATGTCATAAGAATACAAATATGATAAAATTTA    281
                        ************************************************************

B73                     CCTAATGCGTTATCTTCTATCTTGGTGATTTTTTTCTTAGAACCTCAACTCTGATTGTTG    8040
ki11gdnakat3part2       CCTAATGCGTTATCTTCTATCTTGGTGTTTTTTTTCTTAGAACCTCAACTCTGATTGTTG    341
                        *************************** *********************************

B73                     CATATGGTGTATCGATGACAATGAGCCCACAACCTGTACACAGTTTCCTAGTCTTGGATA    8100
ki11gdnakat3part2       CATATGGTGTATCGATGACAATGAGCCCACAACCTGTACACAGTTTCCTAGTCTTGGATA    401
                        ************************************************************

B73                     TCAAGCACAAGTTGTCATGTCACCAAGTCATCCTATGCTGCACTCATTTAATATTGCATA    8160
ki11gdnakat3part2       TCAAGCACAAGTTGTCATGTCACCAAGTCATCCTATGCTGCACTCATTTAATATTGCATA    461
                        ************************************************************

B73                     ATACAATGCAACAGGAATAGCCTAATGATCTCCCTCTTAAGAAATCATTAATCCAACTCC    8220
ki11gdnakat3part2       ATACAACGCAACAGGAATAGCCTAATGATCTCCCTCTTAAGAAATCATTAATCCAACTCC    521
                        ****** ******************************************************

B73                     TTTGCTGCTCTCCTGCTGAGCTCATGGCTGGTCCCTTCCTGGTCTTTTGCAGGTCAGGTT    8280
ki11gdnakat3part2       TTTGCCGCTCTCCTGCTGAGCTCATGGCTGGTCCCTTCCTGGTCTTTTGCAGGTCAGGTT    581
                        ***** ******************************************************

B73                     GATCACCAGAGCCTAGAGGACTGGTGGCTGAGGTCAAGGCTACTCAGTCCTGTTTATGTC    8340
ki11gdnakat3part2       GATCACCAGAGCCTAGAGGACTGGTGGCTGAGGTCAAGGCTACTCAGTCCTGTTTATGTC    641
                        ************************************************************
```

```
B73                 ATTTATATTTTTCGATGTATCTAGTTACATTTGTTCTAAACAAAACAAATCCACTAATTG    8400
ki11gdnakat3part2   ATTTATATTTTTCGATGTATCTAGTTACATTTGTTCTAAACAAAACAAATCCACTAATTG    701
                    ************************************************************

B73                 CTCATTCCAGTTCCTTTTGTAATGCTTTACAATTCTTTGTGTCATTGCGTTTATAGTGCC    8460
ki11gdnakat3part2   CTCATTTCAGTTCCTTTTGTAATGCTTTACAATTCTTTGTGTCATTGCGTTTATAGTGCC    761
                    ****** ***************************************************

B73                 TAATTCTTGTTCAGTTATGTAATTTTCTTCAAGCAAAGCACCCAATTTTGCAGGATGACA    8520
ki11gdnakat3part2   TAATTATTTTTCAGTTATGTATTTTTCTTCAAGCAAAGCACCCAATTTTGCAGGATGACA    821
                    ***** ** ************ ***************************************

B73                 TGATTTTGCCGTTATTTGTCCAAATAATAGGGTTAGAGTTTTTAAATTGGTTCTTCATAC    8580
ki11gdnakat3part2   TGATTTTGCCGTTATTTGTCCAAATAATAGGGTTAGAGTTTTTAAATTGGTTCTTCATAC    881
                    ************************************************************

B73                 TTTTTTCGAACGACGCAGGAGAGCTGCATGTCATTCTATTAAAAAGGAGTAAGAAAAAAT    8640
ki11gdnakat3part2   TTTTTTCGAACGATGCAGAAGAGCTGCATGTCATTCCATTAAAAAGGAGTAAGAAAAAAT    941
                    ************* **** ***************** ************************

B73                 ACAAGTGGGGGACCGAGGCCTAAAACCCACACCCTTACAGTACAGACATAGGCACGCCAC    8700
ki11gdnakat3part2   ACAAGTGGGGGACCGAGGCCCAAAACCCACACCCTTACAGACATAG---GCACGCCACAC    998
                    ******************* ******************          * *  ***

B73                 ACACACGAGGGATAACGACCCAACACAGAAGGGGGTGGGGGGCTTGCTCAAGAGCCCAGC    8760
ki11gdnakat3part2   ACACACGAGGGATAACGACCCAACACAGAAGGGGGTGGGGGGCTTGCTCAAGAGCCCAGC    1058
                    ************************************************************

B73                 CCCACCAACCTTGCGCACAGAAAGCTAAACGCAGAATTACCAGCTAGATACCACAGG---    8817
ki11gdnakat3part2   CCCACCAACCTTGCGCACAGAAAACTAAACGCAGAATTACCAGCTAGACACCACAGGTTG    1118
                    ********************** ********************** ********

B73                 -----------TTACGGCAGACTACAGAAACACTAGGCCTAATCCCCTCAAACACACAAT    8866
ki11gdnakat3part2   CCTGCACAATCTTACGGCAGACTACAGAAACACTAGGCCTAATCCCCTCAAACACACAAT    1178
                              ************************************************

B73                 CGTTCCTGTGCATCTCCCAGGCCACCAAAATAAACAAGGATAGACCCTTCTTCAGCCTTA    8926
ki11gdnakat3part2   CGTTCCTGTGCATCTCCCAGGCCACCAAAATAAACAAGGATAGACCCTTCTTCAGCCTTA    1238
                    ************************************************************

B73                 CAGAGAATTAATGTGAAACTACAAATTACACTGAACTATTGGTGTCAAAATCATTGATTA    8986
ki11gdnakat3part2   CAGAGAATTAATGTGAAACTACAAATTACACTGAACTATTGGTGTCAAAATCATTGATTA    1298
                    ************************************************************

B73                 TTTTACCAGGGAAAAAACAGATGGTTATTTTGGCAGTTTTGGTCCATTGATGTATATAGG    9046
ki11gdnakat3part2   TTTTACCAGGGAAAAAACAGATGGTTATTTTGGCAGTTTTGGTCCATTGATGTATATAGG    1358
                    ************************************************************

B73                 ATACTGTTTTATAATAACAGGCATGGCTGCAAATGAAAAGGCTATGCACCACCTCCTGCC    9106
ki11gdnakat3part2   ATACTGTTTTATAATAACAGGCATGGCTGCAAATGAAAAGGCTATGCACCACCTCCTGCC    1418
                    ************************************************************

B73                 TGGTTTCACCCCAGATGGTATTTTTGTTGAAATTTGGTGGGGATCTGACATCATGCATAA    9166
ki11gdnakat3part2   TGGTTTCACCCCAGATGGTATTTTTGTTGAAATTTGGTGGGGAACTGACATCATGCATAA    1478
                    ****************************************** ****************

B73                 CAGTTCTACGAACCATTGGTATCCCTTTTTTGGGCAACATTCATGTCTGGTAGTTTCCTG    9226
ki11gdnakat3part2   CAGTTCTACGAACCATTGGTATCCCTTTTTTGGGCAACATTCATGTCTGGTAGTTTCCTG    1538
                    ************************************************************

B73                 CTTTATGTAGACACTATTTATGTCTGGTAGTTCAATAGAATTTTGCCTATATCTATACTA    9286
ki11gdnakat3part2   CTTTATGTAGACACTATTTATGTCTGGTAGTTCAATAGAATTTTGCCTATATCTATACTA    1598
                    ************************************************************

B73                 GCGGCATTTACCTGCTAGTTATAATTTACTCTAGATATTTATCTTCACACATGAGAATAC    9346
ki11gdnakat3part2   GCGCCATTTACCTGCTAGTTATAATTTACTCTAGATATTTA------------GAACAC    1645
                    *** ************************************           *** **

B73                 TATTTTTTTCTCATTATTATTTTTCACCAGGCTATTCCCATGTATGCTGCTACTATTGCC    9406
ki11gdnakat3part2   TATTATTTTCTCATTATTATTTTTCACCAGGCTATTCCCATGTATGCTGCTACTATTGCC    1705
                    **** ********************************************************

B73                 ATTGCTACTTCTCTTCTTCCATATGCATCTACCACTTCTGATCCAAATTATAGTTCACTT    9466
ki11gdnakat3part2   ATTGCTACTTCTCTTCTTCCATATGCATCTACCACTTCTGATCCAAATTATAGTTCACTT    1765
                    ************************************************************

B73                 TAGCTTTATCGTAAACCATTTCTTTTTATCTTTGACCAAATTTAAAGGAAAATGTAATAT    9526
ki11gdnakat3part2   TAGCTT-ATCCTAAACCATTTCTTTTTATCTTTGACCAAATTTAAAGGAAAATGTGACAT    1824
                    ****** *** ***************************************** * **
```

```
B73                 CTACAATATCAATCTATTTTCTTAAATTCTCCATTAAATATTTCTTAATAGTGCATCTAT    9586
ki11gdnakat3part2   CTACAATATCAATCTATTTTCTTAAATTCTCCATTAAATATTTCTTAATAGTGCATCTAT    1884
                    ************************************************************

B73                 TCGAACTTATAGATGTTAATATAATTTTCTAAAACTTTGGTCAAAGTTAGAGAAGTCTAA    9646
ki11gdnakat3part2   TCGAACGTATAGATGTTAATATAATTTTCTAAAACTTTGGTCAAAGTTAGAGAAGTCTAA    1944
                    ****** ***************************************************

B73                 CGTAGGAGAAAGCATAAGGAACTACAATTTGAATAGAGGGAATATGTTAGTAACTTACTA    9706
ki11gdnakat3part2   CGTAGGAGAAAGCATAAGGAACTACAATTTGAATAGAGGGAATATGTTACTAACTTACTA    2004
                    ********************************************** **********

B73                 TTGTTCACATTAATGTGCATTATGTTGACTTCTAAATTGCCCAGGCGGAGGCTGGAGAAG    9766
ki11gdnakat3part2   CTGTTCACATTAATGTGCATTATGTTGACTTCTAAATTGCCCAGGCGGAGGCTGGAGAAG    2064
                     ************************************************************

B73                 CGTATTTATATCCCACTTCCAGATTTCGAAAGCAGAAAGGCACTTATCAACATTAATCTT    9826    6
ki11gdnakat3part2   CGTATTTATATCCCACTTCCAGATTTCGAAAGCAGAAAGGCACTTATCAACATTAATCTT    2124
                    ************************************************************

B73                 AGAACAGTTCAGGTATGTGTTGGAGATATCTTTCTGGATCATCTCGTGATATCTTTGTCC    9886
ki11gdnakat3part2   AGAACAGTTCAGGTATGTGTTGGAGATATCTTTCTGGATCATCTCGTGATATCTTTGTCC    2184
                    ************************************************************

B73                 CCTTTCCTTTGTTTCATTTTGAGTCATTGCGAACAAATTGATTTTATCAGACATGCCATG    9946
ki11gdnakat3part2   CCTTTCCTTTGTTTCATTTTGAGTCATTGCGAACAAATTGATTTTATCAGACATGCCATG    2244
                    ************************************************************

B73                 ATGCACGTGTCAAAATTGTTGGCGCTTAATTTTGTGGAATCACATGTACATGCCTGCAGC    10006
ki11gdnakat3part2   ATGCACGTGTCAAAATTGTTGGCGCTTAATTTTGTGGAATCACATGTACATGCCTGCAGC    2304
                    ************************************************************

B73                 ATAACCATTATGTATGTTGCCCGGCAATTTTATTTTTTGAATTTCTCATTTTCCTAATGA    10066
ki11gdnakat3part2   ATAACCATTATGTATGTTGCCCGGCAATTTTATTTTTTGAATTTCTCATTTTCCTAATGA    2364
                    ************************************************************

B73                 TATGTAAATGCCCTAGAAAATAGATACTTATCGAAGCATTGCACCGGTGCTTTTTTTTTT    10126
ki11gdnakat3part2   TATGTAAATGCCCTAGAAAATGGATACTTATCGAAGCATTGCACCGGTGCTTTT----TT    2420
                    ******************** ******************************    **

B73                 GGTCGAACCAATTTGCTCACTACTCTAATTCCATACATTTGGATTGTCAATTACTGTGTC    10186
ki11gdnakat3part2   GGTCGAACCAATTTGCTCACTACTCTAGTTCCATACATTTGGATTGTCAATTACTGTGTC    2480
                    ************************** ******************************

B73                 ATATCTTCAGTGGCTTATTGTTATTTCTGTTATTCTGTACCTCCTTTTGTCTCAACAGAT    10246
ki11gdnakat3part2   ATATCTTCAGTGGCTTATTGTTATTTCTGTTATTCTGTACCTCCTTTTGTCTCAACAGAT    2540
                    ************************************************************

B73                 AGCTGCGGATGTTAACATCGATGAGGTTGCTCGGAGGACAGAAGGCTATAGTGGAGATGA    10306
ki11gdnakat3part2   AGCTGCGGATGTTAACATCGATGAGGTTGCTCGGAGGACAGAAGGCTATAGTGGAGATGA    2600
                    ************************************************************

B73                 CTTGACAAATGTTTGCCGTGATGCTTCAATGAACGGTATGCGGCGCAAGATAGCAGGCAA    10366
ki11gdnakat3part2   CTTGACAAATGTTTGCCGTGAT--------GCACGGTATGCGGCGCAAGATAGCAGGCAA    2652
                    **********************        * ****************************    7

B73                 AACCCGCGACGAGATCAAGAACATGTCAAAGGACGATATAGCCAAGGACCCAGTGGCCAT    10426
ki11gdnakat3part2   AACCCGCGACGAGATCAAGAACATGTCAAAGGACGAGATAGCCAAGGACCCAGTGGCCAT    2712
                    ********************************** ***********************

B73                 GTGCGACTTTGTGGAGGCTCTGGTGAAGGTCCAGAAGAGTGTCTCGCCTGCAGACATAGA    10486
ki11gdnakat3part2   GTGCGACTTTGTGGAGGCTCTGGTGAAGGTCCAGAAGAGTGTCTCGCCTGCAGACATAGA    2772
                    ************************************************************

B73                 AAAGCACGAGAAGTGGATGGCTGAGTTTGGATCTGCCTGAGACCTCGGTCATCTCCTTCA    10546
ki11gdnakat3part2   AAAGCACGAGAAGTGGATGGCTGAGTTTGGATCTGCCTGAGACCTCGGTCATCTCCTTCA    2832
                    ************************************************************

B73                 ACATTGGTTTCTGTGGTTGACACGACAAGTGTATGTTGATATCCGCTGACCGCTGGTGCA    10606
ki11gdnakat3part2   ACATTGGTTTCTGTGGTTGACACGAGAAGTGTATGTTGATATCCGCTGACCGCTGGTGCA    2892
                    ************************ **********************************

B73                 TAGATCAGAGGCACGAACTATCTTGTATATTTTCAGGGATACTACAAATTAAGTTCACGA    10666
ki11gdnakat3part2   TAGATCAGAGGCACGAACTATCTTGTATATTTTCAGGGATACTACGAATTAAGTTCAC--    2950
                    ******************************************* ************
```

```
B73                 TTATTTCATTTCAATCCCTGATATGTACATTCTAGCTGTGAAACGTGTCTCATCAATTAG    10726
ki11gdnakat3part2   ------------------------------------------------------------    2950


B73                 CCGTGGCAA 10735
ki11gdnakat3part2   --------- 2950
```

Mo18w

-Parts 1 and 2 of Mo18w sequence are two non-overlapping contigs.

```
B73                 CGTCTCTTCCCACACCACGCATTTTGTCGGGATTCGGGAACCCTATCGCCGGATCTTCGC    180
Mo18w_gDNA_part1    ----------------------TTTTGTCGGGATTCGGGAACCCTAGAGCCGGATCTTCGC    39
                                          ***********************  *************

B73                 GGCGGCGGCGGAAATGGCGAATCCCCTCGCGGGGCTGCAGGACCACATCAAGCTTGCGCG    240
Mo18w_gDNA_part1    GGCGGCGGCGGAAATGGCGAATCCCCTCGCGGGTCTGCAGGACCACATCAAGCTTGCGCG    99
                    ******************************** *************************

B73                 GGATTACGCGCTCGAGGGCCTATACGACACCTCCATAATCTTCTTCGACGGCGCCATTGC    300     1
Mo18w_gDNA_part1    GGATTACGCGCTCGAGGGCCTATACGACACCTCCATAATATTCTTCGACGGCGCCATTGC    159
                    ************************************ ********************

B73                 TCAGATCAACAAGTGAGCTTCCTATAATCCCCTGACCCCGGTTCCCCAGTTGCCGTATTA    360
Mo18w_gDNA_part1    TCAGATCAACAAGTGAGCTTCCTATAATCCCCTGACTCCGGTTCCCCAGTTGCCGTATTA    219
                    ************************************ ********************

B73                 CGCCGTGGATTCGATCGCTATCAGGCCACTACGGCGAATCGGCGATCAGTGGGTGTGAAT    420
Mo18w_gDNA_part1    CGCCGTGGATTCGATCGCTATCAGGACACTACGGCGAATTGGCGATCGTTGGGTGTGAAT    279
                    ************************ ************* *******  ************

B73                 CGCGACGTCCAGCCCGCCCGGATCTGCGGGTTTGGCCTCACGGCAACGGTTTTCATTTCG    480
Mo18w_gDNA_part1    CGCGACGTCCAGCCCGCCCGGATCTGCGGGTTTGGCCTCACGGCAACGGTTTTCATTTCG    339
                    ************************************************************

B73                 ACTGCTGCTTTCAGTAGTTTAGCAGTTGTCGTTTTGCTCTGTGGCGCATTTTGCTGAAAT    540
Mo18w_gDNA_part1    ACTGCTGCTTTCAGTTGTTTAGCAGTTGTCGTTTTGCTCTGTGGCGCATTTTGCTGAAAC    399
                    *************** ******************************************

B73                 GTTGGCTATGTTGTTGGGTCTATCCCTATTTTTAGTTTGCATTTTTTAAGTGAAATGATA    600
Mo18w_gDNA_part1    GTTGGCTATATTGTTGGGTCTATCCCTATTTTTAGTTTGCATTTTTTAAGTGAAATGATA    459
                    ********* ************************************************

B73                 AAAATATAATTGATTTGCATCCATATTAGGATAAATGATTGT------------------    642
Mo18w_gDNA_part1    AAAATATAATTGGTTTGCATCCATATTAGGACGAATTATTCACATTCCTTATAGTTTAGT    519
                    ************ ******************  *** ***

B73                 --------------------------------AACAATTGAGTACTGTTGGTGCGAAGATA    671
Mo18w_gDNA_part1    AATCAACTACCTATATAGGATAAATGATTGTAACAATTGAGTACTGTTGGTGCGAAGATA    579
                                                    ****************************

B73                 TTTAAAAGCTAAAAAATGTGTTTTTCCTTGTACTTCATGTTAGTATACGATGGATACACT    731
Mo18w_gDNA_part1    TTTAAAAGCTAAAAAATGTGT-TTTCCTTGTACTTCATGTTAGTATACGATGGATACACT    638
                    ******************** ************************************

B73                 GTGCATGTTGAT----------------CCTCTGATTCATAGAAAATGGATGAACTCTCA    775
Mo18w_gDNA_part1    GTGCATGCATCTGACTACTTTCTTTGATCCTCTGATTCATAGAAAATGGATGAACTCTCA    698
                    *******    *               *******************************

B73                 GAAAAGTACGGCCGTACAGGCAAATAAGTGAAAAAAGTGTGAAACAGCTTTATGCAGTGT    835
Mo18w_gDNA_part1    GAAAAGTAC---------------------------------------------------    707
                    *********
```

```
B73                 AAAATTTGTTATGTACTTAGCGTAGCGTATGTATGTGTTAATTGTTACTACTAGTGGCCA    960
Mo18w_gDNA_part2    --------------ATGTACTTAGCGGTATATATGTGTTAATTGTTACTACTAGTGGGCC    46
                               *  **       **** ************************* *

B73                 TTGTATATATA---------CATCATTCAATTTATTAGCATTACAACAATAGTTATATAT    1011
Mo18w_gDNA_part2    ATTGTATATTGTATATATACATATATTCAATTTATTAACATTACAACTATAGTTATATAT    106
                     *       *             ************* ********* ************
```

```
B73                 GTGTTGCCCCCCCCCCCCCCCCCCCCCCCCGCCCCTCCCCCAAGGAAAAATTCTGGCTAC     1071
Mo18w_gDNA_part2    GTGTTGC----------------------CCCCCTCCCCCCAAGGAAAAATTCTGGCTAC     144
                    *******                      * ***  ************************

B73                 GCCCCTAGCTGTATGCTTTATTTTAGTCCTGCAAATTTCAAAATAGTGTGTGGTGTGTCT     1131
Mo18w_gDNA_part2    GCCCCTAGCTGTATGCTTTATTTTAGTCCTGCAAATTTCAAAATAGTGTGTGGTGTGTCT     204
                    ************************************************************

B73                 AAAATAGAACAGTGGAATATTGTCGAAGTTACTGTTAGACAGATAATAACTTTGAAGCAC     1191
Mo18w_gDNA_part2    AAAATAGAACAGTGGAATATTGTCAAAGTTACTGTTAGACAGATAATAGCTTTGAAGCAC     264
                    ********************** ********************** ***********

B73                 TATCCTGAGGGGG---GGGGCTCACATTCTTTCTTATTTAATGATAAAATAACTAGGAAA     1248
Mo18w_gDNA_part2    TATCCTGAGGGGGGGGGGGACTCACATTCTTTCTTATTTAATGATAAAATAACTAGGAAA     324
                    *************   *** ****************************************

B73                 ATGAGTTAAAAGCCTAGATAATGTCTTTTCGTTGTGTTCCGTGTTATTAAGGTTAATTTT     1308
Mo18w_gDNA_part2    ATGAGTTAAAAGCCTAGATAATGTCTTTTCGTTGTGTTCAGTGTTATTAAGGTTAATTTT     384
                    ************************************* ********************

B73                 AACCATACAGGCATCTAACTACTTTGGACGATGCTTTGGTTCGTACGAAATGGATGAACT     1368
Mo18w_gDNA_part2    AACCATACAGGCATCTAACTACTTTGGACGATGCTTTGGTTCGTACGAAATGGATGAACT     444
                    ************************************************************

B73                 GCAAGAAAGCAATCTCTGAAGAAGTGGAAAGTGTGAAACAGTTGGATGCTCAATTAAAGT     1428
Mo18w_gDNA_part2    GCAAGAAAGCAATCACTGAAGAAGTGGAAAGTGTGAAACAGTTGGATGCTCAATTAAAGT     504
                    ************** ********************************************

B73                 CCCTTAAAGAAGCTCCTGGGACGAGGCGGTCCTCATCACCTCCTATTCGCTCCAATAAAT     1488
Mo18w_gDNA_part2    CCCTTAAAGAAGCTCCTGGGACGAGGCGGTCCTCATCACCTCCTATTCGCTCCAATAAAT     564
                    ************************************************************

B73                 CATTTGTTTTCCAACCGTTGGACGAGTATCCAACATCTTCACCAGCTCCTTTTGATGATC     1548
Mo18w_gDNA_part2    CATTTGTTTTCCAACCGTTGGACGAGTATCCAACGTCTTCACCAGCACCTTTTGATGATC     624
                    ********************************** ************ **************

B73                 CTGATGTGTGGGCTCCACCAAGGGATACACCGACCCGAAGACCAACAAGAGGTCAATCTA     1608
Mo18w_gDNA_part2    CTGATGTGTGGGCTCCACCAAGGGATACATCGACCCGAAGACCAACAAGAGGTCAATCTA     684
                    ***************************** ******************************

B73                 GTGCAAGAAAATCCTCCCAAGATGGAGCCTGGGCACGTGGTTCATCAAGGACTGGAACAC     1668
Mo18w_gDNA_part2    GTGCAAGAAAATCCTCCCAAGATGGAGCCTGGGCACGTGGTTC-----------------     727
                    ******************************************

B73                 CTAGCCGAAGCTCAAAACCTAATGGGAGTAAAGGAGGCTCTGTGGTTAAATCATCAACTG     1728
Mo18w_gDNA_part2    ------------------------------------------------------------     727
```

2

Appendix C Contiguous sequences from Sanger sequencing of *ktn1b* cDNA from different NAM inbreds

>B73

ACGCATTTTGTCGGGATTCGGGAACCCTATCGCCGGATCTTCGCGGCGGCGG
CGGAAATGGCGAATCCCCTCGCGGGGCTGCAGGACCACATCAAGCTTGCGCG
GGATTACGCGCTCGAGGGCCTATACGACACCTCCATAATCTTCTTCGACGGC
GCCATTGCTCAGATCAACAAGCATCTAACTACTTTGGACGATGCTTTGGTTCG
TACGAAATGGATGAACTGCAAGAAAGCAATCTCTGAAGAAGTGGAAAGTGT
GAAACAGTTGGATGCTCAATTAAAGTCCCTTAAAGAAGCTCCTGGGACGAGG
CGGTCCTCATCACCTCCTATTCGCTCCAATAAATCATTTGTTTTCCAACCGTTG
GACGAGTATCCAACATCTTCACCAGCTCCTTTTGATGATCCTGATGTGTGGGC
TCCACCAAGGGATACACCGACCCGAAGACCAACAAGAGGTCAATCTAGTGC
AAGAAAATCCTCCCAAGATGGAGCCTGGGCACGTGGTTCATCAAGGACTGGA
ACACCTAGCCGAAGCTCAAAACCTAATGGGAGTAAAGGAGGCTCTGTGGTTA
AATCATCAACTGCCTCTAACAGTTCTGTAAGGAAAGGAAAACCAAGTTCAAG
CAAGGCTGATTCAGCGAGTAGTGATGCTGAGGAAGGTAAGTCCAAGAAGGG
TCAATATGAAGGGCCAGATATGGACTTAGCTGCAATGCTTGAAAGGGATGTT
CTGGATTCTACTCCAGGAGTAAGATGGGATGATGTTGCCGGACTTAGTGAGG
CCAAACGACTCCTCGAGGAAGCAGTTGTGCTTCCTCTCTGGATGCCTGAATAT
TTTCAGGGTATTCGTCGACCTTGGAAAGGAGTTCTTATGTTTGGTCCACCAGG
CACGGGAAAGACTCTTTTGGCAAAGGCAGTGGCTACAGAATGTGGAACAACA
TTCTTCAATGTTTCCTCTGCAACATTGGCCTCTAAATGGCGCGGCGAAAGTGA
GCGCATGGTTCGTTGTTTATTTGATCTTGCGAGGGCCTATGCTCCAAGTACAA
TTTTCATTGATGAAATTGACTCCTTATGCACATCACGTGGAGCATCTGGTGAA
CATGAGTCGTCAAGAAGGGTGAAGTCTGAACTTCTAGTGCAAATTGATGGTG
TAAACAATAGCTCCACCACTGAAGATGGTCAGCCAAAAATTGTTATGGTTCT
AGCTGCAACAAATTTTCCATGGGATATTGATGAGGCACTGAGGCGGAGGCTG
GAGAAGCGTATTTATATCCCACTTCCAGATTTCGAAAGCAGAAAGGCACTTA
TCAACATTAATCTTAGAACAGTTCAGATAGCTGCGGATGTTAACATCGATGA
GGTTGCTCGGAGGACAGAAGGCTATAGTGGAGATGACTTGACAAATGTTTGC
CGTGATGCTTCAATGAACGGTATGCGGCGCAAGATAGCAGGCAAAACCCGCG
ACGAGATCAAGAACATGTCAAAGGACGATATAGCCAAGGACCCAGTGGCCA
TGTGCGACTTTGTGGAGGCTCTGGTGAAGGTCCAGAAGAGTGTCTCGCCTGC
AGACATAGAAAAGCACGAGAAGTGGATGGCTGAGTTTGGATCTGCCTGAGAC
CTCGGTCATCTCCTCAACA

>M37w

CGCATTTTGTCGGGATTCGGGAACCCTATCGCCGGATCTTCGCGGCGGCGGC
GGAAATGGCGAATCCCCTCGCGGGGCTGCAGGACCACATCAAGCTTGCGCGG
GATTACGCGCTCGAGGGCCTATACGACACCTCCATAATCTTCTTCGACGGCGC
CATTGCTCAGATCAACAAGCATCTAACTACTTTGGACGATGCTTTGGTTCGTA

CGAAATGGATGAACTGCAAGAAAGCAATCTCTGAAGAAGTGGAAAGTGTGA
AACAGTTGGATGCTCAATTAAAGTCCCTTAAAGAAGCTCCTGGGACGAGGCG
GTCCTCATCACCTCCTATTCGCTCCAATAAATCATTTGTTTTCCAACCGTTGGA
CGAGTATCCAACATCTTCACCAGCTCCTTTTGATGATCCTGATGTGTGGGCTC
CACCAAGGGATACACCGACCCGAAGACCAACAAGAGGTCAATCTAGTGCAA
GAAAATCCTCCCAAGATGGAGCCTGGGCACGTGGTTCATCAAGGACTGGAAC
ACCTAGCCGAAGCTCAAAACCTAATGGGAGTAAAGGAGGCTCTGTGGTTAAA
TCATCAACTGCCTCTAACAGTTCTGTAAGGAAAGGAAAACCAAGTTCAAGCA
AGGCTGATTCAGCGAGTAGTGATGCTGAGGAAGGTAAGTCCAAGAAGGGTC
AATATGAAGGGCCAGATATGGACTTAGCTGCAATGCTTGAAAGGGATGTTCT
GGATTCTACTCCAGGAGTAAGATGGGATGATGTTGCCGGACTTAGTGAGGCC
AAACGACTCCTCGAGGAAGCAGTTGTGCTTCCTCTCTGGATGCCTGAATATTT
TCAGGGTATTCGTCGACCTTGGAAAGGAGTTCTTATGTTTGGTCCACCAGGCA
CGGGAAAGACTCTTTTGGCAAAGGCAGTGGCTACAGAATGTGGAACAACATT
CTTCAATGTTTCCTCTGCAACATTGGCCTCTAAATGGCGCGGCGAAAGTGAGC
GCATGGTTCGTTGTTTATTTGATCTTGCGAGGGCCTATGCTCCAAGTACAATT
TTCATTGATGAAATTGACTCCTTATGCACATCACGTGGAGCATCTGGTGAACA
TGAGTCGTCAAGAAGGGTGAAGTCTGAACTTCTAGTGCAAATTGATGGTGTA
AACAATAGCTCCACCACTGAAGATGGTCAGCCAAAAATTGTTATGGTTCTAG
CTGCAACAAATTTTCCATGGGATATTGATGAGGCACTGAGGCGGAGGCTGGA
GAAGCGTATTTATATCCCACTTCCAGATTTCGAAAGCAGAAAGGCACTTATC
AACATTAATCTTAGAACAGTTCAGATAGCTGCGGATGTTAACATCGATGAGG
TTGCTCGGAGGACAGAAGGCTATAGTGGAGATGACTTGACAAATGTTTGCCG
TGATGCTTCAATGAACGGTATGCGGCGCAAGATAGCAGGCAAAACCCGCGAC
GAGATCAAGAACATGTCAAAGGACGATATAGCCAAGGACCCAGTGGCCATG
TGCGACTTTGTGGAGGCTCTGGTGAAGGTCCAGAAGAGTGTCTCGCCTGCAG
ACATAGAAAAGCACGAGAAGTGGATGGCTGAGTTTGGATCTGCCTGAGACCT
CGGTCATCT

>NC358

CCACGCATTTTGTCGGGATTCGGGAACCCTATCGCCGGATCTTCGCGGCGGC
GGCGGAAATGGCGAATCCCCTCGCGGGGCTGCAGGACCACATCAAGCTTGCG
CGGGATTACGCGCTCGAGGGCCTATACGACACCTCCATAATCTTCTTCGACG
GCGCCATTGCTCAGATCAACAAGCATCTAACTACTTTGGACGATGCTTTGGTT
CGTACGAAATGGATGAACTGCAAGAAAGCAATCTCTGAAGAAGTGGAAAGT
GTGAAACAGTTGGATGCTCAATTAAAGTCCCTTAAAGAAGCTCCTGGGACGA
GGCGGTCCTCATCACCTCCTATTCGCTCCAATAAATCATTTGTTTTCCAACCGT
TGGACGAGTATCCAACATCTTCACCAGCACCTTTTGATGATCCTGATGTGTGG
GTTCCACCAAGGGATACACCGACCCGAAGACCAACAAGAGGTCAATCTAGTG
CAAGAAAATCCTCCCAAGATGGAGCCTGGGCACGTGGTTCATCAAGGACTGG
AACACCTAGCCGAAGCTCAAAACCTAATGGGAGTAAAGGAGGCTCTGTGGTT
AAATCATCAACTGCCCCTAACAGTTCTGTAAGGAAAGGAAAACCAAGTTCAA
GCAAGGCTGATTCAGCGAGTAGTGATGCTGAGGAAGGTAAGTCCAAGAAGG
GTCAATATGAAGGGCCAGATATGGACTTAGCTGCAATGCTTGAAAGGGATGT

TCTGGATTCTACTCCAGGAGTAAGATGGGATGATGTTGCCGGACTTAGTGAG
GCCAAACGACTCCTCGAGGAAGCAGTTGTGCTTCCTCTCTGGATGCCTGAATA
TTTTCAGGGTATTCGTCGACCTTGGAAAGGAGTTCTTATGTTTGGTCCACCAG
GCACGGGAAAGACTCTTTTGGCAAAGGCAGTGGCTACAGAATGTGGAACAAC
GTTCTTCAATGTTTCCTCTGCAACATTGGCCTCTAAATGGCGCGGCGAAAGTG
AGCGCATGGTTCGTTGTTTATTTGATCTTGCGAGGGCCTATGCTCCAAGTACA
ATTTTCATTGATGAAATTGACTCATTATGCACATCACGTGGAGCATCTGGTGA
ACATGAGTCGTCAAGAAGGGTGAAGTCTGAACTTCTAGTGCAAATTGATGGT
GTAAACAATAGCTCCACCACTGAAGATGGTCAGCCAAAAATTGTTATGGTTC
TAGCTGCAACAAATTTTCCATGGGATATTGATGAGGCACTGAGGCGGAGGCT
GGAGAAGCGAATTTATATCCCACTTCCAGATTCCGAAAGCAGAAAGGCACTT
ATCAACATTAATCTTAGAACAGTTCAGATAGCTGCGGATGTTAACATCGATG
AGGTTGCTCGGAGGACAGAAGGCTATAGTGGAGATGACTTGACAAATGTTTG
CCGTGATGCTTCGATGAACGGTATGCGGCGCAAGATAGCAGGCAAAACCCGC
GACGAGATCAAGAACATGTCAAAGGACGAGATAGCCAAGGACCCAGTGGCC
ATGTGCGACTTTGTGGAGGCTCTGGTGAAGGTCCAGAAGAGTGTCTCGCCTG
CAGACATAGAAAAGCACGAGAAGTGGATGGCTGAGTTTGGATCTGCCTGAGA
CCTCGGTCATCTCCTTCACACA

>Mo18w

X – 7 bp insertion compared to B73 *KTN1B*

CGCATTTTGTCGGGATTCGGGAACCCTAGAGCCGGATCTTCGCGGCGGCGGC
GGAAATGGCGAATCCCCTCGCGGGTCTGCAGGACCACATCAAGCTTGCGCGG
GATTACGCGCTCGAGGGCCTATACGACACCTCCATAATATTCTTCGACGGCG
CCATTGCTCAGATCAACAAAGTAGTGATGCTGAGGAAGGTAAGTCCAAGAAG
GGTCAATATGAAGGGCCAGATAATAGATATGGACTTAGCTGCAATGCTTGAA
AGGGATGTTCTGGATTCTACTCCAGGAGTAAGATGGGATGATGTTGCTGGAC
TTAGTGAGGCCAAACGACTCCTCGAGGAAGCAGTTGTGCTTCCTCTCTGGATG
CCTGAATATTTTCAGGGTATTCGTCGACCTTGGAAAGGAGTTCTTATGTTTGG
TCCACCAGGCACGGGAAAGACTCTTTTGGCAAAGGCAGTGGCTACAGAATGT
GGAACAACGTTCTTCAATGTTTCCTCTGCAACATTGGCCTCTAAATGGCGCGG
CGAAAGTGAGCGCATGGTTCGTTGTTTATTTGATCTTGCGAGGGCCTATGCTC
CAAGTACAATTTTCATTGATGAAATCGACTCCTTATGCACATCACGTGGAGCA
TCTGGTGAACATGAGTCGTCAAGAAGGGTGAAGTCTGAACTTCTAGTGCAAA
TTGATGGTGTAAACAATAGCTCCACCACTGAAGATGGTCAGCCAAAAATTGT
TATGGTTCTAGCTGCAACAAATTTTCCATGGGATATTGATGAGGCACTGAGGC
GGAGGCTGGAGAAGCGAATTTATATCCCACTTCCAGATTTCGAAAGCAGAAA
GGCACTTATCAACATTAATCTTAGAACAGTTCAGATAGCTGCGGATGTTAAC
ATCGATGAGGTTGCTCGGAGGACAGAAGGCTATAGTGGAGATGACTTGACAA
ATGTTTGCCGTGATGCTTCGATGAACGGTATGCGGCGCAAGATAGCAGGCAA
AACCCGCGACGAGATCAAGAACATGTCAAAGGACGACATAGCCAAGGACCC
AGTGGCCATGTGCGACTTTGTGGAGGCTCTGGTGAAGGTCCAGAAGAGTGTC

TCGCCTGCAGACATAGAAAAGCACGAGAAGTGGATGGCTGAGTTTGGATCTG
CCTGAGACCTCATCT

>Ki11_1.6KB

^ - CTTCAATG deletion compared with B73 *KTN1B*

X – retained intron

CGCATTTTGTCGGGATTCGGGAACCCTAGAGCCGGATCTTCGCGGCGGCGGC
GGAAATGGCGAATCCCCTCGCGGGTCTGCAGGACCACATCAAGCTTGCGCGG
GATTACGCGCTCGAGGGCCTATACGACACCTCCATAATATTCTTCGACGGCG
CCATTGCTCAGATCAACAAAAAATGGATGAACTCTCAGAAAAGTACGGCCGT
ACGGGCAAGTGAAAAAAGTGTGAAACAGCTGTATGCAGTGGCGTAGACAAG
GGAGGCGCCGTTATTTATTTATGGGCATCTAACTACTTTGGACGATGCTTTGG
TTCGTACGAAATGGATGAACTGCAAGAAAGCAATCACTGAAGAAGTGGAAA
GTGTGAAACAGTTGGATGCTCAATTAAAGTCCCTTAAAGAAGTTCCTGGGAC
GAGGCGGTCCTCATCACCTCCTATTAGCTCCAATAAATCATTTGTTTTCCAAC
CGTTGGACGAGTATCCAACATCTTCACCAGCATCTTTTGATGATCCTGATGTG
TGGGCTCCACCAAGGGATACATCGACCCGAAGACCAACAAGAGGTCAATCTA
GCGCAAGAAAATCCTCCCAAGATGGAGCCTGGGCACGTGGTTCATCAAGGAC
TGGAACACCTAGCCGAAGCTCAAAACCTAATGGGAGTAAAGGAGGCTCTGCG
GTTAAATCATCAACTGCCTCTAACAGTTCTGTAAGGAAAGGAAGACCAAGTT
CAAGCAAGGCTGATTCAGCGGGTATTCGTCGACCTTGGAAAGGAGTTCTTAT
GTTTGGTCCACCAGGCACGGGAAAGACTCTTTTGGCAAAGGCAGTGGCTACA
GAATGTGGAACAACGTTCTTCAATGTTTCCTCTGCAACATTGGCCTCTAAATG
GCGCGGCGAAAGTGAGCGCATGGTTCGTTGTTTATTTGATCTTGCGAGGGCCT
ATGCTCCAAGTACAATTTTCATTGATGAAATCGACTCCTTATGCACATCACGT
GGAGCATCTGGTGAACATGAGTCGTCAAGAAGGGTGAAGTCTGAACTTCTAG
TGCAAATTGATGGTGTAAACAATAGCTCCACCACTGAAGATGGTCAGCCAAA
AATTGTTATGGTTCTAGCTGCAACAAATTTTCCATGGGATATTGATGAGGCAC
TGAGGCGGAGGCTGGAGAAGCGTATTTATATCCCACTTCCAGATTTCGAAAG
CAGAAAGGCACTTATCAACATTAATCTTAGAACAGTTCAGATAGCTGCGGAT
GTTAACATCGATGAGGTTGCTCGGAGGACAGAAGGCTATAGTGGAGATGACT
TGACAAATGTTTGCCGTGATG^CACGGTATGCGGCGCAAGATAGCAGGCAAA
ACCCGCGACGAGATCAAGAACATGTCAAAGGACGAGATAGCCAAGGACCCA
GTGGCCATGTGCGACTTTGTGGAGGCTCTGGTGAAGGTCCAGAAGAGTGTCT
CGCCTGCAGACATAGAAAAGCACGAGAAGTGGATGGCTGAGTTTGGATCTGC
CTGAGACCTCGGTCATCTCCTCAACA

>Ki11_600bp

CATTTTGTCGGGATTCGGGAACCCTAGAGCCGGATCTTCGCGGCGGCGGCGG
AAATGGCGAATCCCCTCGCGGGTCTGCAGGACCACATCAAGCTTGCGCGGGA
TTACGCGCTCGAGGGCCTATACGACACCTCCATAATATTCTTCGACGGCGCCA

TTGCTCAGATCAACAAGCGGAGGCTGGAGAAGCGTATTTATATCCCACTTCC
AGATTTCGAAAGCAGAAAGGCACTTATCAACATTAATCTTAGAACAGTTCAG
ATAGCTGCGGATGTTAACATCGATGAGGTTGCTCGGAGGACAGAAGGCTATA
GTGGAGATGACTTGACAAATGTTTGCCGTGATGCACGGTATGCGGCGCAAGA
TAGCAGGCAAAACCCGCGACGAGATCAAGAACATGTCAAAGGACGAGATAG
CCAAGGACCCAGTGGCCATGTGCGACTTTGTGGAGGCTCTGGTGAAGGTCCA
GAAGAGTGTCTCGCCTGCAGACATAGAAAAGCACGAGAAGTGGATGGCTGA
GTTTGGATCTGCCTGAGACCTCGGTCATCTCCTTCAACATTGGTTTCTGTGGTT
GACACGAGAAGTGTATGTTGATATCCGCTGACCGCTG

>Ki3_1.6kb

^ - CTTCAATG deletion compared with B73 *KTN1B*

X – retained intron

X – novel 54 bp sequence containing another in-frame stop codon and sharing homology with a Prem1 Gypsy retroelement

TTTTGTCGGGATTCGGGAACCCTAGAGCCGGATCTTCGCGGCGGCGGCGGAA
ATGGCGAATCCCCTCGCGGGTCTGCAGGACCACATCAAGCTTGCGCGGGATT
ACGCGCTCGAGGGCCTATACGACACCTCCATAATATTCTTCGACGGCGCCATT
GCTCAGATCAACAAAAAATGGATGAACTCTCAGAAAAGTACGGCCGTACGG
GCAAGTGAAAAAAGTGTGAAACAGCTGTATGCAGTGGCGTAGACAAGGGAG
GCGCCGTTATTTATTTATGGGCATCTAACTACTTTGGACGATGCTTTGGTTCGT
ACGAAATGGATGAACTGCAAGAAAGCAATCACTGAAGAAGTGGAAAGTGTG
AAACAGTTGGATGCTCAATTAAAGTCCCTTAAAGAAGTTCCTGGGACGAGGC
GGTCCTCATCACCTCCTATTAGCTCCAATAAATCATTTGTTTTCCAACCGTTGG
ACGAGTATCCAACATCTTCACCAGCATCTTTTGATGATCCTGATGTGTGGGCT
CCACCAAGGGATACATCGACCCGAAGACCAACAAGAGGTCAATCTAGCGCA
AGAAAATCCTCCCAAGATGGAGCCTGGGCACGTGGTTCATCAAGGACTGGAA
CACCTAGCCGAAGCTCAAAACCTAATGGGAGTAAAGGAGGCTCTGCGGTTAA
ATCATCAACTGCCTCTAACAGTTCTGTAAGGAAAGGAAGACCAAGTTCAAGC
AAGGCTGATTCAGCGTGAGGTCACGTGCCATCTGAAGATCATCCTGGTACCT
GGATTCTCAAGGCCCAGGGTATTCGTCGACCTTGGAAAGGAGTTCTTATGTTT
GGTCCACCAGGCACGGGAAAGACTCTTTTGGCAAAGGCAGTGGCTACAGAAT
GTGGAACAACGTTCTTCAATGTTTCCTCTGCAACATTGGCCTCTAAATGGCGC
GGCGAAAGTGAGCGCATGGTTCGTTGTTTATTTGATCTTGCGAGGGCCTATGC
TCCAAGTACAATTTTCATTGATGAAATCGACTCCTTATGCACATCACGTGGAG
CATCTGGTGAACATGAGTCGTCAAGAAGGGTGAAGTCTGAACTTCTAGTGCA
AATTGATGGTGTAAACAATAGCTCCACCACTGAAGATGGTCAGCCAAAAATT
GTTATGGTTCTAGCTGCAACAAATTTTCCATGGGATATTGATGAGGCACTGAG
GCGGAGGCTGGAGAAGCGTATTTATATCCCACTTCCAGATTTCGAAAGCAGA
AAGGCACTTATCAACATTAATCTTAGAACAGTTCAGATAGCTGCGGATGTTA

ACATCGATGAGGTTGCTCGGAGGACAGAAGGCTATAGTGGAGATGACTTGAC
AAATGTTTGCCGTGATG^CACGGTATGCGGCGCAAGATAGCAGGCAAAACCC
GCGACGAGATCAAGAACATGTCAAAGGACGAGATAGCCAAGGACCCAGTGG
CCATGTGCGACTTTGTGGAGGCTCTGGTGAAGGTCCAGAAGAGTGTCTCGCC
TGCAGACATAGAAAAGCACGAGAAGTGGATGGCTGAGTTTGGATCTGCCTGA
GACCTCGGTCATCTCCTTCAACA

>CML333_1

X – retained intron

X – first two nucleotides of 3’ RACE primer

CATTTTGTCGGGATTCGGGAACCCTATCGCCGGATCTTCGCGGCGGCGGCGG
AAATGGCGAATCCCCTCGCGGGGCTGCAGGACCACATCAAGCTTGCGCGGGA
TTACGCGCTCGAGGGCCTATACGACACCTCCATAATCTTCTTCGACGGCGCCA
TTGCTCAGATCAACAAGCATCTAACTACTTTGGACGATGCTTTGGTTCGTACG
AAATGGATGAACTGCAAGAAAGCAATCTCTGAAGAAGTGGAAAGTGTGAAA
CAGTTGGATGCTCAATTAAAGTCCCTTAAAGAAGCTCCTGGGACGAGGCGGT
CCTCATCACCTCCTATTCGCTCCAATAAATCATTTGTTTTCCAACCGTTGGACG
AGTATCCAACATCTTCACCAGCTCCTTTTGATGATCCTGATGTGTGGGCTCCA
CCAAGGGATACACCGACCCGAAGACCAACAAGAGGTCAATCTAGTGCAAGA
AAATCCTCCCAAGATGGAGCCTGGGCACGTGGTTCATCAAGGACTGGAACAC
CTAGCCGAAGCTCAAAACCTAATGGGAGTAAAGGAGGCTCTGTGGTTAAATC
ATCAACTGCCTCTAACAGTTCTGTAAGGAAAGGAAAACCAAGTTCAAGCAAG
GCTGATTCAGCGAGTAGTGATGCTGAGGAAGGTAAGTCCAAGAAGGGTCAAT
ATGAAGGGCCAGATATGGACTTAGCTGCAATGCTTGAAAGGGATGTTCTGGA
TTCTACTCCAGGAGTAAGATGGGATGATGTTGCCGGACTTAGTGAGGCCAAA
CGACTCCTCGAGGAAGCAGTTGTGCTTCCTCTCTGGATGCCTGAATATTTTCA
GGGTATTCGTCGACCTTGGAAAGGAGTTCTTATGTTTGGTCCACCAGGCACGG
GAAAGACTCTTTTGGCAAAGGCAGTGGCTACAGAATGTGGAACAACATTCTT
CAATGTTTCCTCTGCAACATTGGCCTCTAAATGGCGCGGCGAAAGTGAGCGC
ATGGTTCGTTGTTTATTTGATCTTGCGAGGGCCTATGCTCCAAGTACAATTTTC
ATTGATGAAATTGACTCCTTATGCACATCACGTGGAGCATCTGGTGAACATG
AGTCGTCAAGAAGGGTGAAGTCTGAACTTCTAGTGCAAATTGATGGTGTAAA
CAATAGCTCCACCACTGAAGATGGTCAGCCAAAAATTGTTATGGTTCTAGCT
GCAACAAATTTTCCATGGGATATTGATGAGGCACTGAGGTTGGCAAACTCTT
ATTCTCATATTCACTTCATTTTAGGTGCTACTGCCTACTTATTATTATGAATAA
GGGTTGGTACCTGGAAGATGCATATGATGGTTCACATAAACGGATAAACCTG
TCATATTTTAGCAGTAGCACCTGATTGCTTGAGTGGTGCTGCTAGTAGCGTTA
GATACTGTCGAAGCCAGGGACAGTTTATTTGATTTCTCAAGACTTTTACAGAA
TCATTTTTTCTCAGTCATGCTGCATTGTCACACCACTGACCACTGTTTATTTGG
TGAGACAAGAAACTATGGTAGTTCCTAACTTCAGG

>CML333_2

X – retained intron

X – first two nucleotides of 3’ RACE primer

TTTTGTCGGGATTCGGGAACCCTATCGCCGGATCTTCGCGGCGGCGGCGGAA
ATGGCGAATCCCCTCGCGGGGCTGCAGGACCACATCAAGCTTGCGCGGGATT
ACGCGCTCGAGGGCCTATACGACACCTCCATAATCTTCTTCGACGGCGCCATT
GCTCAGATCAACAAGCATCTAACTACTTTGGACGATGCTTTGGTTCGTACGAA
ATGGATGAACTGCAAGAAAGCAATCTCTGAAGAAGTGGAAAGTGTGAAACA
GTTGGATGCTCAATTAAAGTCCCTTAAAGAAGCTCCTGGGACGAGGCGGTCC
TCATCACCTCCTATTCGCTCCAATAAATCATTTGTTTTCCAACCGTTGGACGA
GTATCCAACATCTTCACCAGCTCCTTTTGATGATCCTGATGTGTGGGCTCCAC
CAAGGGATACACCGACCCGAAGACCAACAAGAGGTCAATCTAGTGCAAGAA
AATCCTCCCAAGATGGAGCCTGGGCACGTGGTTCATCAAGGACTGGAACACC
TAGCCGAAGCTCAAAACCTAATGGGAGTAAAGGAGGCTCTGTGGTTAAATCA
TCAACTGCCTCTAACAGTTCTGTAAGGAAAGGAAAACCAAGTTCAAGCAAGG
CTGATTCAGCGAGTAGTGATGCTGAGGAAGGTAAGTCCAAGAAGGGTCAATA
TGAAGGGCCAGATATGGACTTAGCTGCAATGCTTGAAAGGGATGTTCTGGAT
TCTACTCCAGGAGTAAGATGGGATGATGTTGCCGGACTTAGTGAGGCCAAAC
GACTCCTCGAGGAAGCAGTTGTGCTTCCTCTCTGGATGCCTGAATATTTTCAG
GGTATTCGTCGACCTTGGAAAGGAGTTCTTATGTTTGGTCCACCAGGCACGGG
AAAGACTCTTTTGGCAAAGGCAGTGGCTACAGAATGTGGAACAACATTCTTC
AATGTTTCCTCTGCAACATTGGCCTCTAAATGGCGCGGCGAAAGTGAGCGCA
TGGTTCGTTGTTTATTTGATCTTGCGAGGGCCTATGCTCCAAGTACAATTTTCA
TTGATGAAATTGACTCCTTATGCACATCACGTGGAGCATCTGGTGAACATGA
GTCGTCAAGAAGGGTGAAGTCTGAACTTCTAGTGCAAATTGATGGTGTAAAC
AATAGCTCCACCACTGAAGATGGTCAGCCAAAAATTGTTATGGTTCTAGCTG
CAACAAATTTTCCATGGGATATTGATGAGGCACTGAGGTCAGGTTGATCACC
AGAGCCTAGAGGACTGGTGGCTGAGGTCAAGGCTACTCAGTCCTGTTTATGT
CATTTATATTTTTCGATGTATCTAGTTACATTTGTTCTAAACAAAACAAATCC
ACTAATTGCTCATTCCAGTTCCTTTTGTAATGCTTTACAATTCTTTGTGTCATT
GCGTTTATAGTGCCTAATTCTTGTTCAGTTATGTAATTTTCTTCAAGCAAAGC
ACCCAATTTTGCAGGATGACATGATTTTGCCGTTATTTGTCCAAATAATAGGG
TTAGAGTTTTT

>CML333_RACE

X – retained intron

X – first two nucleotides of 3’ RACE primer

TTTTGTCGGGATTCGGGAACCCTATCGCCGGATCTTCGCGGCGGCGGCGGAA
ATGGCGAATCCCCTCGCGGGGCTGCAGGACCACATCAAGCTTGCGCGGGATT
ACGCGCTCGAGGGCCTATACGACACCTCCATAATCTTCTTCGACGGCGCCATT
GCTCAGATCAACAAGCATCTAACTACTTTGGACGATGCTTTGGTTCGTACGAA

ATGGATGAACTGCAAGAAAGCAATCTCTGAAGAAGTGGAAAGTGTGAAACA
GTTGGATGCTCAATTAAAGTCCCTTAAAGAAGCTCCTGGGACGAGGCGGTCC
TCATCACCTCCTATTCGCTCCAATAAATCATTTGTTTTCCAACCGTTGGACGA
GTATCCAACATCTTCACCAGCTCCTTTTGATGATCCTGATGTGTGGGCTCCAC
CAAGGGATACACCGACCCGAAGACCAACAAGAGGTCAATCTAGTGCAAGAA
AATCCTCCCAAGATGGAGCCTGGGCACGTGGTTCATCAAGGACTGGAACACC
TAGCCGAAGCTCAAAACCTAATGGGAGTAAAGGAGGCTCTGTGGTTAAATCA
TCAACTGCCTCTAACAGTTCTGTAAGGAAAGGAAAACCAAGTTCAAGCAAGG
CTGATTCAGCGAGTAGTGATGCTGAGGAAGGTAAGTCCAAGAAGGGTCAATA
TGAAGGGCCAGATATGGACTTAGCTGCAATGCTTGAAAGGGATGTTCTGGAT
TCTACTCCAGGAGTAAGATGGGATGATGTTGCCGGACTTAGTGAGGCCAAAC
GACTCCTCGAGGAAGCAGTTGTGCTTCCTCTCTGGATGCCTGAATATTTTCAG
GGTATTCGTCGACCTTGGAAAGGAGTTCTTATGTTTGGTCCACCAGGCACGGG
AAAGACTCTTTTGGCAAAGGCAGTGGCTACAGAATGTGGAACAACATTCTTC
AATGTTTCCTCTGCAACATTGGCCTCTAAATGGCGCGGCGAAAGTGAGCGCA
TGGTTCGTTGTTTATTTGATCTTGCGAGGGCCTATGCTCCAAGTACAATTTTCA
TTGATGAAATTGACTCCTTATGCACATCACGTGGAGCATCTGGTGAACATGA
GTCGTCAAGAAGGGTGAAGTTTGAACTTCTAGTGCAAATTGATGGTGTAAAC
AATAGCTCCACCACTGAAGATGGTCAGCCAAAAATTGTTATGGTTCTAGCTG
CAACAAATTTTCCATGGGATATTGATGAGGCACTGAGGTCAGGTTGATCACC
AGAGCCTAGAGGACTGGTGGCTGAGGTCAAGGCTACTCAGTCCTGTTTATGT
CATTTATATTTTTCGATGTATCTAGTTACATTTGTTCTAAACAAAACAAATCC
ACTAATTGCTCATTCCAGTTCCTTTTGTAATGCTTTACAATTCTTTGTGTCATT
GCGTTTATAGTGCCTAATTCTTGTTCAGTTATGTAATTTTCTTCAAGCAAAGC
ACCCAATTTTGCAGGAGG

Appendix D Amplification of *ktn1b* transcript from two additional samples of cDNA from seedling mesocotyl of different NAM lines

Ext_F-Ext_R (corresponds to Figure 3.8B)
-RNA extraction, cDNA synthesis and PCR as described in Chapter 3 except SuperScript IV used instead of SuperScript III for cDNA synthesis.

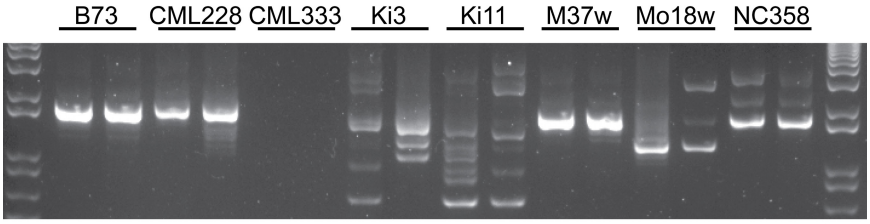

Ext_F-520_R (corresponds to Figure 3.8E)
-same RNA samples as Ext_F-Ext_R reactions but synthesis of cDNA done using M-MuLV Reverse Transcriptase (NEB). PCR as described in Chapter 3.

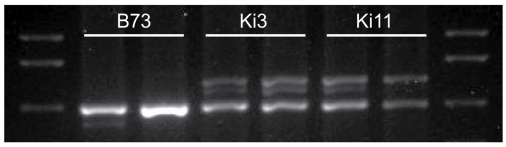

3_F-1020_R (corresponds to Figure 3.8F)
-same cDNA samples as Ext_F-520_R reactions. PCR as described in Chapter 3.

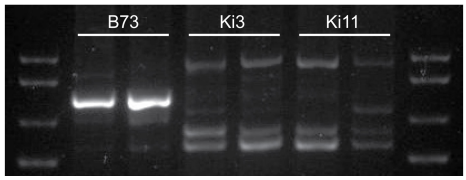

Ext_F-Qo (corresponds to Figure 3.8H)
-Same RNA samples as Ext_F-Ext_R reactions, but synthesis of cDNA done using the 3' RACE primer followed by PCR, as described in Chapter 3.

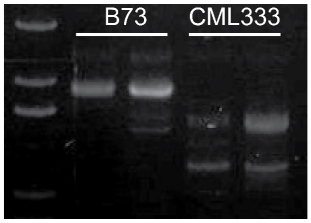

VITA

VITA

Kin Lau was born in Hong Kong but moved at an early age to Kingston, Jamaica where he grew up. He completed his high school education at Campion College in 2006. He then moved north to Davidson College in North Carolina, USA for his undergraduate education and obtained a B.S. in Biology in 2010. While at Davidson, he worked in the lab of Dr. Malcolm Campbell where he learned basic molecular techniques and developed an interest in pursuing a career in science. Upon completion of his undergraduate studies, Kin continued his northward journey, ending up at Purdue University in West Lafayette, Indiana where he worked on his Ph.D. in the lab of Dr. Clifford Weil. Here, he continued his growth as a budding scientist while working on a project characterizing developmental mutants in maize. After obtaining his Ph.D. in Aug 2016, Kin will pursue post-doctoral opportunities to continue building his skill set and qualifications as a plant geneticist.